



DISSERTATION

**Advances in automated flow systems for microfluidic analysis  
with mid-IR detection**

ausgeführt zum Zwecke der Erlangung des akademischen Grades eines  
Doktors der technischen Wissenschaften

unter der Leitung von  
Ao. Univ. Prof. Dr. Bernhard Lendl  
E164-AC  
Institut für Chemische Technologie und Analytik

eingereicht an der Technischen Universität Wien  
Fakultät für Technische Naturwissenschaften und Informatik

von

**Dipl. Ing. Stephan Kulka**  
Matr.-Nr. 9626471  
Hockegasse 15, A-1180 Wien

Wien, im Dezember 2005

## DEUTSCHE KURZFASSUNG

Das Ziel der vorliegenden Arbeit war die Entwicklung automatisierter mikrofluidischer Systeme mit Detektion im mittleren Infrarot (MIR).

Der erste Teil beschäftigt sich mit der Weiterentwicklung einer Mikrodurchflusszelle für online MIR-Detektion in der Kapillarelektrophorese (CE) für Proteine und Analyse ihrer Sekundärstrukturen. Eine mit SU-8 mikrostrukturierte infrarottransparente Durchflusszelle, in welcher auch die Detektion stattfand, wurde zwischen zwei Kapillaren eingesetzt. In dieser Arbeit wurde eine neue Halterung für die Durchflusszelle entwickelt, in der mit Hilfe von O-Ringen die Kapillaren an die Zelle angekoppelt wurden. Die eingesetzten Modellproteine Myoglobin,  $\alpha$ -Lactalbumin und  $\beta$ -Lactoglobulin wurden wegen ihrer deutlich unterschiedlichen Sekundärstrukturen gewählt. Die Trennung der Proteine erfolgte in unbehandelten Kapillaren mit einem Innendurchmesser von 50  $\mu\text{m}$ ; als Puffer wurde Borax mit einem pD von 9.2 verwendet. Die Analyse der Proteine erfolgte in  $\text{D}_2\text{O}$ , damit die starke Absorptionsbande von Wasser bei 1640  $\text{cm}^{-1}$  zu 1210  $\text{cm}^{-1}$  verschoben wurde, um die Analyse der Amide I-Bande zu ermöglichen. Ein Vergleich der Trennung, detektiert mit UV-Vis und Infrarotspektroskopie, zeigte, dass der Einbau der Durchflusszelle keine Auswirkungen auf die Trennleistung des CE-Systems hatte. Die online gewonnenen IR-Spektren wurden mit Referenzspektren verglichen und ergaben eine gute Übereinstimmung.

Im zweiten Teil wurde ein Chip für Kapillarelektrophorese (CE) in Zusammenarbeit mit dem Institut für Industrielle Elektronik und Materialwissenschaften an der TU Wien entwickelt und am Synchrotron ANKA (Karlsruhe, Deutschland) eingesetzt. Synchrotronstrahlung weist im Vergleich mit herkömmlichen Strahlungsquellen eine sehr hohe Brillianz auf, die in erster Linie bei Messungen, in denen der IR-Strahl auf Strukturen unter 50  $\mu\text{m}$  fokussiert wird, zum Tragen kommt. Dadurch ist es möglich, Analysen in einem sehr kleinen Detektionsvolumen durchzuführen, was bei scharfen Peaks wie in CE besonders wichtig ist. In dieser Arbeit wurde ein Chip für die

Kapillarelektrophorese entwickelt, bestehend aus  $\text{CaF}_2$  und dem Polymer SU-8 zur Strukturierung. Diese Entwicklung war notwendig, weil übliche Chipmaterialien infrarotes Licht stark absorbieren. Der Kanal auf dem Chip hatte eine Breite von  $100\ \mu\text{m}$  und eine Höhe von  $10\ \mu\text{m}$ , die auch der optischen Weglänge entspricht und wurde in eine eigens gefertigte Plexiglashalterung eingeschraubt. Die Funktionsweise des CE-Chips wurde mit den anorganischen Ionen Sulfat und Nitrat getestet, die beide starke Absorptionsbanden im Infrarot aufweisen. Weiters wurde der Chip mit Myoglobin getestet, weil durch die höhere Diffusionskonstante das Protein sich nach Anlegen der Spannung langsamer bewegt. Beide Analysen wurden herangezogen, um die Möglichkeiten der Synchrotronstrahlung für mikrofluidische Anwendungen zu beurteilen. Die vorliegenden Ergebnisse zeigen, dass für solche Applikation das Rauschen, welches an der IR-Beamline des Synchrotrons technisch bedingt derzeit noch stark auftritt, Anwendungen in wässriger Lösung limitieren.

Der letzte Teil der Dissertation beschäftigt sich mit der Kopplung von sequentieller Injektionsanalyse (SIA) und Kapillarelektrophorese (CE). Die Möglichkeit von SIA, automatisiert Analyten und Reagenzien zu mischen, chemische Reaktionen und/oder Anreicherungs-schritte durchzuführen, wurde in dieser Arbeit eingesetzt, um die Analyten kurz vor der CE-Trennung zu modifizieren. Die Fähigkeit eines SIA-Systems, durch die Spritzenpumpe Druck in einem Fließsystem auszuüben, wurde zur automatisierten hydrodynamischen Injektion in die Kapillare verwendet. Zur vollständigen Automation der Kopplung wurde in dieser Arbeit Software entwickelt, um die Hochspannungsquelle und den UV-Detektor anzusteuern. Dadurch war eine komplette Automatisierung aller Schritte erreicht. Die analytischen Parameter der Kopplung zwischen SIA und CE wurden anhand der Injektion und Trennung von Adenosin und Adenosinmonophosphat charakterisiert. Dabei wurden eine Standardabweichung im einstelligen Prozentbereich und eine Nachweisgrenze im unteren ppm-Bereich gefunden. Die Möglichkeiten von SIA wurden eingesetzt um verschiedene Konzentrationen von Natriumdodecylsulfat (SDS) automatisiert herzustellen und mit Myoglobin zu mischen. SDS ist ein bekanntes Reagens zur

Denaturierung von Proteinen. Nach erfolgter Mischung wurde Myoglobin in die Kapillare injiziert und mittels Kapillarelektrophorese getrennt. Die Ergebnisse zeigen die verschiedenen entstandenen Konformationen von Myoglobin, abhängig von der Konzentration von SDS.

## ABSTRACT

The goal of this work was the development of automated flow systems for microfluidic analysis using mid-IR detection.

The first part deals with the further development of a micro flow cell for online MIR detection of proteins and their secondary structures. An infrared transparent flow cell structured with the epoxy polymer SU-8 was coupled between two capillaries. In the flow cell the IR detection took place. In this work a new cell holder was developed where the capillaries were attached to flow cell using O-rings. The proteins myoglobin,  $\alpha$ -lactalbumin and  $\beta$ -lactoglobulin were used in this study as they show different secondary structures. The separation of the proteins was carried out in uncoated capillaries with an inner diameter of 50  $\mu\text{m}$  and the buffer used was borax with a pD of 9.2. The strong absorption of water at 1640  $\text{cm}^{-1}$  was shifted down to 1210  $\text{cm}^{-1}$  and thus the analysis of the amide I band became possible when measuring in  $\text{D}_2\text{O}$ . A comparison of the separation as detected with UV-Vis and infrared detection showed that the inclusion of the micro flow cell did not have an influence on the separation itself. The spectra taken online were compared with reference spectra and showed a good agreement.

In the second part a capillary electrophoresis (CE) chip was developed in cooperation with the institute for Industrial Electronics and Material Science and was used at the synchrotron ANKA (Karlsruhe, Germany). Synchrotron radiation possesses a very high brilliance compared to conventional light sources, which becomes relevant in measurements where the IR beam is focussed below 50  $\mu\text{m}$ . Therefore analysis in very small detection volume is possible, which gets important for sharp peaks as in CE. In this work a CE chip made of  $\text{CaF}_2$  and the polymer SU-8 was developed. This development was necessary as the usual materials used for micro chips strongly absorb infrared light. The channel on the chip was 100  $\mu\text{m}$  broad and 10  $\mu\text{m}$  high, which is equal to the optical path length and was mounted in a dedicated Perspex holder. The functionality of the chip was tested with the inorganic ions sulfate and nitrate, which both show strong absorption bands in the infrared. Furthermore, the chip was tested with

myoglobin, because the protein moves slower inside the chip due to its higher diffusion constant. Both applications were studied to assess the potential of synchrotron radiation for microfluidic applications. The obtained results show that for such applications the noise found at the IR beamline of the synchrotron is at the moment still high due to technical reasons.

The last part of this dissertation deals with the coupling of sequential injection analysis (SIA) and capillary electrophoresis (CE). The ability of SIA to automatically mix analytes and reagents, carry out chemical reactions and/or preconcentration steps, was used in this work to modify the analyte shortly before separation inside the CE system. The possibility of a SIA system to pressurize a flow system using its syringe pump was applied to automated hydrodynamic injection into the capillary. For the complete automatization of the hyphenated system software to control the high voltage power supply and the UV detector was developed in this work. Using this software all steps were completely automated. The figures of merit of this system were assessed based on the injection and separation of adenosine and adenosine monophosphate. A standard deviation in the single-digit percentage range and a limit of detection in the low ppm-range was found. The possibilities of SIA were applied to prepare different concentrations of sodium dodecyl sulfate (SDS), a known denaturing agent for proteins, automatically and mix them with myoglobin. After the mixing myoglobin was injected into the capillary and separated with CE. The results show the differently formed conformations of myoglobin, depending on the concentration of SDS.

## ACKNOWLEDGEMENT

I want to thank my supervisor *Bernhard Lendl* who always helped me in situations where things went wrong. He was not only a supervisor but also a friend to count on in difficult private situations.

A big thank you goes to all co-operation partners contributing to this work: *Peter and Edda Svasek* from the Institute of Industrial Electronics and Material Science, who have skilfully built the microfluidic devices and made this project possible; *David Moss* who helped me during my stay at the synchrotron in Karlsruhe, *Ullrich Schade* who gave me deep insights into the operation principles of a synchrotron in Berlin and *Ersilia de Lorenzi* and *Stefania Sabella* in whose lab in Pavia my views about capillary electrophoresis were extended.

The CAVS team always was the place for good ideas, help, fun and more than once my work without their suggestions and their experience would not have gone this way finally. I want to thank *Nina Kaun*, *Wolfgang Ritter*, *Stefan Schaden* and *Johannes Schnöller*, but not to forget our international members as *Guillermo Quintas Soria*, *Ana Dominguez Vidal* and *Mercedes Lopez Pastor* and of course *Josefa Rodriguez Baena*. The former group members who laid the foundation of this work, *Peter Hinsmann* and *Michael Haberkorn* need to be mentioned here as well. I also want to thank all former group members and guests who gave the working group its multicultural flair.

The help of *Johannes Frank* who was always there when strange ideas need to be converted into a practical tool and to *Markus Schaufler* who took care of all wiring, built the electronic devices needed and kept the spectrometer running. Thanks also go to all members of the institute, mainly to the head of the institute professor *Hans Puxbaum*.

Financial support for this work provided by Austrian Science Fund (FWF) within the project P 15531 ÖCH is gratefully acknowledged.

I want to thank *Christian Sperger* who helped me through my first time of this work and who never grew tired listening to me in all matters and all others who endured me in times of bad mood and stress.

Last, but definitely not least I want to thank my family who always supported me.

## TABLE OF CONTENTS

<b>1</b>	<b>INTRODUCTION</b>	<b>1</b>
1.1	Fourier transform infrared spectroscopy	1
1.2	FT-IR spectroscopy in aqueous solution	6
1.3	Synchrotron Radiation	9
1.4	Protein Structure	14
1.5	Flow systems	19
1.6	Capillary Electrophoresis	21
1.7	Miniaturised flow systems	25
1.8	Microstructuring Strategies	26
<b>2</b>	<b>FT-IR DETECTION IN CAPILLARY ELECTROPHORESIS FOR PROTEINS</b>	<b>28</b>
2.1	Detection methods in capillary electrophoresis	28
2.2	Interface for on-line FT-IR detection in CE	29
2.3	Applications for protein samples	31
2.4	Conclusions and Outlook	35
<b>3</b>	<b>INFRARED SYNCHROTRON RADIATION FOR MICRO-CHIP BASED ANALYSIS</b>	<b>36</b>
3.1	Production of the micro-chip	36
3.2	FT-IR spectrometer and synchrotron source	38
3.3	Results and Discussion	39
3.4	Conclusions and Outlook	43
<b>4</b>	<b>SEQUENTIAL INJECTION (SI)-CAPILLARY ELECTROPHORESIS SYSTEM FOR AUTOMATED SAMPLE PREPARATION AND SEPARATION</b>	<b>44</b>
4.1	Development of the software	44
4.2	SIA-CE interface	46



4.2.1	Test of the SIA-CE system	48
4.2.2	Application to myoglobin and sodium dodecyl sulfate	49
4.3	Conclusion and Outlook	50
<b>5 REFERENCES</b>		52
<b>6. APPENDIX</b>		
	Publication I	56
	Publication II	73
	Publication III	80
	Publication IV	101
	Curriculum vitae	126

## LIST OF PUBLICATIONS

- I** Kulka, S.; Lendl, B. “*On-line capillary electrophoresis FT-IR detection for the separation and characterization of proteins*” submitted publication.
- II** Kulka, S.; Kaun, N.; Baena J.R.; Frank, J.; Svasek, P.; Moss, D.; Vellekoop M.J.; Lendl, B. “*Mid-IR synchrotron radiation for molecular specific detection in microchip-based analysis systems*” *Analytical and Bioanalytical Chemistry* **2004**, 378 , 1735-1740.
- III** Kulka, S.; Quintas, G.; Lendl, B. “*Automated sample preparation and analysis using a sequential-injection (SI)-capillary electrophoresis (CE) interface*” submitted publication.
- IV** Kulka, S.; Lendl, B. “*Vibrational spectroscopic detection in capillary electrophoresis (CE)*”. in “*Analysis and detection by capillary electrophoresis*”, eds. Marina, M.L; Rios, A.; Valcarcel, M., Elsevier: Amsterdam, 2005
- V** Kaun, N.; Kulka, S. ; Frank, J.; Schade,U.; Vellekoop, M.J.; Harasek, M. and Lendl, B. “*Towards Biochemical reaction monitoring using FT-IR Synchrotron radiation*” accepted paper

## LIST OF ABBREVIATIONS

<b>ADC</b>	analogue-digital converter
<b>ANKA</b>	Anionenquelle Karlsruhe
<b>ATR</b>	attenuated total reflection
<b>BGE</b>	background electrolyte
<b>CE</b>	capillary electrophoresis
<b>CVD</b>	chemical vapour deposition
<b>EOF</b>	electroosmotic flow
<b>FIA</b>	flow injection analysis
<b>FIR</b>	far infrared
<b>FT-IR</b>	Fourier transform infrared
<b>HPLC</b>	high pressure liquid chromatography
<b>IP</b>	internet protocol
<b>IR</b>	infrared
<b>MCT</b>	mercury cadmium telluride
<b>MEKC</b>	micellar elektrokinetic chromatography
<b>μTAS</b>	micro total analysis system
<b>RSD</b>	root square deviation
<b>SI</b>	sequential injection
<b>SIA</b>	sequential injection analysis
<b>SDS</b>	sodium dodecyl sulfate
<b>TCP</b>	transfer control protocol
<b>UHV</b>	ultra high vacuum
<b>UV</b>	ultraviolet
<b>UV-Vis</b>	ultraviolet-visible

# 1 Introduction

## 1.1 Fourier transform infrared spectroscopy

Infrared (IR) spectroscopy is based on the principle that molecular vibrations and rotations are excited when infrared light is absorbed by the analyte. However, the transition from one vibrational state to the other has to fulfil the requirement that the vibration causes the dipole momentum of the molecule to change. Typical examples of such a situation are molecules like CH<sub>4</sub> or NaH<sub>2</sub>PO<sub>4</sub>. Otherwise, the vibrational mode will not be visible in the IR spectrum of the substance as it is in the case of symmetric molecules like O<sub>2</sub> and N<sub>2</sub>. The energy needed to stimulate a vibrational transition depends on the mass of the atoms and the strength of the bond as described in equation 1.

$$\nu = \frac{1}{2\pi} \sqrt{\frac{F}{\mu}} \quad \text{Equation 1}$$

where  $\nu$  is the frequency of the vibration,  $F$  is the spring constant of the bond and  $\mu$  is the reduced mass of the involved atoms. The reduced mass is used in this equation to describe the combined influence of both atoms on the vibration. The strength of the bond is reflected in different band positions for the same atoms but different bonds (see Table 1). However, the strength of a bond is also influenced by weaker bonds, like hydrogen bonding, which also influence the energy needed to activate the vibration and therefore the band position. In table 1, X stands for C, O or N, in the case of the triple bond only C or N is possible.

	C-X	C=X	C≡X
wavenumber [cm <sup>-1</sup> ]	1300 - 800	1900-1500	2300-2000

Table 1 Different band positions depending on the bond strength

## DEUTSCHE KURZFASSUNG

Das Ziel der vorliegenden Arbeit war die Entwicklung automatisierter mikrofluidischer Systeme mit Detektion im mittleren Infrarot (MIR).

Der erste Teil beschäftigt sich mit der Weiterentwicklung einer Mikrodurchflusszelle für online MIR-Detektion in der Kapillarelektrophorese (CE) für Proteine und Analyse ihrer Sekundärstrukturen. Eine mit SU-8 mikrostrukturierte infrarottransparente Durchflusszelle, in welcher auch die Detektion stattfand, wurde zwischen zwei Kapillaren eingesetzt. In dieser Arbeit wurde eine neue Halterung für die Durchflusszelle entwickelt, in der mit Hilfe von O-Ringen die Kapillaren an die Zelle angekoppelt wurden. Die eingesetzten Modellproteine Myoglobin,  $\alpha$ -Lactalbumin und  $\beta$ -Lactoglobulin wurden wegen ihrer deutlich unterschiedlichen Sekundärstrukturen gewählt. Die Trennung der Proteine erfolgte in unbehandelten Kapillaren mit einem Innendurchmesser von 50  $\mu\text{m}$ ; als Puffer wurde Borax mit einem pD von 9.2 verwendet. Die Analyse der Proteine erfolgte in  $\text{D}_2\text{O}$ , damit die starke Absorptionsbande von Wasser bei 1640  $\text{cm}^{-1}$  zu 1210  $\text{cm}^{-1}$  verschoben wurde, um die Analyse der Amide I-Bande zu ermöglichen. Ein Vergleich der Trennung, detektiert mit UV-Vis und Infrarotspektroskopie, zeigte, dass der Einbau der Durchflusszelle keine Auswirkungen auf die Trennleistung des CE-Systems hatte. Die online gewonnenen IR-Spektren wurden mit Referenzspektren verglichen und ergaben eine gute Übereinstimmung.

Im zweiten Teil wurde ein Chip für Kapillarelektrophorese (CE) in Zusammenarbeit mit dem Institut für Industrielle Elektronik und Materialwissenschaften an der TU Wien entwickelt und am Synchrotron ANKA (Karlsruhe, Deutschland) eingesetzt. Synchrotronstrahlung weist im Vergleich mit herkömmlichen Strahlungsquellen eine sehr hohe Brillianz auf, die in erster Linie bei Messungen, in denen der IR-Strahl auf Strukturen unter 50  $\mu\text{m}$  fokussiert wird, zum Tragen kommt. Dadurch ist es möglich, Analysen in einem sehr kleinen Detektionsvolumen durchzuführen, was bei scharfen Peaks wie in CE besonders wichtig ist. In dieser Arbeit wurde ein Chip für die

Kapillarelektrophorese entwickelt, bestehend aus  $\text{CaF}_2$  und dem Polymer SU-8 zur Strukturierung. Diese Entwicklung war notwendig, weil übliche Chipmaterialien infrarotes Licht stark absorbieren. Der Kanal auf dem Chip hatte eine Breite von  $100\ \mu\text{m}$  und eine Höhe von  $10\ \mu\text{m}$ , die auch der optischen Weglänge entspricht und wurde in eine eigens gefertigte Plexiglashalterung eingeschraubt. Die Funktionsweise des CE-Chips wurde mit den anorganischen Ionen Sulfat und Nitrat getestet, die beide starke Absorptionsbanden im Infrarot aufweisen. Weiters wurde der Chip mit Myoglobin getestet, weil durch die höhere Diffusionskonstante das Protein sich nach Anlegen der Spannung langsamer bewegt. Beide Analysen wurden herangezogen, um die Möglichkeiten der Synchrotronstrahlung für mikrofluidische Anwendungen zu beurteilen. Die vorliegenden Ergebnisse zeigen, dass für solche Applikation das Rauschen, welches an der IR-Beamline des Synchrotrons technisch bedingt derzeit noch stark auftritt, Anwendungen in wässriger Lösung limitieren.

Der letzte Teil der Dissertation beschäftigt sich mit der Kopplung von sequentieller Injektionsanalyse (SIA) und Kapillarelektrophorese (CE). Die Möglichkeit von SIA, automatisiert Analyten und Reagenzien zu mischen, chemische Reaktionen und/oder Anreicherungs-schritte durchzuführen, wurde in dieser Arbeit eingesetzt, um die Analyten kurz vor der CE-Trennung zu modifizieren. Die Fähigkeit eines SIA-Systems, durch die Spritzenpumpe Druck in einem Fließsystem auszuüben, wurde zur automatisierten hydrodynamischen Injektion in die Kapillare verwendet. Zur vollständigen Automation der Kopplung wurde in dieser Arbeit Software entwickelt, um die Hochspannungsquelle und den UV-Detektor anzusteuern. Dadurch war eine komplette Automatisierung aller Schritte erreicht. Die analytischen Parameter der Kopplung zwischen SIA und CE wurden anhand der Injektion und Trennung von Adenosin und Adenosinmonophosphat charakterisiert. Dabei wurden eine Standardabweichung im einstelligen Prozentbereich und eine Nachweisgrenze im unteren ppm-Bereich gefunden. Die Möglichkeiten von SIA wurden eingesetzt um verschiedene Konzentrationen von Natriumdodecylsulfat (SDS) automatisiert herzustellen und mit Myoglobin zu mischen. SDS ist ein bekanntes Reagens zur

Denaturierung von Proteinen. Nach erfolgter Mischung wurde Myoglobin in die Kapillare injiziert und mittels Kapillarelektrophorese getrennt. Die Ergebnisse zeigen die verschiedenen entstandenen Konformationen von Myoglobin, abhängig von der Konzentration von SDS.

## ABSTRACT

The goal of this work was the development of automated flow systems for microfluidic analysis using mid-IR detection.

The first part deals with the further development of a micro flow cell for online MIR detection of proteins and their secondary structures. An infrared transparent flow cell structured with the epoxy polymer SU-8 was coupled between two capillaries. In the flow cell the IR detection took place. In this work a new cell holder was developed where the capillaries were attached to flow cell using O-rings. The proteins myoglobin,  $\alpha$ -lactalbumin and  $\beta$ -lactoglobulin were used in this study as they show different secondary structures. The separation of the proteins was carried out in uncoated capillaries with an inner diameter of 50  $\mu\text{m}$  and the buffer used was borax with a pD of 9.2. The strong absorption of water at 1640  $\text{cm}^{-1}$  was shifted down to 1210  $\text{cm}^{-1}$  and thus the analysis of the amide I band became possible when measuring in  $\text{D}_2\text{O}$ . A comparison of the separation as detected with UV-Vis and infrared detection showed that the inclusion of the micro flow cell did not have an influence on the separation itself. The spectra taken online were compared with reference spectra and showed a good agreement.

In the second part a capillary electrophoresis (CE) chip was developed in cooperation with the institute for Industrial Electronics and Material Science and was used at the synchrotron ANKA (Karlsruhe, Germany). Synchrotron radiation possesses a very high brilliance compared to conventional light sources, which becomes relevant in measurements where the IR beam is focussed below 50  $\mu\text{m}$ . Therefore analysis in very small detection volume is possible, which gets important for sharp peaks as in CE. In this work a CE chip made of  $\text{CaF}_2$  and the polymer SU-8 was developed. This development was necessary as the usual materials used for micro chips strongly absorb infrared light. The channel on the chip was 100  $\mu\text{m}$  broad and 10  $\mu\text{m}$  high, which is equal to the optical path length and was mounted in a dedicated Perspex holder. The functionality of the chip was tested with the inorganic ions sulfate and nitrate, which both show strong absorption bands in the infrared. Furthermore, the chip was tested with



myoglobin, because the protein moves slower inside the chip due to its higher diffusion constant. Both applications were studied to assess the potential of synchrotron radiation for microfluidic applications. The obtained results show that for such applications the noise found at the IR beamline of the synchrotron is at the moment still high due to technical reasons.

The last part of this dissertation deals with the coupling of sequential injection analysis (SIA) and capillary electrophoresis (CE). The ability of SIA to automatically mix analytes and reagents, carry out chemical reactions and/or preconcentration steps, was used in this work to modify the analyte shortly before separation inside the CE system. The possibility of a SIA system to pressurize a flow system using its syringe pump was applied to automated hydrodynamic injection into the capillary. For the complete automatization of the hyphenated system software to control the high voltage power supply and the UV detector was developed in this work. Using this software all steps were completely automated. The figures of merit of this system were assessed based on the injection and separation of adenosine and adenosine monophosphate. A standard deviation in the single-digit percentage range and a limit of detection in the low ppm-range was found. The possibilities of SIA were applied to prepare different concentrations of sodium dodecyl sulfate (SDS), a known denaturing agent for proteins, automatically and mix them with myoglobin. After the mixing myoglobin was injected into the capillary and separated with CE. The results show the differently formed conformations of myoglobin, depending on the concentration of SDS.

## ACKNOWLEDGEMENT

I want to thank my supervisor *Bernhard Lendl* who always helped me in situations where things went wrong. He was not only a supervisor but also a friend to count on in difficult private situations.

A big thank you goes to all co-operation partners contributing to this work: *Peter and Edda Svasek* from the Institute of Industrial Electronics and Material Science, who have skilfully built the microfluidic devices and made this project possible; *David Moss* who helped me during my stay at the synchrotron in Karlsruhe, *Ullrich Schade* who gave me deep insights into the operation principles of a synchrotron in Berlin and *Ersilia de Lorenzi* and *Stefania Sabella* in whose lab in Pavia my views about capillary electrophoresis were extended.

The CAVS team always was the place for good ideas, help, fun and more than once my work without their suggestions and their experience would not have gone this way finally. I want to thank *Nina Kaun*, *Wolfgang Ritter*, *Stefan Schaden* and *Johannes Schnöller*, but not to forget our international members as *Guillermo Quintas Soria*, *Ana Dominguez Vidal* and *Mercedes Lopez Pastor* and of course *Josefa Rodriguez Baena*. The former group members who laid the foundation of this work, *Peter Hinsmann* and *Michael Haberkorn* need to be mentioned here as well. I also want to thank all former group members and guests who gave the working group its multicultural flair.

The help of *Johannes Frank* who was always there when strange ideas need to be converted into a practical tool and to *Markus Schaufler* who took care of all wiring, built the electronic devices needed and kept the spectrometer running. Thanks also go to all members of the institute, mainly to the head of the institute professor *Hans Puxbaum*.

Financial support for this work provided by Austrian Science Fund (FWF) within the project P 15531 ÖCH is gratefully acknowledged.

I want to thank *Christian Sperger* who helped me through my first time of this work and who never grew tired listening to me in all matters and all others who endured me in times of bad mood and stress.

Last, but definitely not least I want to thank my family who always supported me.

## TABLE OF CONTENTS

<b>1</b>	<b>INTRODUCTION</b>	<b>1</b>
1.1	Fourier transform infrared spectroscopy	1
1.2	FT-IR spectroscopy in aqueous solution	6
1.3	Synchrotron Radiation	9
1.4	Protein Structure	14
1.5	Flow systems	19
1.6	Capillary Electrophoresis	21
1.7	Miniaturised flow systems	25
1.8	Microstructuring Strategies	26
<b>2</b>	<b>FT-IR DETECTION IN CAPILLARY ELECTROPHORESIS FOR PROTEINS</b>	<b>28</b>
2.1	Detection methods in capillary electrophoresis	28
2.2	Interface for on-line FT-IR detection in CE	29
2.3	Applications for protein samples	31
2.4	Conclusions and Outlook	35
<b>3</b>	<b>INFRARED SYNCHROTRON RADIATION FOR MICRO-CHIP BASED ANALYSIS</b>	<b>36</b>
3.1	Production of the micro-chip	36
3.2	FT-IR spectrometer and synchrotron source	38
3.3	Results and Discussion	39
3.4	Conclusions and Outlook	43
<b>4</b>	<b>SEQUENTIAL INJECTION (SI)-CAPILLARY ELECTROPHORESIS SYSTEM FOR AUTOMATED SAMPLE PREPARATION AND SEPARATION</b>	<b>44</b>
4.1	Development of the software	44
4.2	SIA-CE interface	46

4.2.1	Test of the SIA-CE system	48
4.2.2	Application to myoglobin and sodium dodecyl sulfate	49
4.3	Conclusion and Outlook	50
<b>5 REFERENCES</b>		<b>52</b>
<b>6. APPENDIX</b>		
	Publication I	56
	Publication II	73
	Publication III	80
	Publication IV	101
	Curriculum vitae	126

## LIST OF PUBLICATIONS

- I** Kulka, S.; Lendl, B. “*On-line capillary electrophoresis FT-IR detection for the separation and characterization of proteins*” submitted publication.
- II** Kulka, S.; Kaun, N.; Baena J.R.; Frank, J.; Svasek, P.; Moss, D.; Vellekoop M.J.; Lendl, B. “*Mid-IR synchrotron radiation for molecular specific detection in microchip-based analysis systems*” *Analytical and Bioanalytical Chemistry* **2004**, 378 , 1735-1740.
- III** Kulka, S.; Quintas, G.; Lendl, B. “*Automated sample preparation and analysis using a sequential-injection (SI)-capillary electrophoresis (CE) interface*” submitted publication.
- IV** Kulka, S.; Lendl, B. “*Vibrational spectroscopic detection in capillary electrophoresis (CE)*”. in “*Analysis and detection by capillary electrophoresis*”, eds. Marina, M.L; Rios, A.; Valcarcel, M., Elsevier: Amsterdam, 2005
- V** Kaun, N.; Kulka, S. ; Frank, J.; Schade,U.; Vellekoop, M.J.; Harasek, M. and Lendl, B. “*Towards Biochemical reaction monitoring using FT-IR Synchrotron radiation*” accepted paper

## LIST OF ABBREVIATIONS

<b>ADC</b>	analogue-digital converter
<b>ANKA</b>	Anionenquelle Karlsruhe
<b>ATR</b>	attenuated total reflection
<b>BGE</b>	background electrolyte
<b>CE</b>	capillary electrophoresis
<b>CVD</b>	chemical vapour deposition
<b>EOF</b>	electroosmotic flow
<b>FIA</b>	flow injection analysis
<b>FIR</b>	far infrared
<b>FT-IR</b>	Fourier transform infrared
<b>HPLC</b>	high pressure liquid chromatography
<b>IP</b>	internet protocol
<b>IR</b>	infrared
<b>MCT</b>	mercury cadmium telluride
<b>MEKC</b>	micellar elektrokinetic chromatography
<b>μTAS</b>	micro total analysis system
<b>RSD</b>	root square deviation
<b>SI</b>	sequential injection
<b>SIA</b>	sequential injection analysis
<b>SDS</b>	sodium dodecyl sulfate
<b>TCP</b>	transfer control protocol
<b>UHV</b>	ultra high vacuum
<b>UV</b>	ultraviolet
<b>UV-Vis</b>	ultraviolet-visible

In the context of this work only mid-infrared light (wavelength 2.5 – 25  $\mu\text{m}$ , wavenumbers 4000 – 400  $\text{cm}^{-1}$ ) was used.

In an infrared spectrum different kind of information can be obtained. The structural information derived from an infrared spectrum may indicate specific functional groups depending on their band position as described in equation 1. However, the whole spectrum, especially the fingerprint area below 1500  $\text{cm}^{-1}$  can be used for the identification of unknown samples when compared to reference spectra collected in a library. Applying the law of Lambert-Beer (equation 2) quantitative analysis in infrared spectroscopy can be performed.

$$A = \varepsilon * c * d \qquad \text{Equation 2}$$

where A is the absorbance,  $\varepsilon$  the substance-specific molar absorptivity, c the concentration of the sample and d the optical pathlength of the cell. Increasing the concentration allows the preparation of a calibration curve which can be applied to the samples of unknown concentration. The same procedure can be carried out for sample mixtures if a multivariate calibration based on different spectral features is feasible. Another kind of information often overlooked does not depend on the concentration of one or a few analytes but lies again in the spectral features. Using infrared spectroscopy latent variables and their changes due to chemical processes, like the viscosity or the octane number can be studied again using multivariate models.

Infrared spectra are obtained in a non-destructive way and no labelling is required being an advantage compared to other analytical techniques like fluorescence or mass spectrometry. However, as the absorptivity in the mid-IR is low, the sensitivity of infrared spectroscopy is lower than in other common detection techniques. Therefore IR spectroscopy generally is not considered to be a trace analysis technique.

There are two types of infrared spectrometers available. The older type is the dispersive IR spectrometer, the more modern are Fourier transform infrared spectrometer (FT-IR). In both cases the IR radiation is emitted from a continuous light source. The most often used light source is a globar, a rod made out of

silicon carbide heated electrically reaching a temperature of about 1500 Kelvin. This light source can be described using Planck's law characterising a blackbody<sup>1</sup>

$$U_{\tilde{\nu}}(T) = \frac{C_1 \tilde{\nu}^3}{e^{C_2 \tilde{\nu}/T} - 1} \quad \text{Equation 3}$$

Where  $C_1$  and  $C_2$  are the first and second radiation constants, having the values

$$C_1 = 1.191 \cdot 10^{-12} \text{ Wcm}^{-2}\text{sr}^{-1}(\text{cm}^{-1})^4$$

$$\text{and } C_2 = 1.439 \text{ Kcm}$$

In equation 3 the influence of temperature and wavenumbers on the spectral intensity can be clearly seen. Higher temperatures lead to a higher emission power but also to a shift of the emission maximum to shorter wavenumbers, thus for obtaining energy in the mid-IR range the temperature of the globar is set to 1200-1500 K as a compromise.

The basic principle of an FT-IR spectrometer is depicted in Figure 1. Infrared light is emitted from a continuous light source (globar) and is split at the beamsplitter in two parts. One light beam hits a fixed mirror, while the other beam travels to the moveable mirror. The light from both mirrors unite again at the beamsplitter and are sent to the detector. The principle of an interferometer lies in the different distances the light coming from the moveable mirror needs to travel, denoted retardation of the light  $\delta$ . Therefore different interference patterns depending on the position of the moveable mirror are formed. In case of  $\delta$  of 0 or  $\lambda$  (and multiples) the interference is constructive and for  $\lambda/2$  (and multiples) it is destructive. The interferogram shows the relation between the retardation and the intensity in the time-domain. In a mathematical operation, a Fourier transformation the spectrum relating the frequency (in IR wavenumbers are more common) to the intensity is obtained, thus being the frequency-domain. An interesting characteristic of Fourier transformation is that a peak having a small width in one domain becomes very broad in the other. The typical example is a



single line from a monochromatic light source in the frequency domain (spectrum) which is a cosine wave in the interferogram.

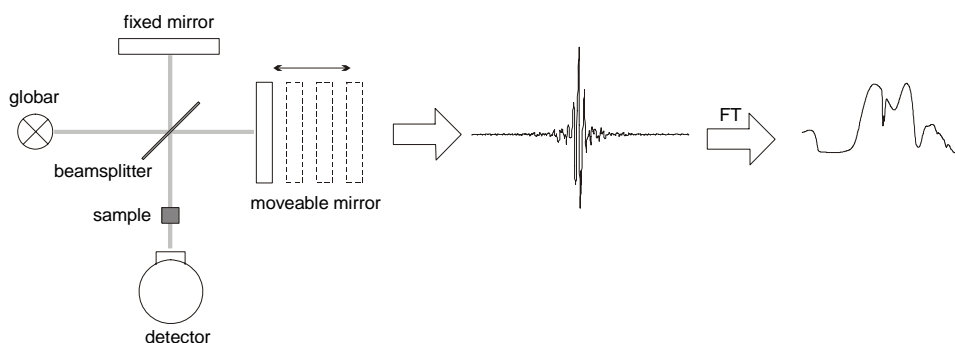


Figure 1 Scheme of spectra acquisition with an FT-IR spectrometer

From a practical point of view the interferogram which should be recorded until infinity needs to be cut off. There are various apodisation functions (e.g. a boxcar) available which are multiplied with the measured interferogram and then the Fourier transformation of the modified interferogram is calculated. In a real spectrometer the analog data coming from the detector needs to be digitized using an analog-digital converter (ADC). For a correct conversion the sampling rate of the analog function has to be at least  $2 \cdot \nu_{\max}$  (Nyquist theorem). This implies that the bandwidth of the function to be digitized needs to be known before. If the sample rate is too low for some frequencies they can be folded into the region of the desired bandwidth giving unwanted artifacts. Therefore filters are employed in infrared spectroscopy to reduce the bandwidth of the globar to prevent aliasing features.

Dispersive instruments (Figure 2) are equipped with monochromators in order to select radiation of a certain wavelength to reach the detector meaning that only a fraction of the whole intensity is passed through the sample. By scanning the whole wavenumber range of interest the spectrum is obtained. The IR light is sent

through a resizable slit depending on the desired spectral resolution, thus decreasing the light intensity even more.

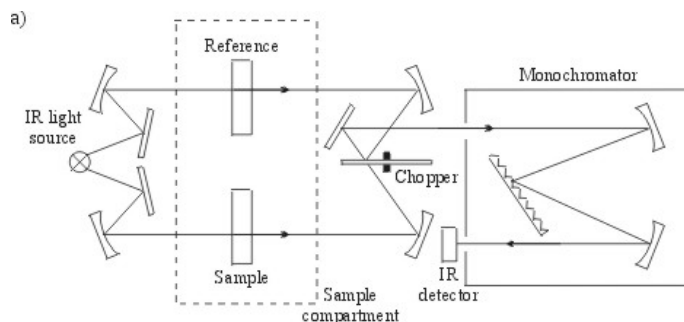


Figure 2 Scheme of a dispersive IR spectrometer

The advantages of FT-IR spectrometers compared to dispersive instruments can be summarised as follows<sup>1</sup>:

- **Multiplex-Advantage ( Fellgett-advantage):**  
FT spectrometers provide higher sensitivity and shorter measurement time due to the simultaneous detection of all spectral frequencies.
- **Throughput-Advantage (Jacquinot-advantage):**  
As FT instruments are constructed without any slits, the intensity reaching the detector is significantly higher than in the case of dispersive spectrometers which require slits to limit the detected wavenumber range in order to achieve the desired spectral resolution.
- **Calibration-Advantage (Connes-advantage):**  
In contrast to dispersive instruments where a reference material is required to calibrate the frequencies, FT spectrometers do not need to be calibrated in this respect as the retardation of the mirror is determined with the help of a helium-neon (He-Ne) reference laser with an exactly known constant wavelength of  $0.632817 \mu\text{m}$  ( $15802 \text{ cm}^{-1}$ ).

The multiplex- and throughput-advantage of FTIR spectrometers result in an improved signal to noise ratio, which is about 100 times better than for dispersive instruments, and therefore basically only FT-IR instruments are in use nowadays.

## 1.2 FT-IR spectroscopy in aqueous solution

The main difficulty using infrared spectroscopy in aqueous solution lies in the strong absorption of water itself. H<sub>2</sub>O has two main regions of absorbance, namely the bending vibration, which is located around 1640 cm<sup>-1</sup> and the stretching vibration absorbing strongly in the entire region between 3600 and 3000 cm<sup>-1</sup> (see Figure 3). At 2125 cm<sup>-1</sup> a combination band of the bending and libration mode can be found. The low intensity below 1000 cm<sup>-1</sup> comes from the strong absorption of the CaF<sub>2</sub> window of the flow cell. At 686 cm<sup>-1</sup> the libration mode of water can be found (not shown).

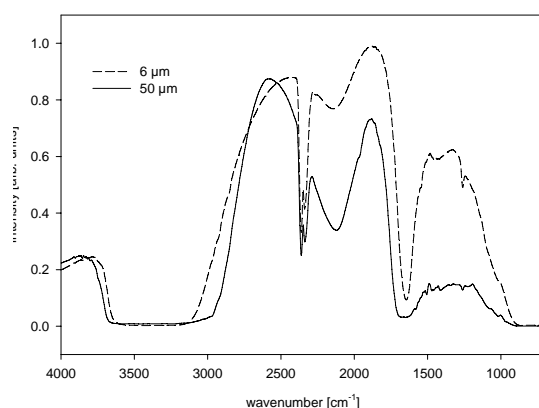


Figure 3. Single channel transmission spectrum of water in a flow cell with 6 μm and 50 μm

As can be seen in Figure 3, the absorption of water can become so high that the light in this region gets blocked nearly completely, thus analysis of samples absorbing in this region is impossible due to lacking light intensity arriving at the detector and the resulting high noise in this region. Therefore, for carrying out measurements in aqueous phase flow cells with a path length below 8 μm have to be used in this region to ensure enough light throughput and therefore an acceptably low noise level.

Widely used when measuring aqueous solutions is attenuated total reflection (ATR) infrared spectroscopy. This technique is based on the principle that light travelling in a material having a higher refractive index  $n_1$  penetrates a fraction of a wavelength into the material with a lower refractive index  $n_2$  (Figure 4).

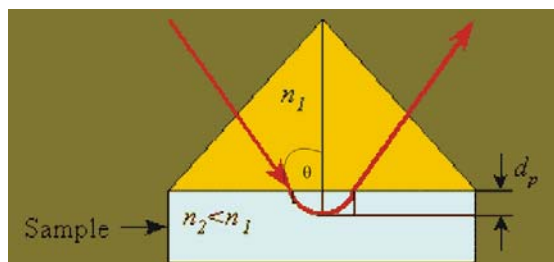


Figure 4 View of an ATR crystal

The depth of penetration ( $d_p$ ) of the evanescent wave is defined as the distance from the crystal-sample interface where the intensity of the evanescent decays to  $1/e$  (37%) of its original value. From Equation 4 the depth of penetration depending on the wavelength of the incident light  $\lambda$ , the angle of the incident light and the refractive indices of the ATR material and the sample can be calculated.

$$d_p = \frac{\lambda}{2 * \pi * n_1 * \sqrt{(\sin^2 \theta - (n_2 / n_1)^2)}} \quad \text{Equation 4}$$

Where  $n_1$  is the refractive index of the ATR crystal,  $n_2$  is the refractive index of the rare medium (function of wavelength) and  $\theta$  is the angle of incidence. The penetration depth is about 2-3  $\mu\text{m}$  at 2000  $\text{cm}^{-1}$ .

As another option, heavy water ( $\text{D}_2\text{O}$ ) can be used as a solvent instead of water, shifting the strong absorption at 1640  $\text{cm}^{-1}$  to 1210  $\text{cm}^{-1}$ , thus enabling spectroscopy in the region of interest (see Figure 5). This strong change in the energy of the vibration (expressed in wavenumbers) can be explained due to the high mass difference between  $\text{D}_2\text{O}$  and  $\text{H}_2\text{O}$ .

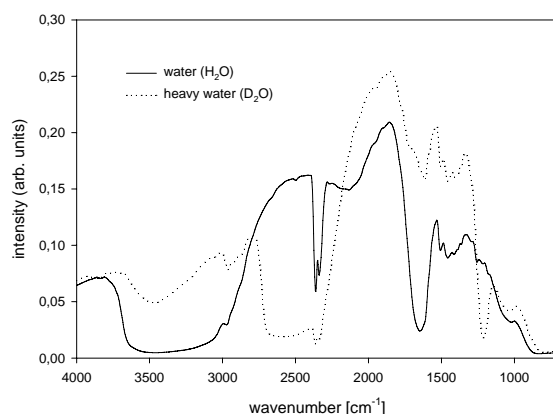


Figure 5 Single channel transmission spectrum of water and heavy water in a flow cell of 25  $\mu\text{m}$

Taking spectra using the ATR technique is simple and allows measurements in water. However, due to the small optical path realised the sensitivity of this method is lower than when using a transmission cell. Especially when using biochemical samples like proteins, interactions with the surface of the ATR unit can lead to structural changes of the analytes and to an unwanted coating of the surface difficult to be removed again.

Measurements in a transmission cell using  $\text{D}_2\text{O}$  allow higher optical path lengths and therefore better sensitivity. As the optical path length in a transmission cell is larger than in the case of an ATR crystal interaction of the sample with the surface leads to less loss of throughput and thus deposition of analytes onto the surface poses fewer problems in a transmission cell. However, the use of  $\text{D}_2\text{O}$  brings difficulties like the formation of HDO due to proton exchange with the sample giving a very strong band centered at  $1450\text{ cm}^{-1}$ . Besides handling of heavy water needs to be carried out carefully and with caution as it is hygroscopic. The normal procedure of handling  $\text{D}_2\text{O}$  is to work in a glove box which was purged with dry air before and to seal all flasks containing solutions with  $\text{D}_2\text{O}$ , thus fairly increasing the complexity of the sample preparation. The choice of the technique therefore depends strongly on the system to be analysed and the restrictions it applies.

### 1.3 Synchrotron Radiation

Synchrotron radiation is electromagnetic radiation generated by electrons moving nearly as fast as light through magnetic fields. The synchrotron radiation is a relativistic quantum effect as the radiation pattern shows a much smaller angular spread  $\Theta$  than in the case of a non-relativistic particle (Figure 6)<sup>2</sup>

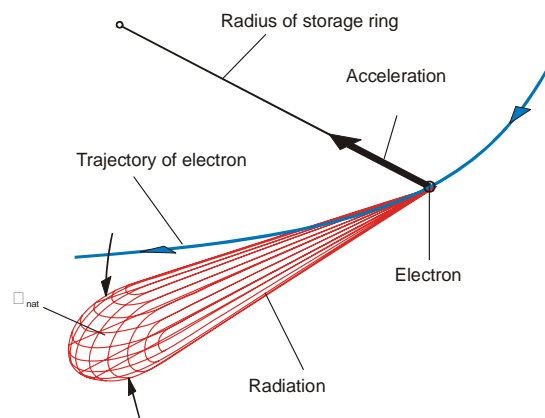


Figure 6 Generation of synchrotron radiation

Technically synchrotron radiation is generated by a diode gun in the so-called microtron where the electrons are accelerated as the synchrotron is not able to speed up stationary electrons. Then the electrons are injected into the synchrotron, a small ring where the electrons are induced to move nearly as fast as light. Finally the electrons are transferred into the storage ring where the synchrotron radiation is emitted when passing magnets. A schematic view of a synchrotron source is shown in Figure 7 where it can be seen that the synchrotron light gets guided out of the storage ring at the position of the magnets (at the so-called beamlines). Synchrotron light contains all frequencies from X-ray to FIR.

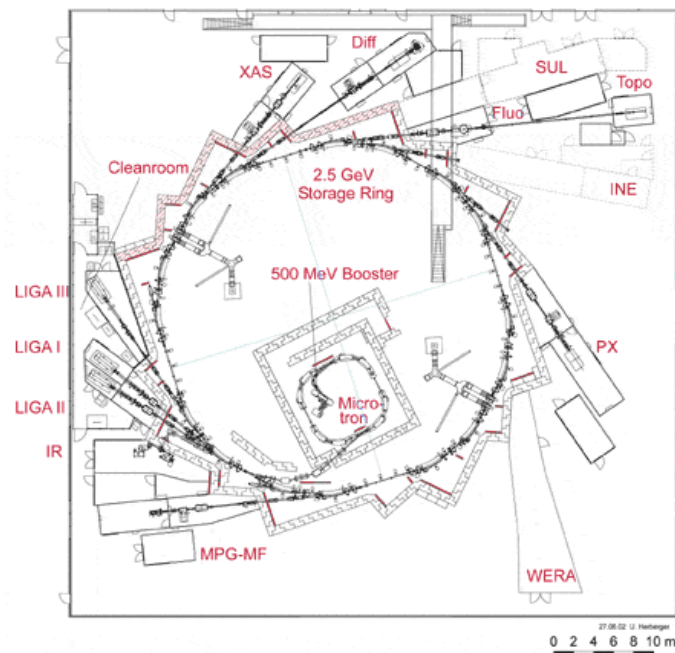


Figure 7 Schematic view of a synchrotron source including beamlines

Inside the storage ring ultrahigh vacuum (UHV) ensures that the electrons only lose their energies upon collision onto the wall or into themselves so that the energy of the beam only decays slowly. In the case of the IR beamline a CVD diamond window between the storage ring and the IR spectrometer shields the UHV of the storage ring from the experimental setup at the beamline. As CVD diamond is only transparent from UV (225 nm) to the FIR the light passing this window can be focussed directly with the help of mirrors into the spectrometer (Figure 8).

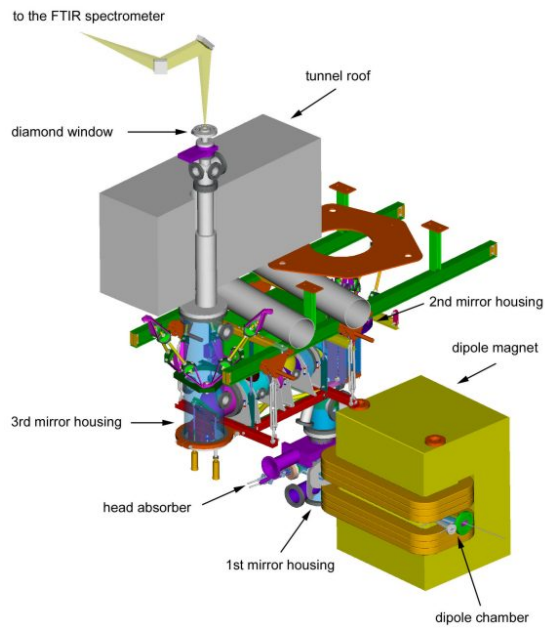


Figure 8 Mechanical and vacuum layout of the IR beamline

The characteristics of synchrotron IR radiation are<sup>3</sup>:

- High brilliance, exceeding other natural and artificial light sources by many orders of magnitude
- High collimation, i.e. small angular divergence of the beam
- Low emittance, i.e. the product of source cross section and solid angle of emission is small
- High level of polarization (linear or elliptical)
- Pulsed light emission (pulse durations at or below one nanosecond)

Brilliance is defined as the amount of photons per area, solid angle and time counted in a defined wavelength range as defined in Planck's law (Equation 3). Together with intensity and divergence it defines the quality of a light source. As can be seen in Figure 9 the difference in brilliance between typical synchrotron sources and a 1200 K blackbody representing a conventional light source in infrared spectroscopy is at least a factor of 1000.



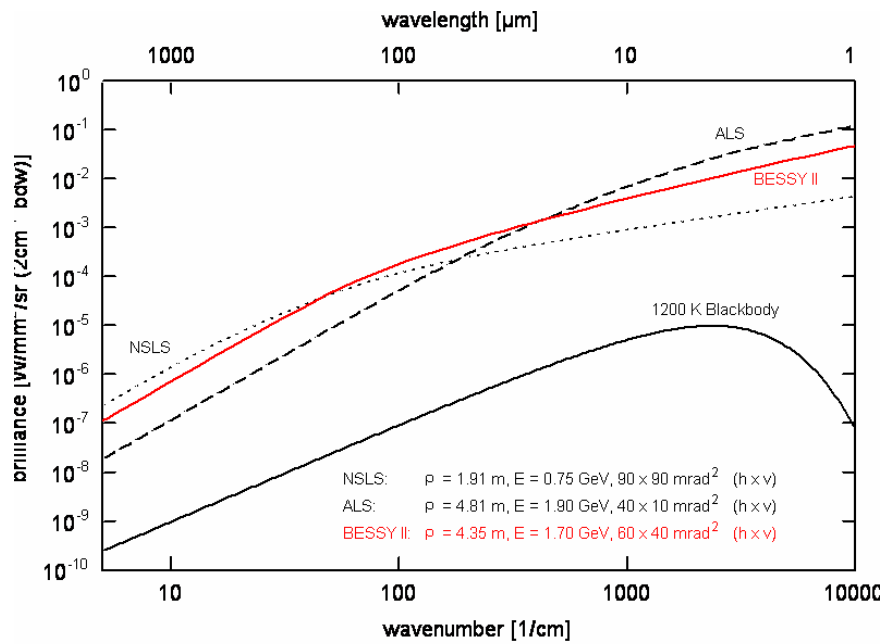


Figure 9 Comparison between synchrotron light and a blackbody<sup>4</sup>

Using the higher brilliance of the synchrotron allows analysing smaller samples as there the losses going to smaller apertures are lower than compared to a conventional light source (Figure 10).

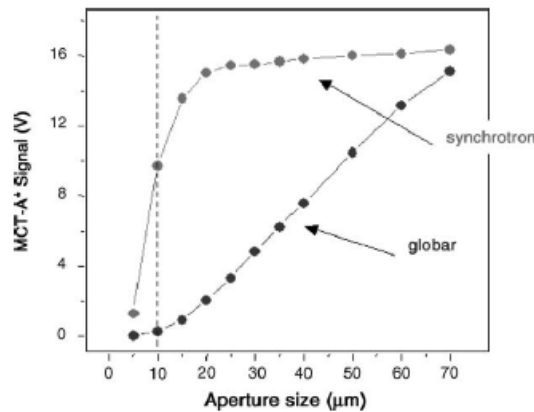


Figure 10 Comparison between globar and synchrotron depending on aperture size<sup>5</sup>

This either makes analysis of smaller samples like single cells possible, or analysis of larger samples with a higher spatial resolution. However, in all applications the diffraction limit of light needs to be considered, with a single objective it lies around  $2\lambda/3$  and with a confocal microscopes where objectives are

placed before and after the sample the spatial resolution can be increased to  $\lambda/2$ .<sup>3</sup> Typical examples of spatial resolutions depending on the wavenumber and the optic setup can be found in table 2.

Wavenumber	4000 cm <sup>-1</sup>	500 cm <sup>-1</sup>
Single objective	1.7 $\mu\text{m}$	13 $\mu\text{m}$
Confocal microscope	1.25 $\mu\text{m}$	10 $\mu\text{m}$

Table 2 Comparison between optic setups and spatial resolution depending on the wavenumber<sup>3</sup>

The small spot size possible due to synchrotron radiation allows the study of two different experimental setups. In the case of a continuous-flow mixer as described in Hinsmann where two flow sheets are superimposed the reaction going on can be monitored in more detail if the spot size when following the mixing channel is as small as possible. In the case of a CE chip the smaller spot size enables the detection of sharper peaks, thus lower dilution can be obtained using synchrotron light. In this work a CE chip was studied. As Figure 11 shows the noise obtained in a synchrotron is even better when an aperture of 100  $\mu\text{m}$  is used. However, the noise produced by the synchrotron due to inherent technical issues is still too high for obtaining spectra with a sufficient signal-to-noise ratio to study complex (bio)chemical processes.

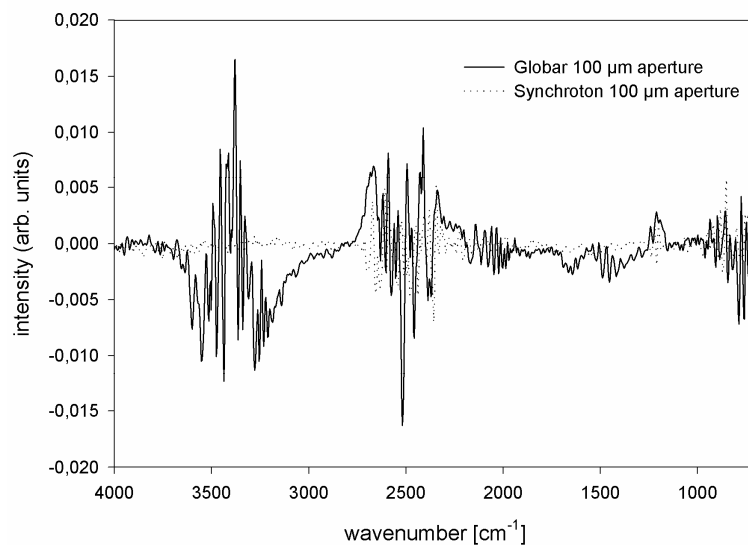


Figure 11 Comparison of noise between a globar and synchrotron light

## 1.4 Protein Structure

The biochemical function of a protein is defined through its structure. The simplest structure is the chain of amino acids, called primary structure. However, this structure does not exist in organisms as proteins form three-dimensional structures. The building blocks of these structures are the  $\alpha$ -helix, the  $\beta$ -strands and  $\beta$ -turns, being the most important secondary structure elements. The sterical arrangement in space is governed by the amino acids themselves as the peptide bond is quite rigid as it has partial double bond character. The two angles  $\phi$  and  $\psi$  define the rotation around the plane of the bond. The angle  $\phi$  is a measure for the rotation of the N-C<sub>a</sub> bond and  $\psi$  for C-C<sub>a</sub> (see Figure 12).

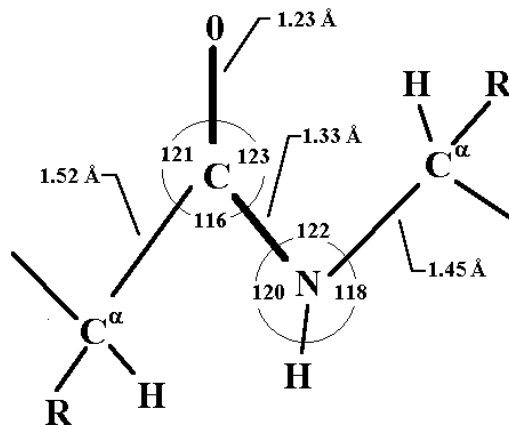


Figure 12 View of the bond angles and length of the peptide bond<sup>6</sup>

The so-called Ramachandran plot is a diagram showing the statistical distribution of the two angles for a protein molecule or a class of proteins (Figure 13)

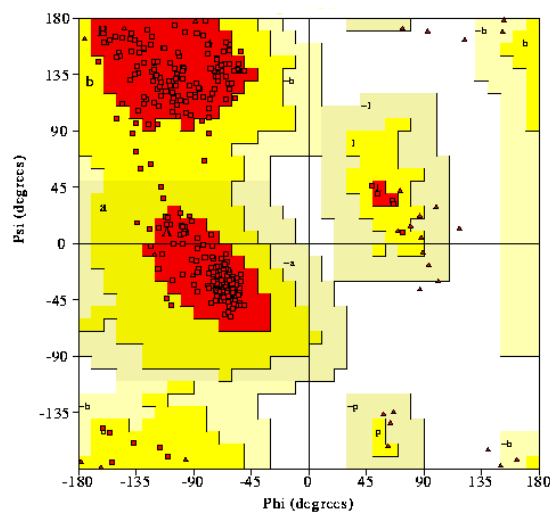


Figure 13 Ramachandran plot showing possible combinations of angles  $\phi$  and  $\psi$

Depending on the angles existing in a protein different motifs can be distinguished. These motifs can be found together in the same protein molecules. In the alpha-helix the amino acids are arranged in a right-handed helical structure achieving a turn every 3.6 amino acid residues. The  $n^{\text{th}}$  oxygen from the carbonyl bond forms a hydrogen bond with the  $(n+4)^{\text{th}}$  hydrogen of the same molecule (see

Figure 14). This motif is tightly packed and looks like a cylinder, also used as a symbol for alpha-helices when describing proteins.

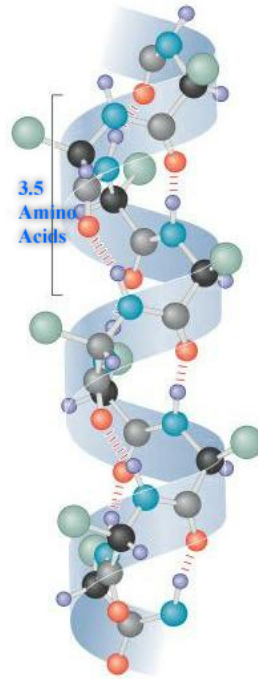


Figure 14 View of a  $\alpha$ -helix

The  $\beta$ -sheet (also  $\beta$ -pleated sheet) consists of two or more amino acid sequences within the same protein that are arranged adjacently and in parallel, but with alternating orientation such that hydrogen bonds can form between the two strands (see Figure 15). The N-H group of strand forms hydrogen bonds with the C=O groups of the adjacent strand. Therefore the anti-symmetric form of this motif is more stable and thus more common than the symmetric form as in this conformation the hydrogen bonds do not have the same strength as in the anti-symmetric conformation.

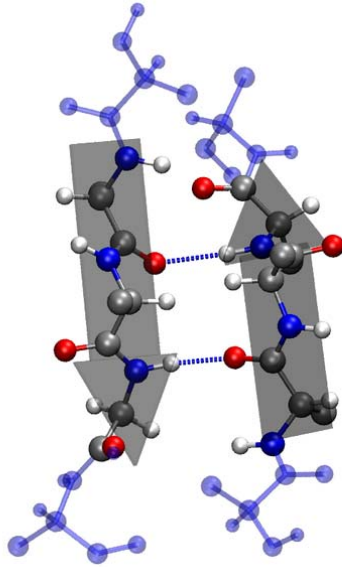


Figure 15 View of an antisymmetric  $\beta$ -sheet

Another motif are the  $\beta$ -turns connecting the other secondary structures (mostly  $\beta$ -sheets). This motif is stabilised by a hydrogen bond of the  $n^{\text{th}}$  C=O group and the  $(n+3)^{\text{th}}$  N-H group. Very common  $\beta$ -turns can be found in changes of directions in the protein structure.

The tertiary structure defines the spatial arrangement of amino acids not as closely together as in the secondary form, so this structure defines the fold of a protein. Finally, when counting subunits of a protein formed by more than one polypeptide chain another structure, the quaternary structure can be defined.

Normally only proteins in their native state have a biological function, however there are partially unfolded/refolded states where proteins still have a biological role. Very often, though these non-native proteins are the cause for illnesses. A typical example is the class of proteins, which upon partially unfolding form plaques and these plaques are the cause of amyloidosis responsible for diseases like Alzheimer or Parkinson.<sup>7</sup> Therefore, the study of proteins and their folding processes receives more and more attention as the role between folded state and biological role is still not fully understood.

Infrared spectroscopy is a valuable tool for studying protein structures and their changes as the band positions indicating the secondary structure elements are

variable due to different hydrogen bond strength. The characteristic IR bands of the peptide bond are listed in the table below.

Amide band	Approximate wavenumber [ $\text{cm}^{-1}$ ]	Vibrational mode
A	~3300	NH stretching in resonance
B	~3100	With 1 <sup>st</sup> amide II overtone
I	1610-1695	C=O stretching
II	1480-1575	N-H bending and C=N stretching
III	1220-1320	C=N stretching and N-H bending
IV	625-765	O=C-N bending, mixed with other modes
V	640-800	Out-of plane N-H bending
VI	535-605	Out-of-plane C=O bending
VII	~200	Skeletal torsion

Table 3 Characteristic IR bands of the peptide bond<sup>8</sup>

The most important vibration for assessing the secondary structure is the amide I band<sup>9</sup> as it is the most intense. However, there are reports where the amide II and III have been used to infer the secondary structure<sup>10,11</sup>. In this work only the amide I was studied. The assignment of band positions to certain structure elements is still not completely elucidated, though much is already known. Typical values for the most important protein structures are summarised in table 4.

Structure element	Wavenumber [ $\text{cm}^{-1}$ ]
$\alpha$ -helix	1640-1662
$\beta$ -sheet	1622-1640
$\beta$ -turn	1660-1690

Table 4 Band positions for secondary structure elements<sup>6</sup>

Measurements in heavy water ( $\text{D}_2\text{O}$ ) not only allow higher path length due to less absorption in the area of the protein bands, but also enables to study the rate and

extent of the exchange of N-, O- and S-bound protons. These exchange rate depend on the global and local accessibility and the  $pK_a$  value and thus giving information about the protein structure as a whole<sup>12</sup>. The deuterated amide bonds are denoted amide I' and amide II' and so on. A general problem when using  $D_2O$  is that HDO overlaps the amide II' band. When working in  $D_2O$  the position of all bands changes, the shift being largest in the case of acidic hydrogen atoms like in N-H (amide II). This has to be considered when changes in band position due to external effects, like temperature or chemicals are studied.

When analysing proteins the different structure elements can be contained in the same molecule, thus giving an average in the band position in the IR spectrum. So far, there are two approaches to tackle this issue. One is based on curve fitting, where input parameters, like the number of component bands and their positions are chosen and then the analysis is performed based on different algorithms. The method looks promising, but the question how to choose the input parameters remains difficult.<sup>13</sup> A complete different approach is taken by pattern recognition, where IR spectra of proteins with a known structure are used as a calibration matrix. In this context mathematical methods like partial least squares analysis or factor analysis are used. Although this method overcomes the bias inherent in peak-fitting methods, difficulties arise in getting the correct calibration matrix as still the function between IR spectrum and three-dimensional structure is not fully understood. Still under development are neural networks enhancing pattern recognition methods promising better recognition rates as more correct calibration matrices will be available.<sup>14</sup>

## 1.5 Flow systems

The idea behind flow systems is the automatization of liquid handling like sample preparation or reaction of the sample with reagent(s). Thus, the reproducibility and precision is increased and human errors mostly precluded. Besides, the sample throughput can be increased, coupled with a decrease in sample and reagent consumption and analysis time.



Flow injection analysis<sup>15,16</sup> (FIA) systems basically consist of a peristaltic pump providing a carrier flow, an injection valve through which the sample is injected into the stream and a detection unit (Figure 5a). The constituent of flow injection analysis is the injection in a non-segmented carrier stream achieving a controlled dispersion of the sample and a controlled timing. On the way to the detection system the sample can be modified passing different reactors and/or being mixed with reagents, thus enabling the detection system to retrieve the information sought.

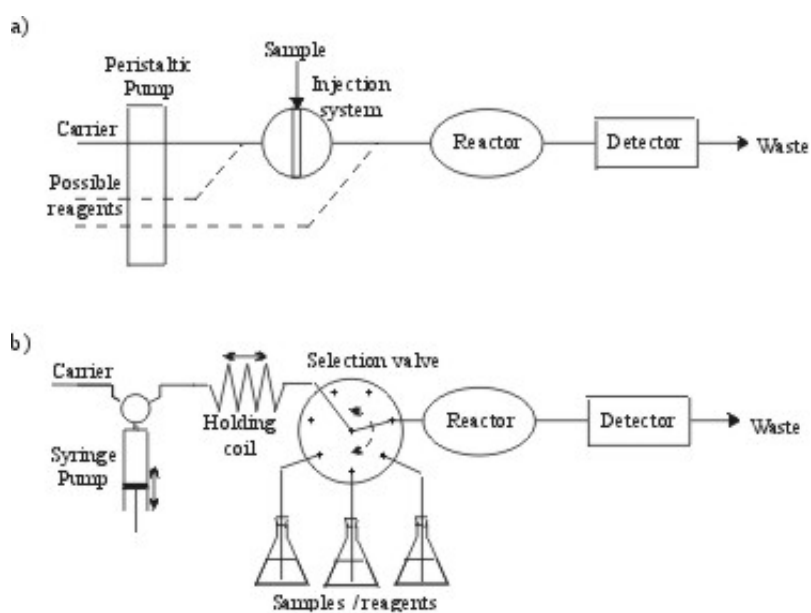


Figure 16 Schematic view of a) flow injection analysis system (FIA) and b) sequential injection analysis system (SIA)

Sequential injection analysis<sup>17,18</sup> (SIA, Figure 16b) systems represent the next level of system automation, as the whole experimental setup is fully computer controlled. Opposite to FIA, in SIA a syringe pump is used to aspire reagents and the sample via a selection valve and to stack them sequentially in a holding coil. Upon a flow reversal, the content of the holding coil is propelled towards the detection system. Again, similar modifications as described in the case for FIA can be carried out. Changes in flow rate and volume are accomplished by adjusting these values using the control computer, thus making the system very flexible in changing these experimental variables. Due to the ease of the setup SIA

systems are more robust than FIA systems. Due to the principle of flow reversal sample and reagent consumption are lower than in FIA, however the sample throughput is lower as well.

These flow systems can be combined with basically any detection system, like UV-Vis, fluorescence or infrared spectroscopy<sup>19</sup>, thus a wide range of analytical problems can be tackled using flow systems.

## 1.6 Capillary Electrophoresis<sup>20</sup>

Capillary electrophoresis (CE) is a separation technique based on differential electrophoretic mobilities of charged analytes under the influence of an externally applied electrical field. The velocity  $v$  of an ion can be expressed by

$$v = \mu_e E \quad \text{Equation 5}$$

where  $\mu_e$  is the electrophoretic mobility and  $E$  is the applied electrical field. The electrophoretic mobility can be defined as follows:

$$\mu_e = \frac{q}{6 \pi \eta r} \quad \text{Equation 6}$$

with  $q$  = ion charge,  $\eta$  = solution viscosity,  $r$  = ion radius. From this equation it is evident that the mobility increases with decreasing size and increasing charge of molecules.

However, there is another important constituent in capillary electrophoresis, the so-called electro-osmotic flow (EOF), the bulk flow inside the capillary. As the silanol groups at the capillary wall are charged negatively counterions build up near the surface to maintain charge balance forming a double-layer so that overall the whole area is electrically neutral. Close to the capillary wall there is a thin layer of liquid bound to the solid surface (rigid layer) showing an elastic behaviour compared to the bulk of the solution which is viscous (diffuse layer). Together these layers form a double-layer where the potential difference is formed, the so-called zeta potential (Figure 17). The zeta potential is the potential

at any given point in the double layer and decreases exponentially with increasing distance from the capillary wall surface.

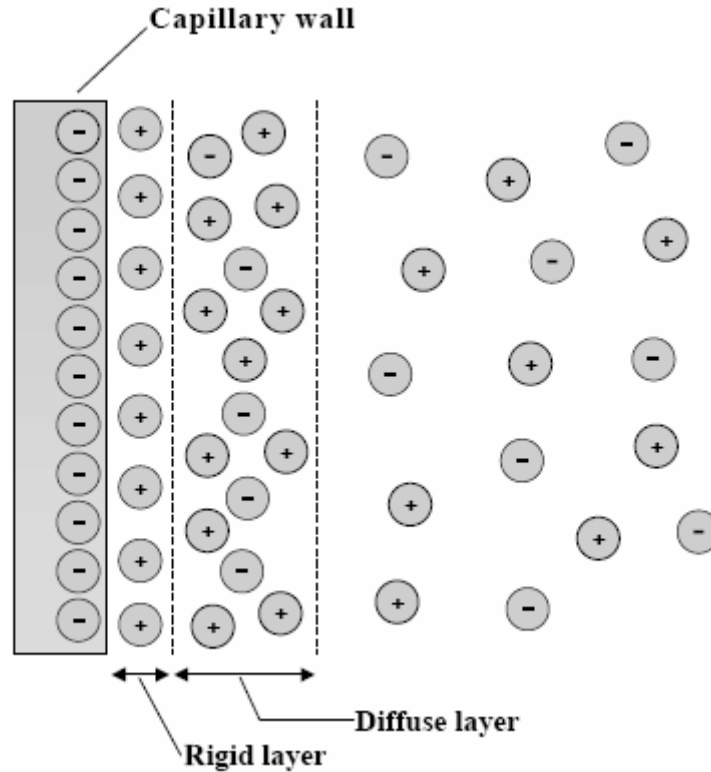


Figure 17 Formation of double layer and the resulting zeta potential

When a voltage is applied across the capillary, cations in the diffuse layer are free to migrate towards the cathode, carrying the bulk solution with them. (Figure 18).

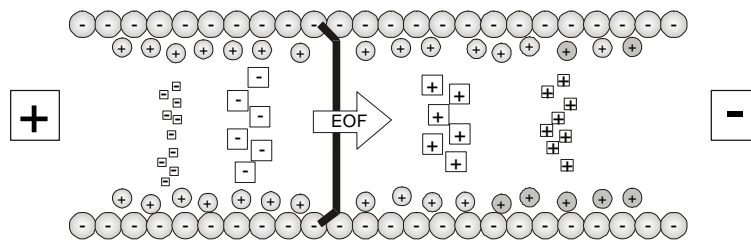


Figure 18 Direction of the EOF in an untreated capillary

The zeta potential is influenced strongly by the pH value of the electrolyte determining the amount of dissociated silanol groups, thus getting stronger the higher the pH value. Another strong modifier of the zeta potential is the ionic

strength of the electrolyte as it directly influences the double-layer as increased ionic strength results in a compressed double-layer. The magnitude of the EOF is expressed in terms of mobility:

$$\mu_{EOF} = \frac{\varepsilon\zeta}{\eta} \quad \text{Equation 7}$$

where  $\varepsilon$  is the electric permittivity of the liquid,  $\eta$  the viscosity of the liquid and  $\zeta$  the zeta potential.

The EOF shows a unique feature as it exhibits a flat flow profile because its driving force (i.e., charge on the capillary wall) is uniformly distributed along the capillary, which means that no pressure drops are encountered and the flow velocity is uniform across the capillary. In contrast to laminar flow as in HPLC, the flat flow profile does not directly contribute to dispersion of the solute zones.

Another benefit of the EOF is that it causes a net movement of nearly all species regardless of charge in the same direction as the magnitude of the EOF in most cases is much larger than the mobility of the ionic species. Hence, also anions will be flushed towards the cathode due to the influence of the EOF.

Most applications of CE so far have been separations of ionised species in aqueous solutions, although non-aqueous solvents are used for not water-soluble analytes<sup>21</sup>. Another mode of operation allows the separation of neutral analytes as a charged surfactant is added to the background electrolyte. The surfactant forms micelles into which the analytes are incorporated and thus moved towards the detector inside the micelle. In this work only capillary zone electrophoresis (CZE) in aqueous media was used.

In CE the separation is performed in narrow-bore fused-silica capillaries with an inner diameter typically between 25  $\mu\text{m}$  and 75  $\mu\text{m}$ . The electrical fields can be high (up to 300  $\text{Vcm}^{-1}$ ) as the large surface to volume ratio of the capillary allows efficient dissipation of the generated Joule heat. Instrumentation in CE is quite simple; a scheme of a typical CE set-up is depicted in Figure 19. The system consists of two buffer reservoirs, a high voltage power supply with electrodes and a fused silica capillary with the optical detection window. The capillary is filled with carrier electrolyte, sample is injected into the capillary by replacing one of

the buffer vials by the sample reservoir and applying either an electrical field or pressure. After replacing the sample vial with the buffer reservoir, high voltage (up to 30 kV) is applied and the separation performed.

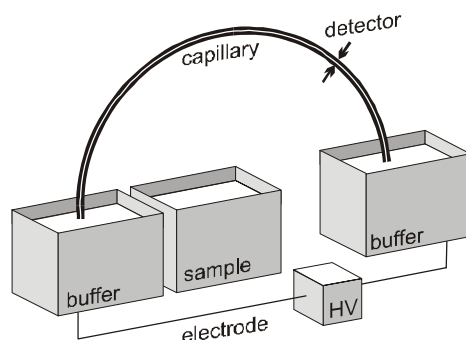


Figure 19 Scheme of a typical CE setup

Capillary electrophoresis attracted quite some interest over the last years mainly as the separation power of CE is higher than in HPLC. The reason is that due to the flat flow profile inside the capillary the radial diffusion can be neglected; only the longitudinal diffusion plays a role in solute-zone broadening. The plate number  $N$  in CE can be expressed as

$$N = \frac{\mu_e E l}{2D} \quad \text{Equation 8}$$

where  $\mu_e$  is the electrophoretic mobility (Equation 6),  $E$  the electric field,  $l$  the length of the capillary and  $D$  the diffusion coefficient. Various works have shown [ref.] that CE is superior to HPLC regarding selectivity, resolution and theoretical plate number, mainly in the field of protein analysis. However, as the inner diameter of a capillary is small compared to an average HPLC column and an untreated capillary shows surface charges, proteins and other macromolecules tend to stick to the wall. One approach to overcome this problem is coating of the capillary wall<sup>22,23</sup> reducing the electrostatic and covalent interactions between the samples and the walls. Still, these restrictions of CE make the use of highly concentrated sample solutions difficult, especially when dealing with macromolecules. Therefore, research is carried out to find on-capillary

preconcentration methods, like stacking<sup>24</sup> and sweeping<sup>25</sup> to prevent overloading of the capillary and still obtaining results having a satisfactory signal-to-noise ratio.

## 1.7 Miniaturised flow systems

In analytical chemistry the trend goes more and more to lower sample consumption, mainly in the field of biochemistry and pharmaceutical chemistry where samples can be very expensive or difficult to obtain in the desired quality. For some time already, miniaturised flow systems known by terms like “lab on a chip” or “micro total analysis system ( $\mu$ TAS)”<sup>26,27</sup> have been introduced in various fields. However, it is necessary to distinguish two different types of miniaturised flow systems<sup>28</sup>. In time-constant systems relevant time variables remain the same. A typical example is the downscaling of FIA where the only advantage lies in the lower carrier and reagent consumption. Therefore also less waste has to be disposed of. The same is valid for diffusion-controlled systems. However, reducing the size of the system leads a decrease in analysis time proportional to the square of the system size. Therefore the reduction in size leads to substantially lower analysis time and thus allows more separation in the same time leading to a higher sample throughput. Therefore “sensor-like” performance which enables parallel determination becomes possible with such miniaturised flow systems. A typical example here is capillary electrophoresis on a chip<sup>29</sup>. In this work this flow system was studied in more detail.

However, detection in microsystems is a challenge, since optical path lengths in the micrometer range drastically reduce the sensitivity of common detection methods like UV-Vis or fluorescence. As mid-IR detection is already confined to a small optical path length due to strong solvent absorption (see section 1.2), there is no loss of sensitivity upon miniaturization.

## 1.8 Microstructuring Strategies<sup>30</sup>

Nowadays two strategies for structuring small objects are available, the bulk and the surface micromaching. The bulk micromaching defines structures by selectively etching inside a substrate (mainly silicon) and is used extensively in the semiconductor industry. Surface micromaching, as the name indicates, is based on the deposition and etching of different structural layers. Surface micromachining can involve as many layers as needed with a different mask (producing a different pattern) on each layer. The most common starting materials (substrate) are glass or plastic as these materials are cheaper than silicon. The structuring layers are deposited using techniques like spin-coating where the material (photo resist) is distributed evenly and in a thin layer on the substrate. Photo resists are mostly polymers like PMMA or the epoxy polymer SU-8 containing a light-sensitive component and a solvent. Like in photography, there are negative and positive resists, in the case of a negative one the solubility of the exposed parts decreases, while for the positive resists it increases. Using a photomask and the light of the correct wavelength the structures to be removed in the next step are defined. After light exposition and polymerisation a developer solution is used, dissolving the soluble structures. In figure 20 these steps are summarised.

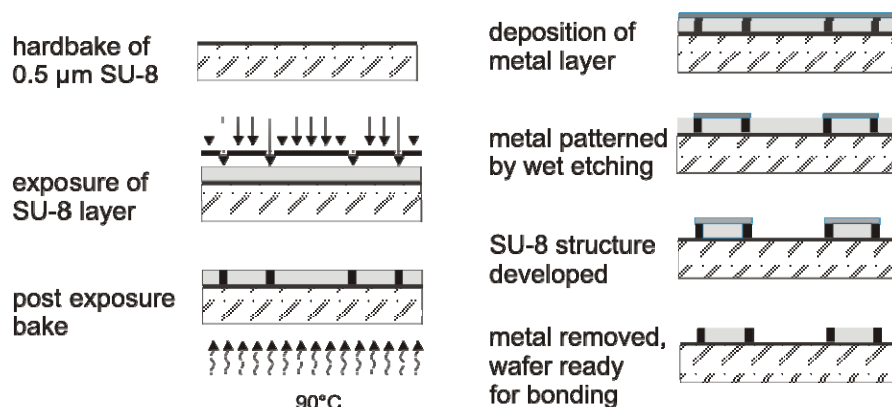


Figure 20 Steps for producing a micro-structured chip

In this work SU-8, an epoxy polymer was used for defining the structures and  $\text{CaF}_2$  as a starting material<sup>31</sup>. The choice of  $\text{CaF}_2$  as a starting material was made necessary as infrared light gets absorbed by standard materials like glass or plastic, while  $\text{CaF}_2$  is infrared-transparent and the typical material for windows used in infrared spectroscopy. SU-8 is a negative photo-resist and the developing wavelength is 365 nm. As first step after the spin-coating a soft-bake is carried out to remove remaining solvent. Then the structures are exposed to UV-light using the photo-mask and in a post exposure bake the SU-8 polymerises through a cationic photoamplification mechanism. In the development step the not polymerised SU-8 is removed and in the final hardbake the two  $\text{CaF}_2$  discs are put together (bonded). The two micro chips developed in this work were both made after this scheme, but depending on the use there have been differences as described below.

The flow cell for the interface between CE and FT-IR (chapter 2) had a titanium layer between the two  $\text{CaF}_2$  discs acting as optical. The metal layer has to be completely isolated from the liquid avoiding electrolysis upon application of the high voltage. In several cells this isolation layer did not work well enough and soon bubbles due to electrolysis of the background electrolyte were formed. The flow channel itself was 150  $\mu\text{m}$  wide and 15  $\mu\text{m}$  thick (optical path length). For details on the production process refer to publication I.

In the electrophoresis chip a Ag metal layer was deposited after the post-exposure-bake. Therefore areas of unexposed SU-8 were covered with metal and thus were not removed in the development process. After removing the metal layer the soft SU-8 remaining beside hard polymerised SU-8 helped to bond together the two  $\text{CaF}_2$  discs. The necessary force for the bonding was therefore reduced and the structures were not deformed. The channel was 100  $\mu\text{m}$  wide and 10  $\mu\text{m}$  high. For technical details on the production process refer to publication II.



## 2 FT-IR detection in capillary electrophoresis for proteins

### 2.1 Detection methods in capillary electrophoresis<sup>32,33</sup>

Due to the small dimension of a capillary and the resulting small optical path length and the low amount of sample available detection in CE poses a challenge. Therefore CE is not a trace analysis technique, as the concentration of the sample normally needs to be high due to these constraints. The most common detection method is UV-Vis absorption spectroscopy due to its universal applicability and its ease of operation, but other methods like laser induced fluorescence<sup>34</sup>, mass spectrometry, electrochemical detection, conductivity, chemiluminescence, refractive index and Raman scattering<sup>35</sup> have been employed.

The use of infrared spectroscopy as a detection technique for CE has only been developed recently as several difficulties need to be overcome:

- CE is normally operated with aqueous buffers that strongly absorb in the mid-IR spectral region
- The fused-silica material of usual CE capillaries is not transparent starting from 2500 cm<sup>-1</sup> to lower wavenumbers
- Sample amounts injected into the CE capillary are usually very small (in the nL range)
- Low absorptivities of the analytes in infrared

Köhlhed et al.<sup>36</sup> have showed the possibility of hyphenating CE with online FT-IR spectroscopic detection. In their work an IR-transparent flow cell was positioned between two capillaries and infrared light was passed through it using a beam condenser.<sup>37</sup> This study showed that the integration of the IR flow cell into the CE system did not influence the migration of the analytes. This system was applied to the analysis of adenosine, adenosine monophosphate and guanosine using capillary zone electrophoresis (CZE) as separation technique. Another application

was the separation of five neutral analytes, namely paracetamol, caffeine, p-nitrobenzylalcohol, m-nitrophenol and p-nitrophenol using micellar electrokinetic chromatography (MEKC)<sup>38</sup>. The possibility of detecting and separating diastereomers was also demonstrated as diastereomers show different physical properties making it possible to separate them and to distinguish them in infrared spectroscopy. This analysis was carried out in non-aqueous media using CZE. An application where sugars in fruit juices were analysed with this technique was shown by Kölhed.<sup>39</sup>

Another possibility developed by de Haseth et al.<sup>40</sup> used deposition of the eluate from the CE onto a ZnSe window using a nebulizer interface. This approach however, does not allow real-time information about the sample and is also limited to volatile background electrolytes and non-volatile analytes. The advantage of this method lies in the preconcentration of the analyte and the possibility to decouple the separation and detection step, thus not imposing any time constraints in the detection process. As solid state IR spectra are generated they should be comparable with library spectra. This method was applied to caffeine, salicylic acid, p-aminobenzoic acid and sodium benzoate.

## 2.2 Interface for on-line FT-IR detection in CE

The interface used in this work was very similar to the one used by Kölhed et al.<sup>21</sup> As was shown the used flow cell together with the connected capillaries constituted a feasible interface for on-line FT-IR detection in CE. This was achieved by a micro-machined flow cell as described in chapter 1.8. This flow cell was constructed in a way that the maintenance of the current upon application of the voltage was assured. Finally, the flow cell did not contribute to band broadening or affected the separation.

The production of the flow cell was described in outlines in chapter 1.8 and in detail in publication I. A scheme of the flow cell is shown in Figure 21

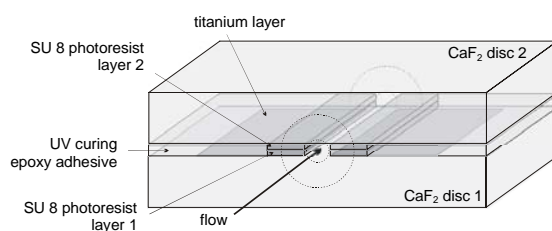


Figure 21 Scheme of infrared flow cell

In this work a new flow cell holder (Figure 22) for simpler changing of the capillaries was designed.

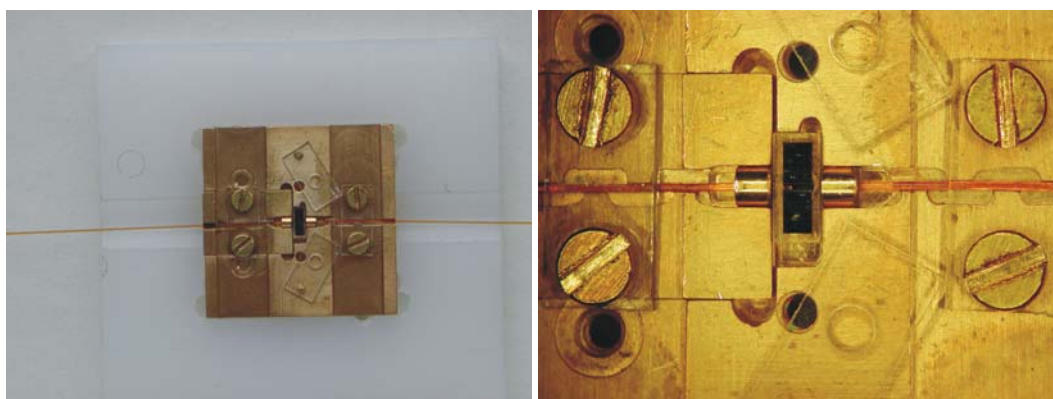


Figure 22 Flow cell with the capillaries attached (left), close up of the interface (right)

Using the previous cell holder it was necessary to cut the capillaries with a dice saw to achieve a very smooth surface. On one end of each capillary to be coupled to the flow cell a drop of an epoxy polymer was put on while passing dry air through the capillary preventing the epoxy polymer clogging the capillary. Then the polymer was cured under UV light for 15 minutes and finally the formed O-ring could be used after a waiting period of 24 hours. This procedure was cumbersome as it involved not only the use of a dice saw but also the application of the epoxy polymer proved to be difficult to be reproduced. If one of these steps was not carried out diligently, the connection between the capillaries and the flow cell could not be accomplished.

In the new holder one side of the supporting block was movable to exert pressure on the cell and the commercial O-rings used to tighten the interface between cell and capillaries (Figure 22). The capillaries were coupled to the flow cell through bolts ensuring that the capillaries were at the same level as the flow channel of the

cell. The exerted pressure also aligned the flow cell inside the supporting block. The O-rings used had an inner diameter of 500  $\mu\text{m}$  and consisted of rubber (Flume GmbH, Essen, Germany). This arrangement allowed for quick and easy changes of the capillaries without the cumbersome procedure of preparing capillaries as in the previous interface.

## 2.3 Applications for protein samples

The proteins studied in this work were myoglobin,  $\alpha$ -lactalbumin and  $\beta$ -lactoglobulin. The proteins were chosen for their secondary structures as myoglobin only consists of  $\alpha$ -helices and  $\alpha$ -lactalbumin mainly of  $\alpha$ -helices while  $\beta$ -lactoglobulin is a typical example of a pleated ( $\beta$ -sheet) structure. The separation was carried out in a 20 mM borax buffer dissolved in deuterium oxide ( $\text{D}_2\text{O}$ ) as it was necessary to shift the maximum of the solvent absorption away from the absorption of the protein (see chapter 1.2). The protein samples were dissolved in the buffer to prevent precipitation of the proteins. All liquid handling was performed in a glove box which was purged before using  $\text{D}_2\text{O}$  with dry air for at least an hour as  $\text{D}_2\text{O}$  is highly hygroscopic. The separation was optimised using a UV-detector (Figure 23). The separation of the proteins was achieved with a baseline separation, an important prerequisite for infrared detection. The proteins migrated in the order myoglobin,  $\alpha$ -lactalbumin and finally  $\beta$ -lactoglobulin. It can be seen in Figure 23 that  $\beta$ -lactoglobulin forms two isoforms which could be separated using these experimental conditions showing the separation power of capillary electrophoresis.

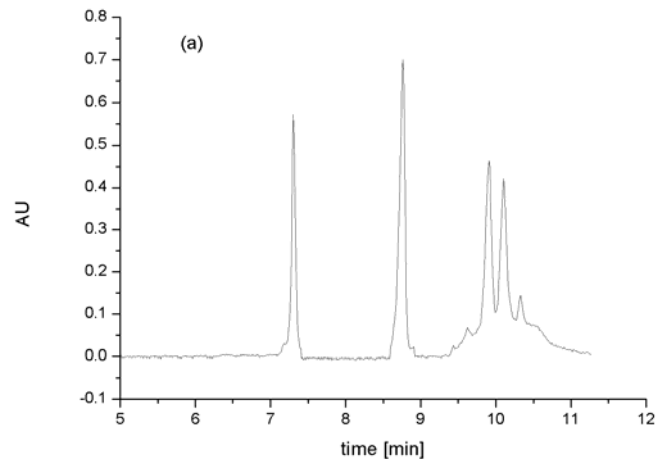


Figure 23 Typical electropherogram of myoglobin, lactalbumin and lactoglobulin

The infrared detection was carried out using a dedicated optical setup, a beam condenser equipped with a sensitive MCT detector. The beam condenser was placed inside a Perspex box purged constantly with dry air. The intensities of the analytes in the infrared detection were integrated from 1350 to 1700  $\text{cm}^{-1}$  and thus a trace was created (Figure 24).

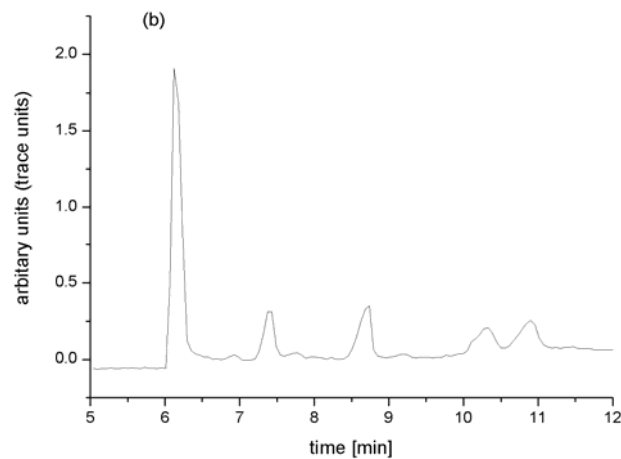


Figure 24 Trace of the electropherogram recorded in IR

As can be seen in Figure 24, there is an additional peak compared to the UV electropherogram. The explanation lies in the formation of HDO due to the proton

exchange of the protein samples with the solvent ( $D_2O$ ). As HDO is a neutral molecule its migration speed equals the mobility of the EOF and can therefore be employed as an EOF marker in IR spectroscopy as the absorptivity of HDO is strong. The other peaks are the same as in the UV electropherogram shown above. These figures give proof that the developed flow cell is applicable also for protein samples.

In the three-dimensional recording of the separation with IR spectroscopy it is clearly visible how the secondary structure of the proteins gets reflected in the IR spectrum (Figure 25).

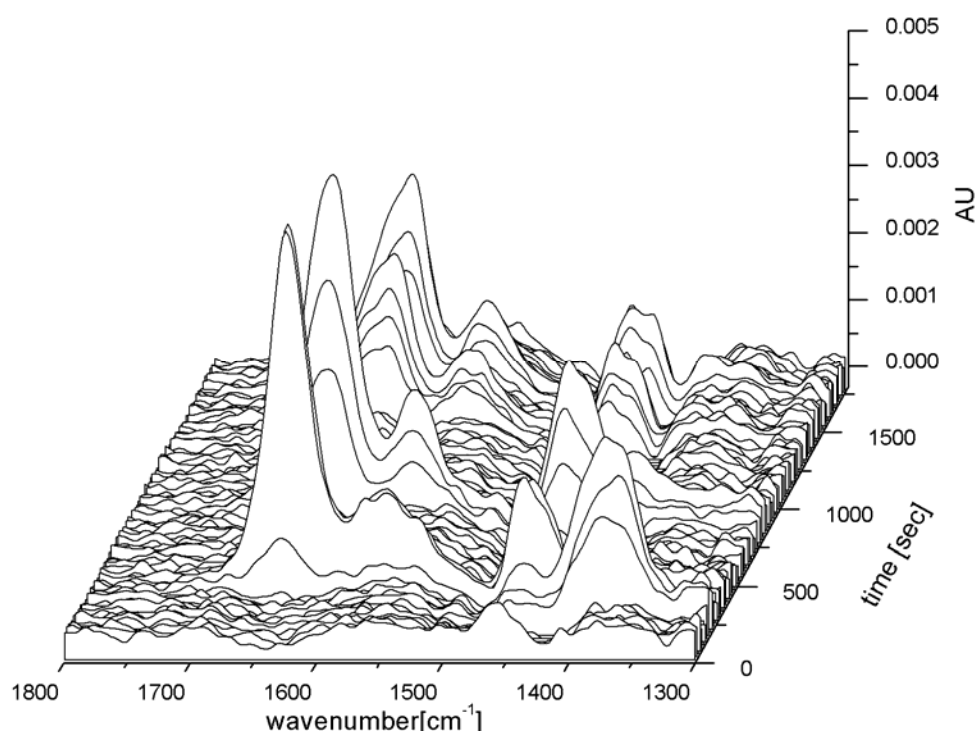


Figure 25 Three-dimensional IR electropherogram of the proteins

Comparison of extracted spectra of the CE run with reference spectra from attenuated total reflection (ATR) spectroscopy show the accordance of the features and thus the possibility to detect protein samples in this way (Figure 26). The more intense peak at the position of the amide II' band in the case of the ATR reference spectra is explained by the formation of HDO. As the reference spectra

were taken on the ATR crystal without an inert atmosphere the hygroscopic D<sub>2</sub>O formed HDO with the water vapour of the surrounding air.

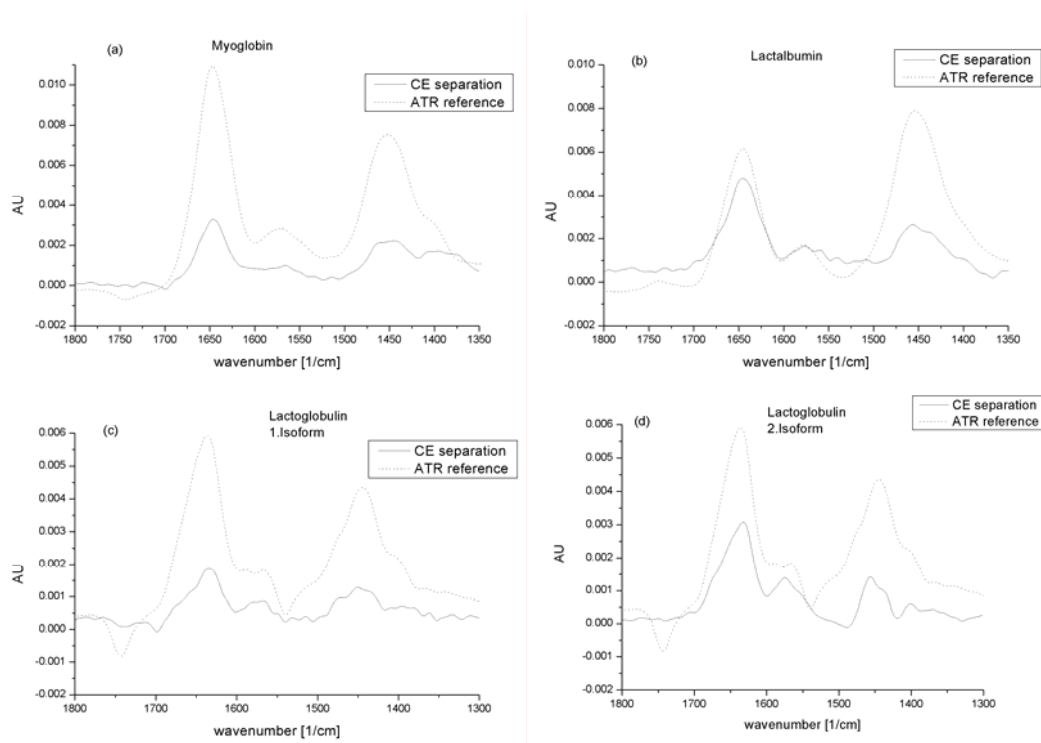


Figure 26 comparison of extracted (CE) and reference spectra (ATR); (a) myoglobin, (b) lactalbumin, (c) lactoglobulin 1. isoform, (d) lactoglobulin 2 isoform

With the experimental conditions chosen 4-5 FTIR spectra were recorded for every protein passing the flow cell used for transmission measurements. Whereas the peak position (amid I band) of the on-line recorded FTIR spectra were in good agreement with those of reference spectra an improvement in signal-to-noise needs to be made to allow a more detailed analysis of the recorded FTIR spectra. As the separation is so fast that only 50 scans can be coadded the noise proves to be too high to enable further studies of the protein structure.

Beside the proton exchange with the sample, also a proton exchange with the epoxy polymer SU-8 takes place as studies with stopped flow showed. However, as all measurements were performed with a continuous flow the detection of the analytes was not affected through this proton exchange. There was one problem showing that the production of the flow cells is not yet under full control. In quite some flow cell the metal layer got contact with the background electrolyte after

some time working with the cell. The effect was always the same, upon application of voltage the electrolyte underwent electrolysis and gas bubbles were formed. Therefore no analysis using these cells could be carried out. As the metal layer only acts as an optical aperture, in the next generation of flow cells it was removed and the detection of the CE separation was performed using an IR microscope. However, the optical setup was not purged with dry air and thus the noise was higher than the one in the beam condenser. Therefore, detection of the protein samples using the IR microscope was not feasible. The concentrations of the sample could not be increased to higher values than  $4 \text{ gL}^{-1}$  as the sample started to stick to the wall and finally the performance of the separation decreased as the peaks broadened strongly.

## 2.4 Conclusions and Outlook

In this work this CE-FTIR system was successfully applied for the first time to a separation of proteins identifying different secondary structures. The use of deuterium oxide shifted the bending vibration down to  $1210 \text{ cm}^{-1}$  while in water it is  $1640 \text{ cm}^{-1}$  covering the absorption of the amide I vibration. Future developments should include capillary electrochromatography as a separation technique as many analytical problems can be solved better using this technique and quite some analytes do not have useful absorptivities in the UV-Vis area while in infrared they show distinct features. Further improvements in the detection systems would enable the study of the secondary structures in more details as the signal-to-noise ratio would improve.



### 3 Infrared synchrotron radiation for micro-chip based analysis

Miniaturization of analytical tools has become a very active field of research in the last years. The area studied in this work is capillary electrophoresis on a microchip as the separation times are short and the resolution good due to the high electric field. Until now, all applications of CE on a chip have been carried out in glass or plastic substrates as these materials are easy to handle and micro machining techniques are widely available for them [ref]. In this work a CE microchip fabricated using  $\text{CaF}_2$  as a starting material for infrared detection was developed and applied.

#### 3.1 Production of the micro-chip

The production of the chip is described in outlines in chapter 1.8 and in more detail in publication II. The geometry of the produced structure is shown in Figure 27.

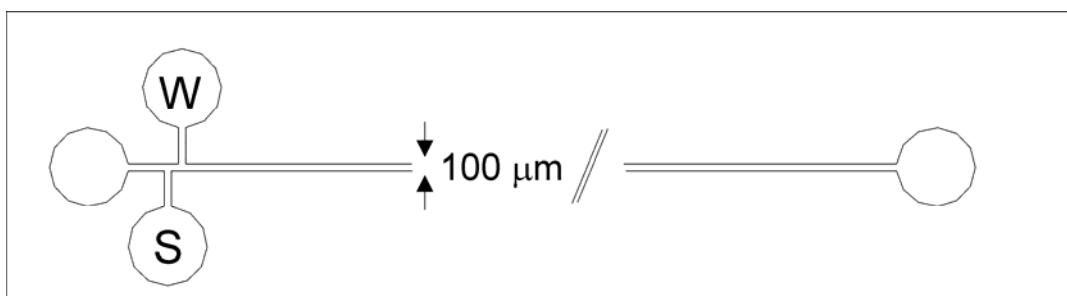


Figure 27 Schematic drawing of the CE chip made on a  $\text{CaF}_2$  wafer. The device is loaded by introducing the sample via hydrodynamic pumping from port S to waste (W).

For capillary zone electrophoresis it was considered of importance to produce channels made out of one type of material as the surface material has an impact on

the separation itself. Therefore, prior to producing the SU-8 structures on the CaF<sub>2</sub> wafers they were coated with a 0,5 μm thick SU-8 layer and exposed to oxygen plasma for two minutes to make them hydrophilic so that another layer of SU-8 could be deposited. Due to the small thickness of the SU-8 layer the throughput for mid-IR measurements was not impaired despite of the fact that the SU-8 characteristic bands were clearly visible in the recorded spectrum (Figure 28).

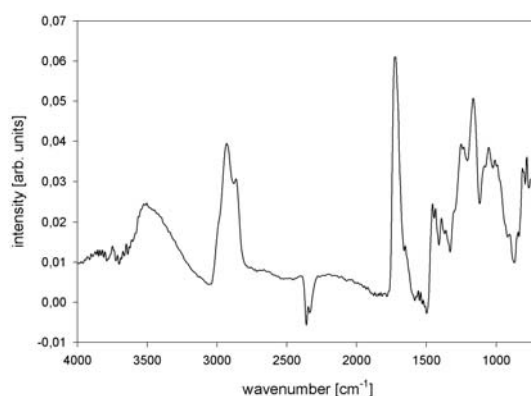


Figure 28 Absorption spectrum of the epoxy polymer SU-8

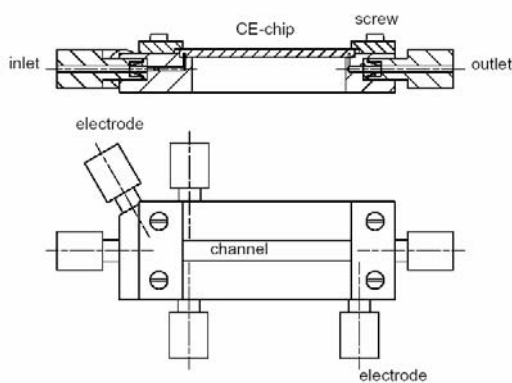


Figure 29 Schematic view of support for CE micro-chip

The produced microchip was placed in a dedicated support made out of PMMA to facilitate the supply of the chip with reagents and the electrodes as required for the experiments. The connections to the support were all standard flow injection threaded fittings for simple liquid handling (Figure 29).

The openings of the chips were sealed to the support with commercially available O-rings (Flume, Germany) to ensure tightness. The O-rings were made out of rubber and had an inner diameter of 0.5 mm. This arrangement made it possible to exchange chips easily. The support carrying the chip was screwed onto a metal plate fitting the xy-stage of the IR-microscope attached to the synchrotron source. The capillary electrophoresis system was built in-house and consisted of a high voltage power supply (Spellman, New York) and two platinum electrodes fitted inside standard Teflon tubings. The electrodes were attached to the chip by screwing the corresponding fittings into the support such that the electrodes touched the running buffer.

### 3.2 FT-IR spectrometer and synchrotron source

In CE the peaks are normally sharp, therefore dilution of these peaks in a high detection volume should be prevented. On going to micro-chips the volumes get reduced, but the same applies for the optical path length. As described in chapter 1.3 the high brilliance of the synchrotron radiation allows for the analysis in such small detection volumes.

In this work, the IR light used was generated at the synchrotron source ANKA (Karlsruhe, Germany). The synchrotron light was guided through a diamond window and coupled into the IR spectrometer. For details about synchrotron light please refer to chapter 1.3. A Bruker 66v FT-IR spectrometer (Bruker Optik, Germany) equipped with a MCT detector was used throughout all the experiments. The IR beam was coupled to the IR microscope (Bruker IRscope II)

using two parabolic mirrors. The scanner of the spectrometer was operated at a HeNe laser modulation frequency of 100 kHz. Fifty spectra were co-added for each spectrum with a spectral resolution of  $8\text{ cm}^{-1}$ . Reference spectra of myoglobin were recorded using a three reflection diamond ATR (attenuated total reflection) unit from SensIR (Danbury, CT) attached to a Bruker Matrix-F spectrometer.

### 3.3 Results and Discussion

The chip was connected to an air tight flow system to enable automation of the liquid handling and to study hygroscopic analytes. Therefore the chip needed to be constructed with a sealing top. All chips reported so far consist of open channels where pressure differences are compensated automatically<sup>41</sup>. The most common injection method is electrokinetic (EK) injection as the pressure-driven injection generates dispersion already at the injection. In this work, however, EK injection proved to be slow as the support has a dead volume about a magnitude larger than the volume of the chip. Therefore injection was performed hydrodynamically using a syringe pump equipped with a microliter Hamilton syringe. Before use the whole chip was flushed with the running buffer for cleaning purposes. This was accomplished by introducing buffer at the inlets of the separation channel and the sample port by means of a three channel syringe pump. For sample loading the two exits of the separation channel were blocked and the sample was introduced using the syringe pump. In this way the sample double tee (Figure 27) was filled. After loading of the sample a potential of 3 kV was applied corresponding to an electrical field of 680 V/cm.

For testing purposes nitrate and sulfate in water were used, as both analytes show very strong absorption in IR. The signal of the analytes were large enough to be

detected easily, however, the chip was overloaded as figures 30 and 31 show where the peak of the analyte decreases only after quite some time.

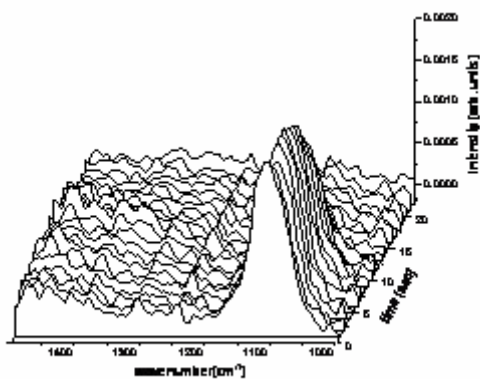


Figure 30 Three-dimensional IR plot of sulfate in the chip

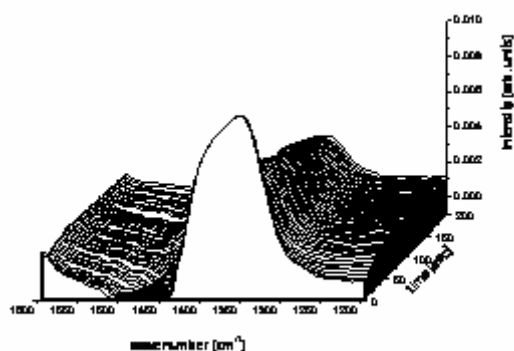


Figure 31 Three-dimensional IR plot of sulfate in the chip

As the migration speed of the inorganic analytes were too fast to obtain a separation, a protein (myoglobin) having a much higher diffusion constant was injected. Figure 32 shows the electropherogram of myoglobin. The peak of the amide I' band is clearly visible and sharp. However, the amide II' is heavily

overlapped by H<sub>2</sub>O, though all samples were prepared carefully inside a glove box.

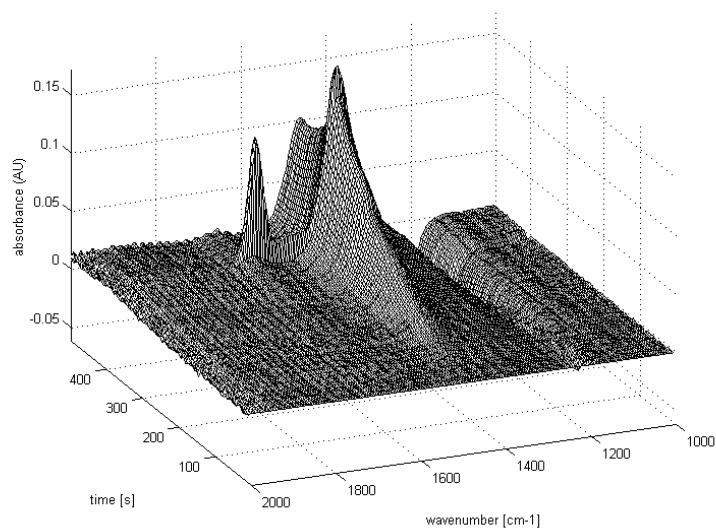


Figure 32 IR electropherogram of myoglobin in the CE micro-chip

The FTIR spectra corresponding to the peak maximum was extracted from the dataset and compared with a reference spectrum taken of the analyte using an ATR unit. A characteristic peak at  $1648\text{ cm}^{-1}$ , being the C=O stretch vibration of the protein, can be clearly seen in both spectra (Figure 33).

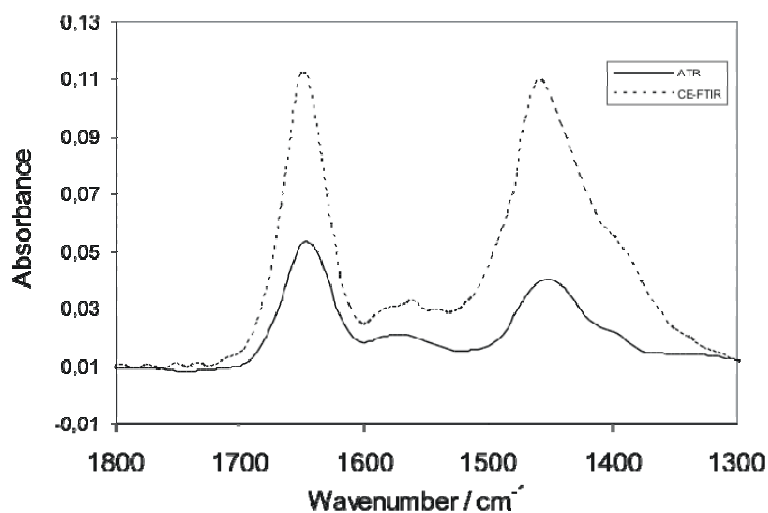


Figure 33 Comparison of FTIR spectra of the analyte (dashed line) as recorded during the experiment shown in figure 15 with a reference spectra (solid line).

As can be seen in Figure 33 the intensity of the amide I' band (the amide II' band is overlapped by HDO) is much higher than in the case of the ATR reference spectrum. This finding indicates when using synchrotron light even in structures of 100  $\mu\text{m}$  higher absorption can be realised due to the higher brilliance. However, as already mentioned in chapter 1.3 the noise level of the synchrotron is still too large for studying processes with small changes of the analytes and their respective IR spectra. This data was recorded during a measurement campaign of four days at the synchrotron ANKA in Karlsruhe.

Carrying out an experiment at a synchrotron light source is very different to making the same experiment at home in the lab. The main difficulty lies in the decaying beam intensity of the synchrotron as the amount of electrons decreases over time. Although this decay is steady an assessment of the intensity differences proves to be difficult as baseline shifts occur frequently. Therefore long-time measurements need to be planned carefully with an eye on the stability of the

beam and mathematical treatment of the data is necessary. Mainly in the infrared region the loss of spectral intensity of the synchrotron beam in the first hour can be observed, rendering measurements in this time for purposes like in this work difficult as the noise of the synchrotron is even higher as during the remaining life time of the beam.

### 3.4 Conclusions and Outlook

The developed technology for IR-chip fabrication based on the combination of CaF<sub>2</sub> and SU-8 structuring technology has proven to be a versatile and effective means to produce devices for use with IR synchrotron radiation source. Using a microchip designed for capillary electrophoresis a protein was successfully injected and recorded as it passed the detector window. From the recorded FTIR spectra the identity of the analyte could be confirmed by comparison with reference spectra.

It is expected that the developed microchip for separation monitoring using IR synchrotron detection can be advantageously be used for a plentiful amount of applications once the noise level at a synchrotron is reduced to amounts as achieved with a globar and a large aperture. The attractiveness of FTIR detection for microchip electrophoresis is seen in its molecular specific information content and especially in its capability to tell the folding state as well as the secondary structures of proteins in solution.



## 4 Sequential injection (SI)-Capillary electrophoresis system for automated sample preparation and separation

The analytical process as a whole is complex and involves four generic steps.<sup>42</sup> The first step involves preliminary steps to prepare the analytes for the measurement, the second step is the measurement and transducing step and the third step consists in the data acquisition and processing. Often these three steps are integrated, even though only partly. The fourth step involves calibration operations using standards. The lack of integration and automation leads to manual intervention, thus being error-prone and time-consuming. Using a flow-system allows the integration of all four steps overcoming some of the cumbersome difficulties.

Kuban<sup>43</sup> and Fang<sup>44</sup> have demonstrated such interfaces for the coupling of flow injection analysis (FIA) and capillary electrophoresis, while Ruzicka<sup>45</sup> has implemented such an interface using a micro sequential analysis system (SIA), the so-called lab-on-a-valve. In this work conventional SIA pumps and valves were used to construct the interface and software for controlling the whole experimental set-up.

### 4.1 Development of the software

As the experimental set-up consisted of many different devices, new programmes based on the software Sagittarius, written by Michael Haberkorn, were developed. Sagittarius consists of a server (the so-called master) and as many clients as there are physical devices. The architecture of Sagittarius is a client-server architecture

based on the Transfer Control Protocol (TCP), a well-known protocol for exchanging data (together with the Internet Protocol, IP, the main protocol of the Internet) and therefore the integration of new clients is carried out without difficulties. As the communication between master and client is based on TCP, control of clients can be exerted via a network giving more flexibility.

One client developed for this work was a data acquisition and control software for a Dionex Ultimate UV detector. The goal of the software was to be able to fully control the detector via the master including data acquisition and setting of experimental variables like detection wavelengths and measurement time (Figure 34).

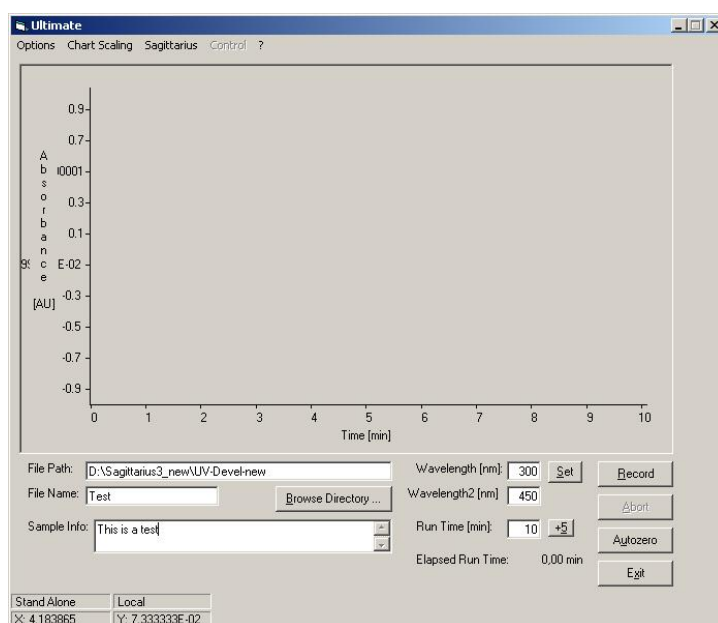


Figure 34 Screenshot of the UV-Client

The second client was designed to interface to a digital-analog card used to control the high voltage (HV) power supply CZE1000R from Spellman as this HV power supply only contained a terminal block for analog signals. Again in this case the goal was the full control of the device using the master (Figure 35).

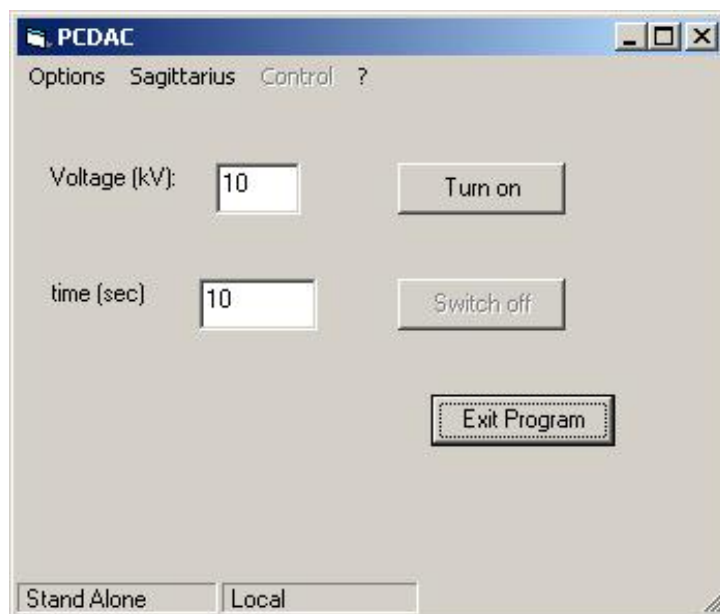


Figure 35 Screenshot of the client for controlling the high voltage power supply

## 4.2 SIA-CE interface

The interface between the SIA system and the CE consisted mainly of two T-pieces containing the electrode (grounded), the capillary, an inlet and an outlet (waste). A schematic view of the interface and the whole set-up is shown in figure 36.

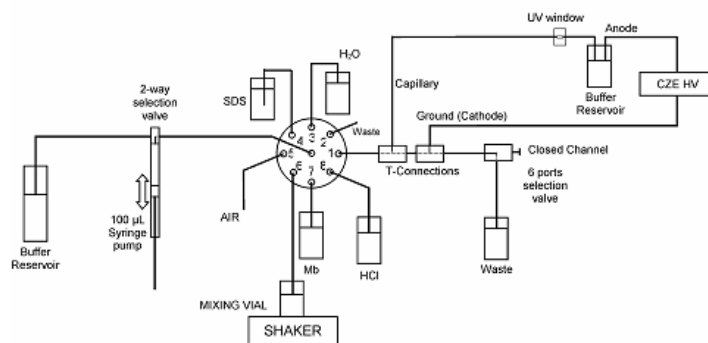


Figure 36 Schematic view of the developed SIA-CE interface

For introducing liquids into the capillary the system was pressurized by closing a two-port valve leading to the waste, thus forcing the pumped liquid into the capillary. First the sample was flushed through the interface with the injection valve open to ensure that the sample was close to the capillary inlet, then the injection valve was closed, the syringe could pressurize the system and sample was injected into the capillary. In the next step the interface was rinsed with the background electrolyte (BGE), then the voltage was applied and the separation started while BGE was replenished at a low flow rate using the same pump. The whole injection process was carried out in 2 minutes while the separation time depended on analytes separated and the voltage applied. The SI system was used in the same way to perform conditioning and cleaning in a fully automated way depending on the stage of the experiment. Using the SI system enables to perform the necessary steps in any order. The sample handling was carried out using the SIA system and the sample was mixed with the reagents in an external mixing chamber, thus decoupling the sample preparation step from the separation process. This gives the possibility to perform further sample preparation steps on the sample, like solid or liquid-liquid extraction or heating.

#### 4.2.1 Test of the SIA-CE system

The system was tested with adenosine and adenosine monophosphate which were mixed off-line to ensure complete mixing. The samples prepared were injected using the SI system as described and the voltage was applied to separate the analytes. The background electrolyte was a 20 mM Borax solution (pH 9.2) and the voltage applied was 10 kV resulting in a current of 16  $\mu$ A.

The electropherogram in Figure 37 shows that the injection and the subsequent separation worked reproducibly (RSD of 5.4%,  $n=5$ ). The inset in Figure 37 shows a decrease of the RSD at an increase of injected sample. As a compromise between overloading the capillary and a low RSD an injection volume of 40 nL (about 4 % of the whole capillary volume) was chosen and used throughout this work.

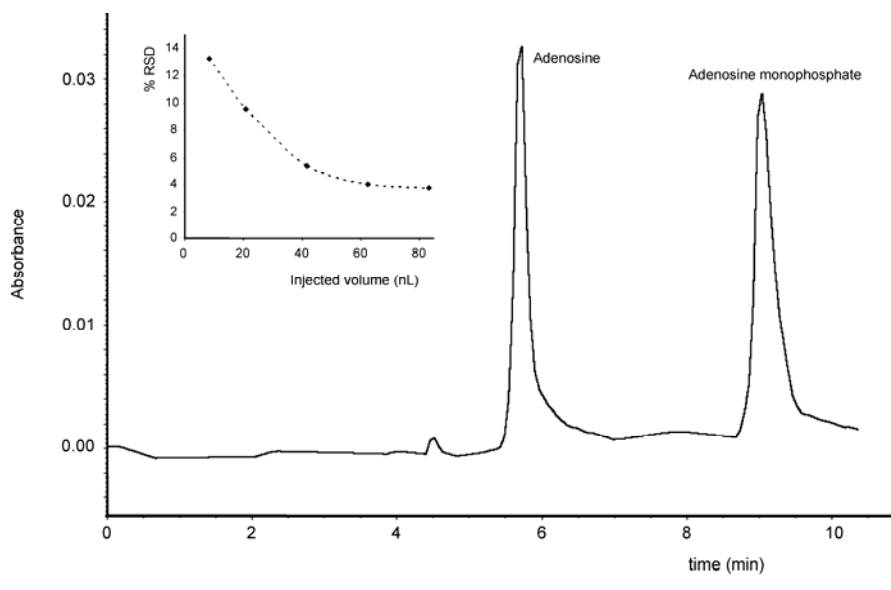


Figure 37 Typical electropherogram after injection using the SI system; inset showing the influence of the injection volume on the mean error

For assessing the figures of merit of the developed interface, it was calibrated between 0 and 500 mgL<sup>-1</sup> giving the calibration curves shown in Figure 37. The limit of detection was calculated to be 0.5 mgL<sup>-1</sup> (obtained from the standard deviation of 6 measurements of a standard solution of 50 mgL<sup>-1</sup>).

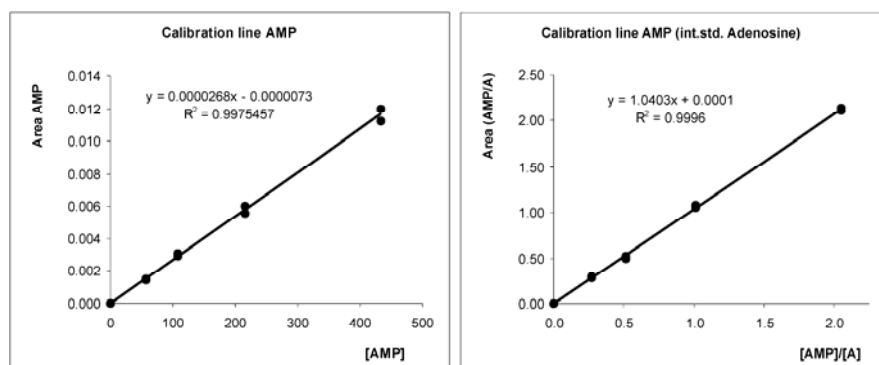


Figure 38 Calibration curves of adenosine and adenosine monophosphate in the range between 0 and 500 mgL<sup>-1</sup>

#### 4.2.2 Application to myoglobin and sodium dodecyl sulfate

As described in Section 1.4 only proteins in their native state exhibit a biological function intended from the organism. However, refolding and unfolding processes occur due to several reasons like heat or denaturing agents while the actual folding mechanism is still not fully understood.

In this study the SI system was employed to investigate the reaction between myoglobin and sodium dodecylsulfate (SDS), which is a known strong denaturing agent. The concentration of myoglobin was kept constant at 1.7 gL<sup>-1</sup> while the concentration of the added SDS was varied using the SIA system. The mixture obtained was injected into the CE system as described and the formed conformations of myoglobin were separated. Figure 39 shows clearly that with increasing concentration of SDS the area of the second peak as well as the

migration time increased indicating that a second conformation was formed moving slower towards the detector.

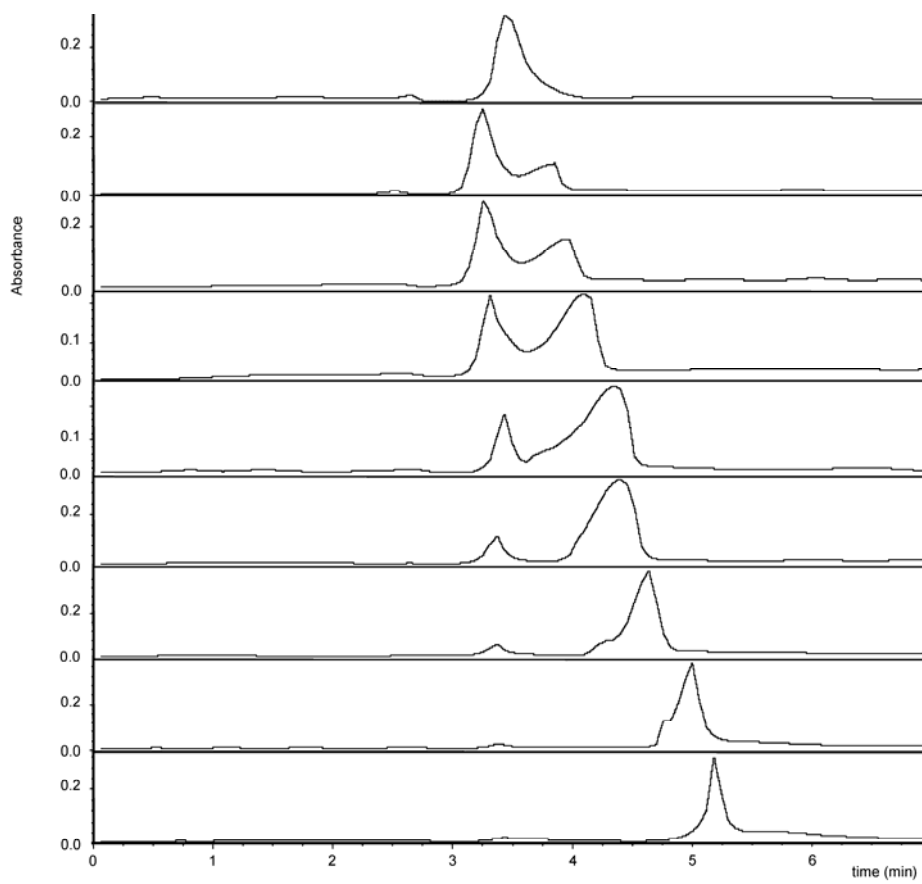


Figure 39 Electropherogram showing the influence of SDS on the formation of myoglobin conformations and their migration times

### 4.3 Conclusion and Outlook

In this work a successful SIA-CE interface using commercially available pumps and valves was developed. The possibilities given by SIA were employed and the automated injection gave reproducible results (RSD of 5.4%,  $n = 5$ , injection volume 40 nL). The limit of detection obtained in the separation of adenosine and adenosine monophosphate was  $0.5 \text{ gL}^{-1}$ . When all components were automated

using self-written software the SI system was employed for integration of the sample preparation, injection and detection process.

The developed flow system allows further studies in two main topics in the future. When hyphenated to capillary zone electrophoresis a broad field of applications like different kinds of sample preparation steps immediately prior to sample injection could be performed as well as inserting the flow cell for infrared detection following UV detection for complex chemical systems. Other separation techniques like capillary electrochromatography could be used as separation technique coupled to the SI system enabling the analysis of more complex mixtures. The other field of application would take advantage of the highly reproducible dispersion profile by the SIA system. Using “electronic dilution” in this system might be an appropriate technique to study time- and concentration-dependent processes.



## 5 References

---

<sup>1</sup> Griffiths, P.R.; deHaseth, J. "Fourier Transform Infrared Spectroscopy", John Wiley & Sons: New York, 1986

<sup>2</sup> Williams, G.P. "Synchrotron and Free Electron Laser Sources of Infrared Radiation" in Chalmers, J.M.; Griffiths, P., Handbook of Vibrational Spectroscopy.; John Wiley & Sons Ltd.: 2002, 341-348

<sup>3</sup> Roy, P; Brubach, J.-B.; Calvani, P.; deMarzi, G.; Filabozzi, A.; Gerschel, A.; Giura, P.; Lupi, S.; Marcouille, O.; Mermet, A.; Nucara, A.; Orphal, J.; Paolone, A.; Vervloet, M. Nuclear Instruments and Methods in Physics Research A 467-468 (2001) 426-436

<sup>4</sup> Schade, U. personal communication

<sup>5</sup> Miller, L.M.; Smith, R.J. Vibrational Spectroscopy 38 (2005) 237-240

<sup>6</sup> Creighton, T.E. "Proteins: Structures and Molecular Principles", W.H. Freeman and Co., New York, 1983

<sup>7</sup> Foguel, D.; Silva, J.L. Biochemistry 43 (2004) 11361-11370

<sup>8</sup> Fabian H; Mäntele, W "Infrared Spectroscopy of Proteins" in Chalmers, J.M.; Griffiths, P., Handbook of Vibrational Spectroscopy.; John Wiley & Sons Ltd.: 2002., 3399-3425

<sup>9</sup> Barth, A.; Zscherp, C. Quarterly Review of Biophysics 35 (2002) 369-430

<sup>10</sup> Oberg, K.A.; Ruyschaert, J.-M.; Goormaghtigh, E. European Journal of Biochemistry 271 (2004) 2937-2948

<sup>11</sup> Schweitzer-Stenner, R.; Eker, F.; Huang, Q.; Griebenow, K.; Mroz, P.A.; Kozlowski, P.M. Journal of Physical Chemistry B 106 (2002) 4294-4304

<sup>12</sup> Goormaghtigh, E.; Cabiaux, V.; Ruyschaert, J.-M. "Determination of soluble and membrane protein structure by Fourier Transform Infrared Spectroscopy" in "Subcellular biochemistry, physicochemical methods in the study of biomembranes", eds Hilderson, H.J, Ralston, B.G. Plenum Press, New York, 1994, 329-450

<sup>13</sup> Surewicz, W.K; Mantsch, H.H; Chapman, D. Biochemistry, 32 (1993) 389

- 
- <sup>14</sup> Pancorska, P.; Fabian, H.; Yoder, G.; Baumruk, V.; Keiderling, T.A. *Biochemistry*, 35 (1996) 13904
- <sup>15</sup> Ruzicka, J.; Hansen, E.H. "Flow Injection Analysis", John Wiley & Sons: New York, 1988 (2<sup>nd</sup> Ed.)
- <sup>16</sup> Fang, Z.-L. "Flow Injection: Separation and Preconcentration" VCH: Weinheim, 1993
- <sup>17</sup> Ruzicka, J.; Marshall, G.D. *Analytica Chimica Acta*, 237 (1990) 329-343
- <sup>18</sup> Economou, A. *Trends in Analytical Chemistry* 24 (2005) 416-425
- <sup>19</sup> Lendl, B.; Kellner, R. *Mikrochimica Acta* 119 (1995) 73-79
- <sup>20</sup> Weinberger, R. "Practical Capillary Electrophoresis" Academic Press Inc.: San Diego, CA, 1993
- <sup>21</sup> Hinsmann, P.; Arce, L.; Svasek, P.; Lämmerhofer, M.; Lendl, B. *Applied Spectroscopy* 58 (2004) 662-666
- <sup>22</sup> Cordova, E.; Gao, J.; Whitesides, G.M. *Analytical Chemistry* 69 (1997) 1370-1379
- <sup>23</sup> Leinweber, F.C.; Stein, J.; Otto, M. *Fresenius Journal of Analytical Chemistry* 370 (2001) 781-788
- <sup>24</sup> Stroink, T.; Paarlberg, E.; Waterval, J.C.M.; Bult, A.; Underberg, W.J.M. *Electrophoresis* 22 (2001) 2375-2383
- <sup>25</sup> Quirino, J.P.; Terabe, S. *Analytical Chemistry* 72 (2000) 1023-1030
- <sup>26</sup> Reyes, D.R.; Iossifidis, D.; Auroux, P.-A.; Manz, A. *Analytical Chemistry* 74 (2002) 2623-2636
- <sup>27</sup> Vilkner, T.; Janasek, D.; Manz, A. *Analytical Chemistry* 76 (2004) 3373-3386
- <sup>28</sup> Manz, A.; Harrison D.J.; Verpoorte, E.; Widmer, H.M. *Advances in Chromatography* 33 (1993) 1-66

- 
- <sup>29</sup> Dolnik, V.; Liu, S.; Jovanovich, S. *Electrophoresis* 21 (2000) 41-54
- <sup>30</sup> Madou, M. "Fundamentals of micofabrication" CRC Press: Boca Raton, 2002 (2<sup>nd</sup> Ed.)
- <sup>31</sup> Svasek, P.; Svasek, E.; Lendl, B.; Vellekoop, M. *Sensors and Actuators A* 115 (2004) 591-599
- <sup>32</sup> Swinney, K.; Bornhop, D.J. *Electrophoresis* 21 (2000) 1239-1250
- <sup>33</sup> Marina, M.L; Rios, A.; Valcarcel, M "Analysis and detection by capillary electrophoresis" Elsevier: Amsterdam, 2005
- <sup>34</sup> Flurer, C.L. *Electrophoresis* 24 (2003) 4116-4127
- <sup>35</sup> Kulka, S.; Lendl, B.; "Vibrational spectroscopic detection in capillary electrophoresis" in "Analysis and detection by capillary electrophoresis", eds. Marina, M.L; Rios, A.; Valcarcel, M., Elsevier: Amsterdam, 2005
- <sup>36</sup> Kölhed, M.; Hinsmann, P.; Svasek, P.; Frank, J.; Karlberg, J.; Lendl, B. *Analytical Chemistry* 74 (2002) 3843-3848
- <sup>37</sup> Hinsmann, P.; Haberkorn, M.; Frank, J.; Svasek, P.; Harasek, M.; Lendl, B. *Applied Spectroscopy* 55 (2001) 241-251
- <sup>38</sup> Kölhed, M.; Hinsmann, P.; Lendl, B.; Karlberg, B. *Electrophoresis* 24 (2003) 687-692
- <sup>39</sup> Kölhed, M.; Karlberg, B. *Analyst* 130 (2005) 772-778
- <sup>40</sup> Jarman, J.L.; Todebush, R.A.; de Haset, J.A. *Journal of Chromatography A* 976 (2002) 19-26
- <sup>41</sup> Greenwood, P.A.; Greenway, G.A. *Trends in Analytical Chemistry* 21 (2002) 726-740
- <sup>42</sup> Valcarcel, M.; "The Analytical Process" in "A Modern Approach to Analytical Science", eds. Kellner, R; Mermet, J.-M.; Otto, M.; Valcarcel, M.; Widmer, H.M., Wiley: Weinheim, 2004
- <sup>43</sup> Kuban, P.; Karlberg, B. *Analytica Chimica Acta* 404 (2000) 19-28

---

<sup>44</sup>Fang, Z.L.; Liu, Z.S.; Shen, Q. *Analytica Chimica Acta* 346 (1997) 135-43

<sup>45</sup> Wu, C.-H.; Scampavia, L.; Ruzicka, J. *Analyst* 127 (2002) 898-905

# I

Kulka, S.; Lendl, B.

*“On-line capillary electrophoresis FT-IR detection for the separation and characterization of proteins”*

Submitted publication

**On-line capillary electrophoresis FT-IR detection for the separation and  
characterization of proteins**

S. Kulka and B. Lendl\*

Institute for Chemical Technologies and Analytics

Vienna University of Technology

Getreidemarkt 9/164

A-1060 Vienna, Austria

Tel.: +43-1-58801-15140

Fax.: +43-1-58801-15199

Email: [Bernhard.lendl@tuwien.ac.at](mailto:Bernhard.lendl@tuwien.ac.at)

Abstract

Capillary electrophoresis (CE) with on-line FTIR spectroscopic detection was used to separate a mixture of three model proteins and to provide information on the dominant secondary structures of the separated proteins. On-line FTIR transmission measurements were achieved using a micro machined flow cell made out of CaF<sub>2</sub> and SU-8 polymer which was attached to the fused silica capillaries using commercial O-rings. The IR beam was focused on the detection window using an off-axis parabolic mirror attached to an external optical port of the spectrometer. As the absorption of water heavily overlaps the so-called amide I band of the proteins the separations were carried out in heavy water (D<sub>2</sub>O). The model proteins studied were myoglobin,  $\alpha$ -lactalbumin and  $\beta$ -lactoglobulin having different secondary structures. It could be shown that the performance of the

separation was comparable to conventional UV-Vis detection and that the peak position of the proteins studied were the same as obtained in reference measurements using the ATR technique.

Key words: Capillary electrophoresis, FTIR spectroscopy, protein separation, protein structure

## **Introduction**

Capillary electrophoresis (CE) has evolved to a powerful and increasingly important separation technique in analytical chemistry [1-3]. Especially in biochemical analysis, CE has found widespread use mainly because of its high separation efficiency and low sample consumption. In CE separation is achieved in narrow bore fused silica capillaries. In general these capillaries with an inner diameter of 50-150  $\mu\text{m}$  are filled with a buffer solution that produce a charged inner capillary wall. Application of a high voltage across the capillary results in bulk electroosmotic flow inside the capillary. Due to different electrophoretic mobilities of the analytes injected into the capillary they migrate inside the capillary with a different velocity thus achieving separation. Detection in CE is difficult for several reasons. First the amount of sample available for detection is small because only a few nanoliters of sample are injected into the capillary. Furthermore, especially considering on-capillary UV-Vis detection, sensitivity is limited by the small bore diameter of the capillaries. Finally the need to apply a high potential during separation presents challenges for off-line detection techniques. When analyte labelling is possible high sensitive on-capillary detection can be achieved by laser induced fluorescence [4,5]. Important structural information

can be obtained by coupling mass spectrometry on-line to the capillary [6-8]. In this case volatile buffers need to be used in order to assure long-term stability. For mid-infrared spectroscopic detection both off-line as well as on-line measurements have been reported so far [9-12]. The attractive feature of off-line detection based on sample deposition and solvent, and if possible, buffer elimination is access to the full analyte spectrum. These spectra measured in condensed phase would allow application of standard spectral libraries for spectrum comparison and identification of unknown analytes. So far several working interfaces have been reported indicating the feasibility of this concept [9,10]. However, recently, more reports on successful on-line FTIR detection have been shown [11-14]. The appealing aspects of on-line detection may be seen in the universality of the concept which allows to accommodate all variants of capillary electrophoresis including micellar electrokinetic chromatography where micelles are formed inside the capillary to assist the separation of neutral analytes. In transmission measurement using dedicated IR transparent flow cells inserted between two pieces of capillaries part of the spectrum is blocked due to strong absorption of the liquid phase. On-line detection based on the attenuated total reflection technique circumvents this problem due to the efficiently reduced optical path. The usefulness of on-line FTIR detection has been demonstrated on the separation and quantification of adenosine, guanosine and adenosine-5'-monophosphate (AMP) in the ng-region using conventional capillary zone electrophoresis [13]. MEKC has also been demonstrated for the separation of 5 analytes reporting on successful qualitative and quantitative results [12]. The maturity of CE-FTIR has recently been shown on the separation and quantification of sugars in soft-drinks [15]. The particular advantages of the molecular specific information contained in the vibrational spectra has been highlighted on the on-line discrimination



of enantiomers during a chiral separation performed in non aqueous media. Interaction of the analyte molecules with the chiral selector produced diastereomers with clearly distinct spectral features allowing for their discrimination. A further research area where infrared spectrometry can provide important information is protein analysis. Main application of FTIR spectroscopy may be seen in studying protein dynamics as well as in the elucidation of the secondary structure [16,17]. It is the latter aspect that makes FTIR spectroscopy a highly interesting detection method in capillary electrophoresis. This paper reports on the first protein separation in capillary electrophoresis with on-line FTIR spectroscopy and discusses the obtained results.

### **Experimental Section**

**IR-flow cell:** The flow cell made of CaF<sub>2</sub> windows and SU-8 polymer was fabricated as outlined in detail previously [12]. Basically, it consisted out of two CaF<sub>2</sub> disks where on one of them the polymer was applied and using UV light and a photomask the channel structure was formed. The second CaF<sub>2</sub> disk was used to close the formed structure to get the complete flow cell.

The channel for IR detection was 2 mm long with a cross section of 150 \* 15 µm. For the connection between the flow cell and the capillaries an improved interface has been developed. The flow cell was put into a custom-built supporting block allowing fine adjustment of cell and capillaries. The capillaries were coupled to the flow cell through bolts ensuring that the capillaries were at the same level as the flow channel of the cell. One side of the supporting block was movable to exert pressure on the cell and the O-rings used to tighten the interface between cell and capillaries. The exerted pressure also aligned the flow cell inside the supporting block. The O-rings used had

an inner diameter of 500  $\mu\text{m}$  and consisted of rubber (Flume GmbH, Essen, Germany). Therefore the time-consuming and tedious process of fabricating the O-rings could be circumvented. This arrangement allowed for quick and easy changes of the capillaries.

**FTIR spectroscopy.** A schematic view of the experimental setup including the capillary electrophoresis system and the system for on-line FT-IR detection is shown in Fig.1. For spectrum acquisition a Bruker Equinox 55 FT-IR spectrometer (Bruker Optik GmbH, Karlsruhe, Germany) was used. To enable the IR beam to be focused correctly, the IR flow cell was placed in an external beam condenser, constructed in-house [18], which was placed in a Perspex housing and purged with dry air. The IR beam from an external optical port of the spectrometer was focused on the cell by means of an off-axis parabolic mirror (focal length 69 mm) and then using three more mirrors was directed to a highly sensitive mercury cadmium telluride (MCT) detector (Fig.1). The scanner of the spectrometer was operated at a HeNe laser modulation frequency of 150 kHz, fifty scans were coadded for each spectrum with a spectral resolution of  $8\text{ cm}^{-1}$  (background spectra 500 coadditions).

Reference measurements of the analytes were obtained by attenuated total reflection (ATR), using a diamond ATR cell (SensIR, Danbury, CT) with a circular surface of 3 mm and three internal reflections. For these measurements the MIR version of a Bruker Matrix-F was used, the scanner velocity was set to 40 kHz and 256 scans were coadded for each spectrum.

**Electrophoresis:** The capillary electrophoresis CE system, which was built in-house consisted of a high-voltage power supply (Brandenburg, Thornton Heath, UK), two platinum electrodes and untreated fused-silica capillaries (i.d. 50  $\mu\text{m}$ , o.d. 375  $\mu\text{m}$ ,

Polymicro Technologies, Phoenix, AZ). The separation voltage applied (at the injection end of the capillary) was +20kV, resulting in a current of 12  $\mu$ A measured over a 100-k $\Omega$  resistance. New capillaries were preconditioned with 0.1 M NaOH, distilled water and running buffer before the first use. The capillary surface was refreshed at start-up each day using 0.1 M NaOH and buffer. Between the runs the capillaries were cleaned with 50 mM SDS [19], distilled water and buffer. The total length of the capillary was 60 cm and the length from the injection point to the IR cell was 40 cm (fig. 1). Hydrodynamic injection of the samples was performed by lifting the injection side of the capillary 30 cm for 15 seconds, resulting in sample injection volumes of 10 nL. During the optimisation of the separation conditions a CV<sup>4</sup> UV-visible detector (ISCO, Lincoln, NE) set at 200 nm and an ELDS Pro 1.0 laboratory data system (Chromatography Data System, Kungshög, Sweden) was used. For on-line UV detection a detection window was made by burning away a small piece of the surrounding polyamide coating of the capillary.

**Reagents:** Myoglobin,  $\alpha$ -lactalbumin and  $\beta$ -lactoglobulin, D<sub>2</sub>O and borax were all of analytical grade (Fluka, Buchs, Switzerland) and were used as received. Solutions of 2 mg/mL of the proteins were made in 20 mM borax buffer in heavy water. The preparation of the buffer and also the dissolving of the proteins were carried out in a glove box after purging with dry air for an hour. A 20 mM borax buffer in heavy water was used as a running buffer without adjusting the pD value any more (pD 9.2). The buffer was filtrated through a 0.2  $\mu$ m syringe filter before use and was then degassed for 15 min using a shaker inside the glove box.

## Results and Discussion

The aim of the experiments was to separate a mixture of proteins using capillary electrophoresis and to record their FTIR spectra “on-the-run”. The most relevant part of the protein spectra is the region of the amid I band which, unfortunately, heavily overlaps with the bending vibration of water. As the available micro-machined flow cell had an optical path of 15  $\mu\text{m}$  the experiments had to be conducted in heavy water in order to shift the bending vibration of the solvent down to  $1210\text{ cm}^{-1}$ . In doing so the important amide region could be studied with the available flow cell.

To facilitate electrophoretic separation the conductivity of the background electrolyte and the samples was matched by dissolving the analytes in 20 mM Borax which was also used as background electrolyte. Because of H-D exchange in the protein some HDO is formed in the sample solutions. Figure 2 shows characteristic electropherograms obtained upon injection of 10 nL of a sample mixture containing the three selected model proteins at concentrations of 2 mg/ml each. First the trace shown in Fig 2a was obtained using UV detection at a capillary length of 60 cm (detector at 40 cm). Subsequently the capillary was cut and the IR cell inserted at the position of the UV detection and the separation repeated. For purpose of comparison with the UV electropherogram a single trace was calculated from the recorded FTIR spectra (Figure 2b). For this purpose each recorded spectra was integrated between  $1430$  and  $1660\text{ cm}^{-1}$  and this value plotted as a function of time. Comparison of the obtained electropherograms reveals 5 peaks in the separation using IR detection whereas only 4 peaks have been obtained when using the UV detection. In capillary electrophoresis, a so-called “EOF” (electroosmotic flow) peak is frequently observed. This peak results from the difference between sample matrix from which the analytes are removed and the background electrolyte during the separation. In this particular

case the EOF peak is not observed in the UV because the sample matrix was practically identical with the separation buffer. However, due to the H-D exchange, which took place after dissolving the proteins in the buffer, significantly more HDO was present in the injected solution than in the separation buffer. Because of the strong spectral differences between HDO as compared to D<sub>2</sub>O, the EOF peak could be observed in the electropherogram when using on-line FTIR detection. The other peaks in the electropherograms can be attributed to the separated proteins. The separation power of the capillary electrophoresis can be seen by the two isoforms of  $\beta$ -lactoglobulin, which could be separated allowing their individual investigation by FTIR spectrometry.

In figure 3 a section of the obtained FTIR electropherogram is shown. The signal-to-noise of the experimental set-up was sufficient to record several FTIR spectra during the passage of the separated proteins through the detector. Representative spectra of each peak have been extracted from the recorded data set and are compared with reference spectra of the corresponding proteins (Fig. 4a-d). In the reference spectra a strong peak at about 1450 cm<sup>-1</sup> can be detected which is absent in the protein spectra recorded on-line during the CE separation. This peak results from HDO, which was present in the protein solution, probably due to the H-D exchange in the protein. The absorbance values obtained for the amide I band in the on-line recorded protein spectra are in the order of a few milli-absorbance units. Therefore, the signal to noise ratio of the spectra is not sufficient to perform a detailed analysis of the band shape of the amide I band. However, a comparison of the position of the peak maxima of the amide I band in the on-line recorded spectra and the reference spectra was possible (table 1). The position of the amide I band is an indicator of the secondary structure of a protein. It can be clearly seen that the structure of myoglobin and  $\alpha$ -lactalbumin

is predominantly helical ( $\alpha$ -structure), while the position of the bands for the isoforms of  $\beta$ -lactoglobulin indicate that this protein mainly takes a pleated structure ( $\beta$ -sheet conformation).

From the good agreement of the band positions we can conclude that the signal to noise ratio was sufficient to tell the dominant secondary structure of the separated proteins during the CE separation.

### **Conclusion**

Separation and on-line detection of a mixture of proteins using capillary electrophoresis with FTIR spectroscopic detection has been shown for the first time. With the experimental conditions chosen 4-5 FTIR spectra were recorded for every protein passing the flow cell used for transmission measurements. Whereas the peak position (amid I band) of the on-line recorded FTIR spectra were in good agreement with those of reference spectra an improvement in signal to noise needs to be made to allow a more detailed analysis of the recorded FTIR spectra.

### **Acknowledgement**

The authors are grateful for financial support received within the project 15531 of the Austrian Science Fund.

## Reference List

- [1] N. Anastos, N.W. Barnett, S. Lewis *Talanta* **2005**, *67*, 269-79.
- [2] P.G. Righetti *Journal of Chromatography, A* **2005**, *1079*, 24-40.
- [3] M. Lämmerhofer *Journal of Chromatography, A* **2005**, *1068*, 3-30.
- [4] M. Lacroix, V. Poinso, C. Fournier, F. Couderc *Electrophoresis* **2005**, *26*, 2608-21.
- [5] C.L. Flurer *Electrophoresis* **2003**, *24*, 4116-27.
- [6] M.R. Monton, S. Terabe *Analytical Sciences* **2005**, *21*, 5-13.
- [7] P. Schmitt-Kopplin, M. Englmann *Electrophoresis* **2005**, *26*, 1209-20.
- [8] D.C. Simpson, R.D. Smith *Electrophoresis* **2005**, *26*, 1291-305.
- [9] J.L. Jarman, R.A. Todebush, J.A. de Haseth *Journal of Chromatography A* **2002**, *976*, 19-26.
- [10] R.A. Todebush, L.-T. He, J.A. de Haseth *Analytical Chemistry* **2003**, *75*, 1393-99.
- [11] B. Lendl, M. Kölhed, P. Hinsmann, M. Haberkorn, P. Svasek, B. Karlberg *Micro Total Analysis Systems 2002, Proceedings of the mTAS 2002 Symposium, 6th, Nara, Japan, Nov.3-7, 2002* **2002**, *1*, 599-601.
- [12] P. Hinsmann, L. Arce, P. Svasek, M. Lämmerhofer, B. Lendl, *Applied Spectroscopy* **2004**, *58*, 662-66.
- [13] M. Kölhed, P. Hinsmann, P. Svasek, J. Frank, B. Karlberg, B. Lendl *Analytical Chemistry* **2002**, *74*, 3843-48.
- [14] B.M. Patterson, N.D. Danielson, A.J. Sommer *Analytical Chemistry* **2004**, *76*, 3826-32.
- [15] M. Kölhed, B. Karlberg *Analyst* **2005**, *130*, 772-78.
- [16] A. Barth, C. Zscherp *Quarterly Review of Biophysics* **2002**, *35*, 369-430.
- [17] H. Fabian, W. Mäntele in J.M. Chalmers, P. Griffiths, *Handbook of Vibrational Spectroscopy*; John Wiley & Sons Ltd.: 2002., p.3399.
- [18] P. Hinsmann, M. Haberkorn, J. Frank, P. Svasek, M. Harasek, B. Lendl *Applied Spectroscopy* **2001**, *55*, 241-51.
- [19] D.K. Lloyd, H. Wätzig *Journal of Chromatography B* **1994**, *663*, 400-05.

Table 1 comparison between the CE separation and the reference spectra

Protein	wavenumber reference	wavenumber CE separation
myoglobin	1646 cm <sup>-1</sup>	1648 cm <sup>-1</sup>
α-lactalbumin	1646 cm <sup>-1</sup>	1646 cm <sup>-1</sup>
β-lactoglobulin 1.isoform	1634 cm <sup>-1</sup>	1635 cm <sup>-1</sup>
β-lactoglobulin 2.isoform	1634 cm <sup>-1</sup>	1633 cm <sup>-1</sup>



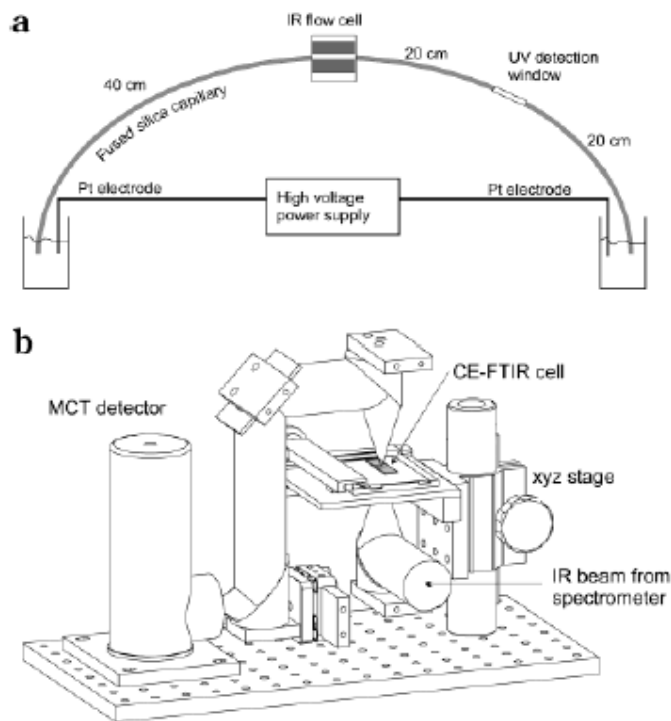


Figure 1 (a) schematic diagram of the experimental setup. (b) optical setup: the IR beam from the spectrometer is focused on the flow channel of the CE-FT-IR cell by means of a parabolic mirror and then on a highly sensitive MCT detector.

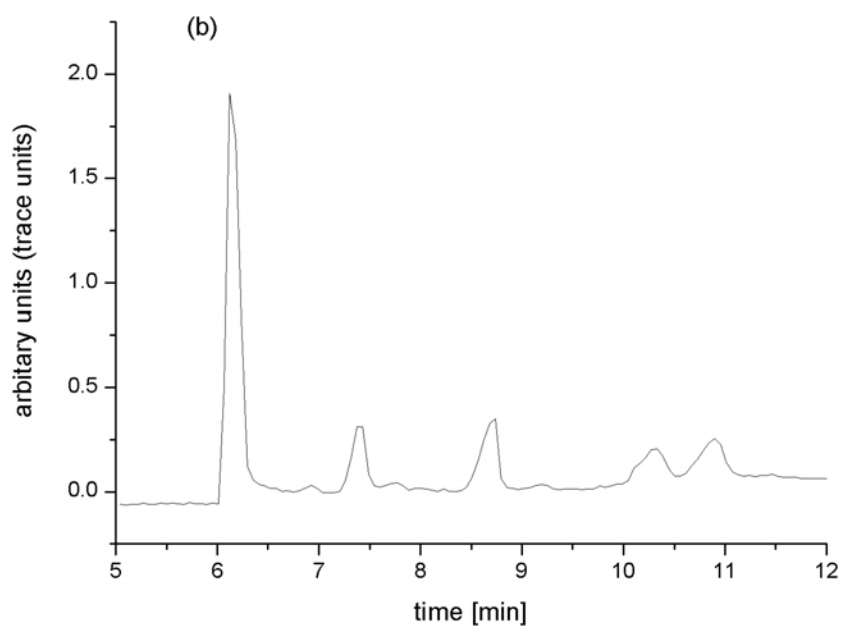
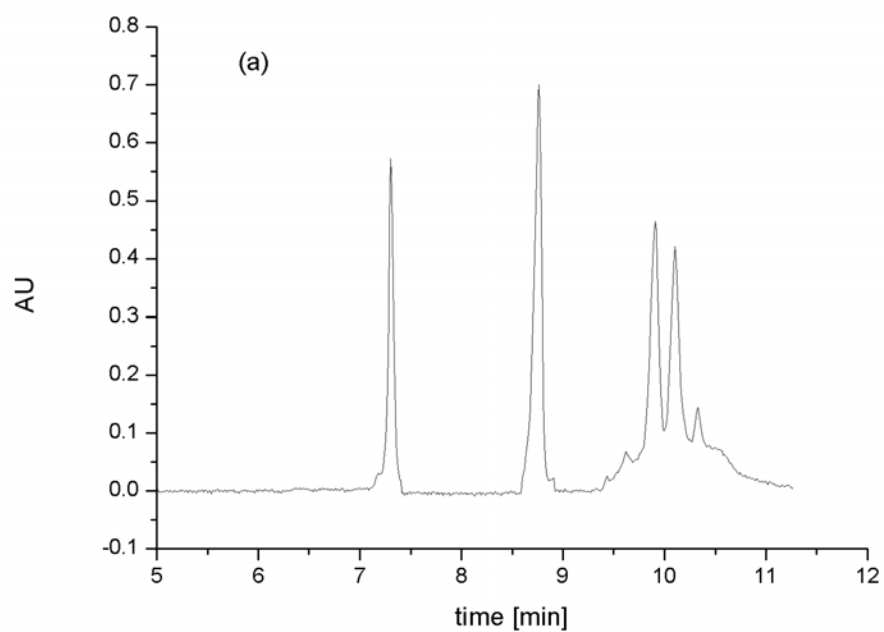


Figure 2 (a) typical electropherogram recorded with a UV detector. (b) IR trace as integration over time showing the CE separation (first peak EOF)

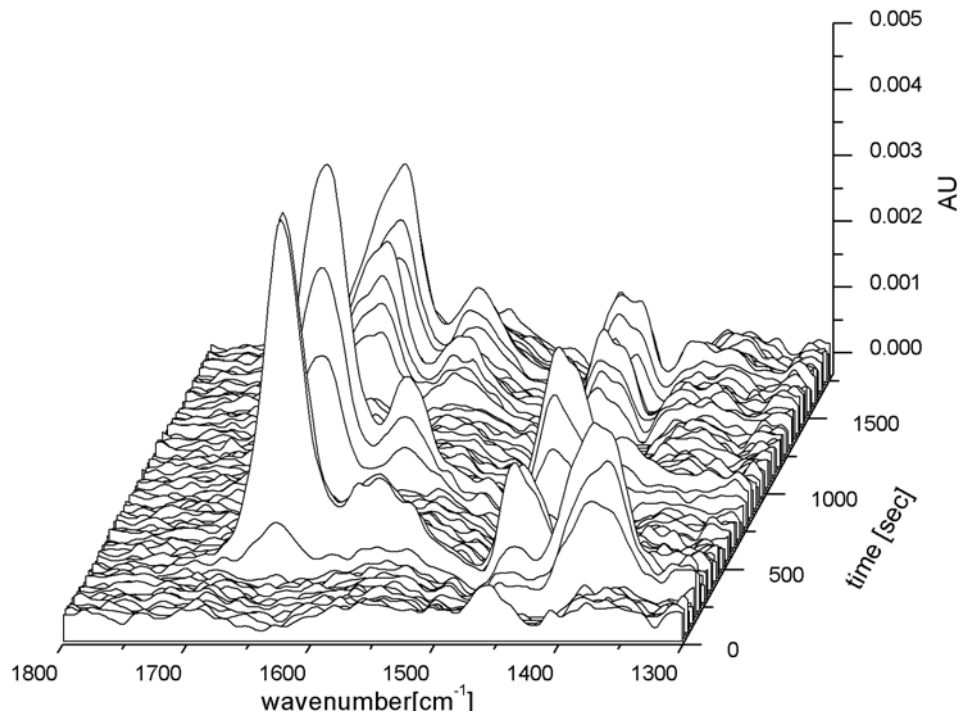
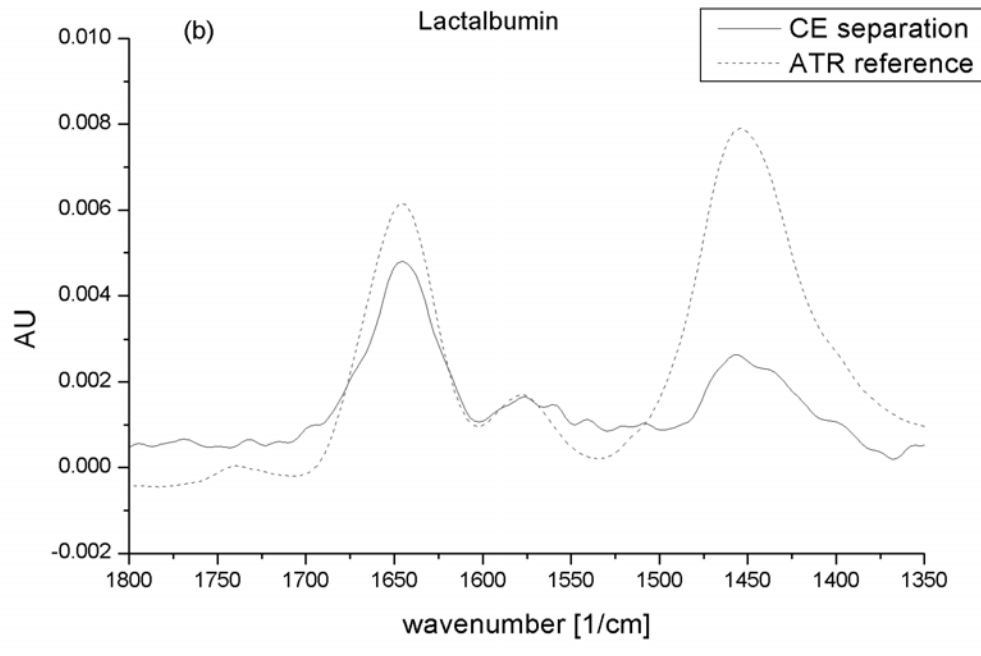
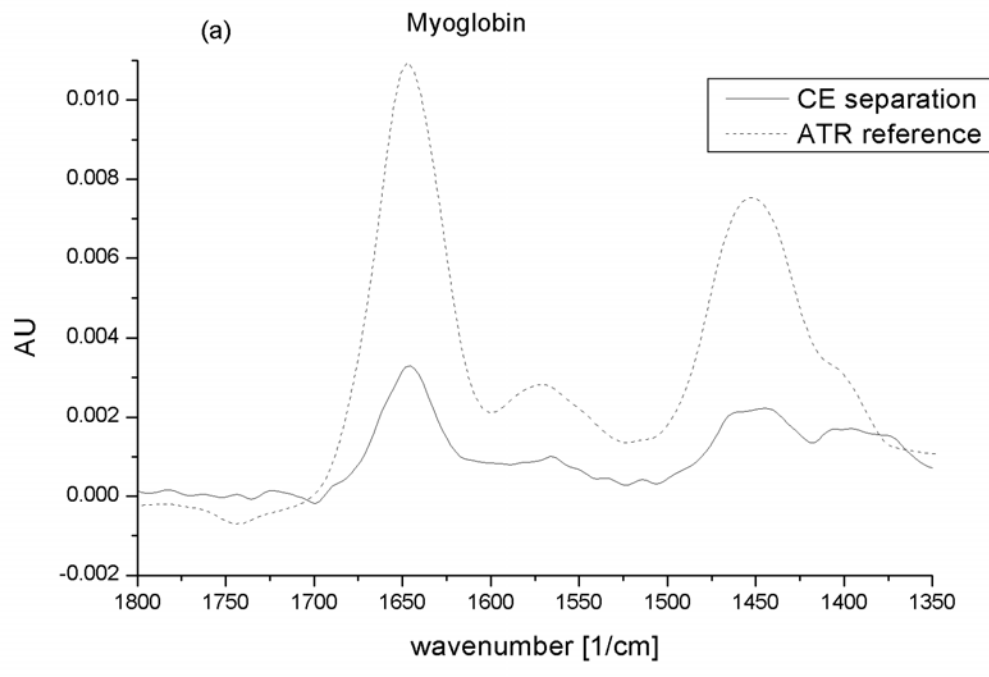


Figure 3 three-dimensional plot of the separation showing the separation and the spectral differences obtained using FTIR as a detection system



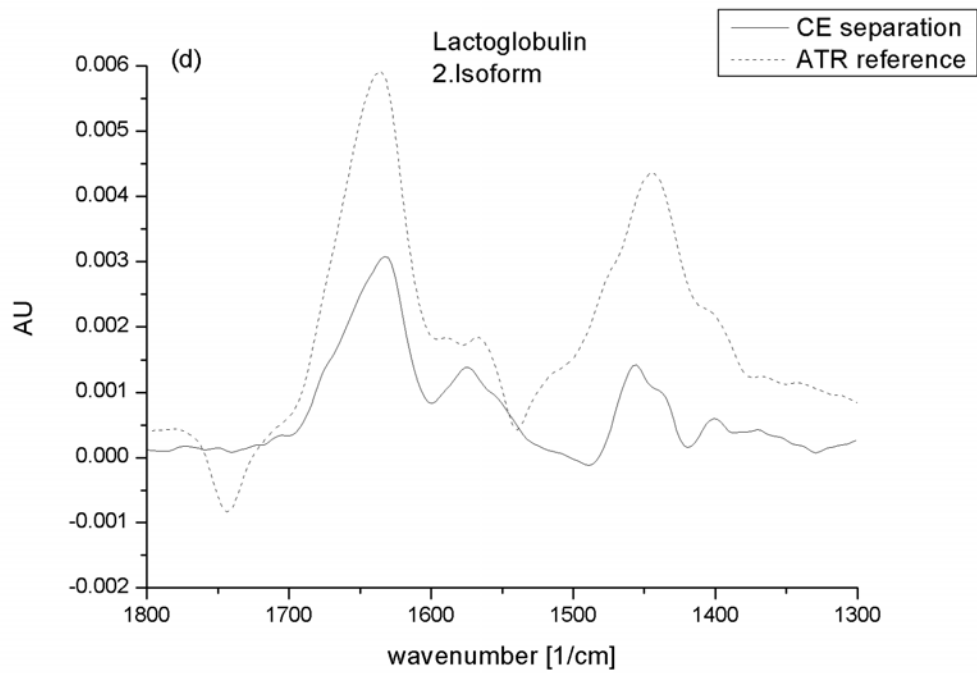
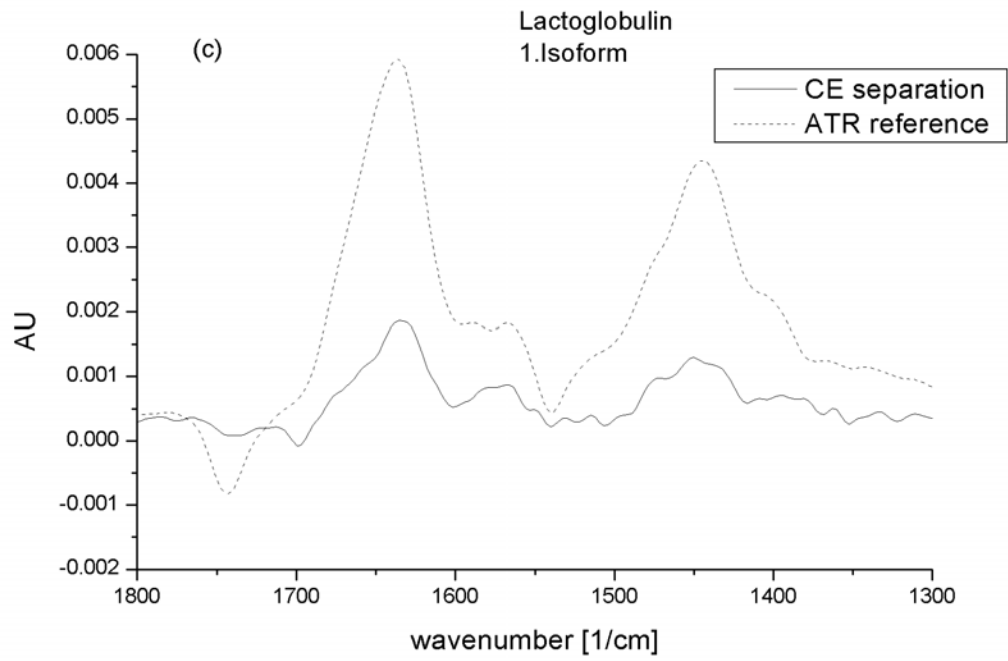


Figure 4 comparisons between the spectra from the CE run and the ATR reference measurement (a) myoglobin, (b)  $\alpha$ -lactalbumin, (c)  $\beta$ -lactoglobulin 1.isoform , (d)  $\beta$ -lactoglobulin 2.isoform

## II

Kulka, S.; Kaun, N.; Baena, J.R.; Frank, J.; Svasek, P.; Moss, D.; Vellekoop M.J.; Lendl, B.

*"Mid-IR synchrotron radiation for molecular specific detection in microchip-based analysis systems"*

Analytical and Bioanalytical Chemistry **2004**, 378, 1735-1740

S. Kulka · N. Kaun · J. R. Baena · J. Frank · P. Svasek  
D. Moss · M. J. Vellekoop · B. Lendl

## Mid-IR synchrotron radiation for molecular specific detection in microchip-based analysis systems

Received: 2 October 2003 / Revised: 30 January 2004 / Accepted: 2 February 2004 / Published online: 2 March 2004  
© Springer-Verlag 2004

**Abstract** Microstructures constructed from SU-8 polymer and produced on CaF<sub>2</sub> base plates have been developed for microchip-based analysis systems used to perform FTIR spectroscopic detection using mid-IR synchrotron radiation. The high brilliance of the synchrotron source enables measurements at spot sizes at the diffraction limit of mid-IR radiation. This corresponds to a spatial resolution of a few micrometers (5–20 μm). These small measurement spots are useful for lab-on-a-chip devices, since their sizes are comparable to those of the structures usually used in these devices. Two different types of microchips are introduced here. The first chip was designed for time-resolved FTIR investigations of chemical reactions in solution. The second chip was designed for chip-based electrophoresis with IR detection on-chip. The results obtained prove the operational functionality of these chips, and indicate the potential of these new devices for further applications in (bio)analytical chemistry.

**Keywords** Synchrotron radiation · Time resolved IR spectroscopy · Capillary electrophoresis · Lab-on-a-chip · SU-8

### Introduction

Miniaturization of chemical analysis systems remains a major driving force in the development of advanced instrumentation for analytical chemistry. Frequently, the ultimate goal of miniaturization is seen as the development of self-contained sensor-like analysis systems known as “lab-on-a-chip” devices or micro total analysis systems. However, to obtain significant advantages from chip-based liquid handling, complete miniaturization of the whole analysis system is not usually required.

Especially when dealing with instrumentally complex detection systems like mass spectrometry [1], nuclear magnetic resonance [2] or vibrational spectroscopic techniques (infrared and Raman) [3, 4], microchips may be viewed rather as valuable add-ons to these powerful detectors rather than as stand-alone micro-systems. In many cases, an appropriate microchip for fluid handling may extend the problem-solving capabilities of these detectors due to the added degree of experimental flexibility. An example of this is the use of microchips for the study of (bio)chemical reactions with high time resolution and minimum sample consumption via Fourier transform mid-infrared spectrometry [4, 5, 6]. In this case, miniaturization and integration of micro-mixers in IR transmission cells enables fast diffusive mixing by the generation of short diffusion distances inside the mixer. These devices allow complete diffusive mixing of two solutions in less than 100 ms and the simultaneous recording of the reaction-induced spectral changes on-chip. From these changes, details about the reaction under study may be deduced, and intermediates characterized. In a similar way, fast mixers have been used to study chemical reactions via mass spectrometry, although in this case with substantially lower time resolution since only off-chip measurements are possible [7].

Within the group of optical techniques based on absorption measurements, mid-IR detection holds a special position; in contrast to absorption measurements at shorter wavelength (UV-Vis or NIR spectrometry) no loss in sensitivity is incurred upon miniaturization. This is because

---

S. Kulka · N. Kaun · J. R. Baena · J. Frank · B. Lendl (✉)  
Institute of Chemical Technologies and Analytics,  
Vienna University of Technology,  
Getreidemarkt 164-AC, 1060 Vienna, Austria  
e-mail: blendl@mail.zserv.tuwien.ac.at

P. Svasek  
Ludwig Boltzmann Institute of Biomedical Microtechnology,  
Vienna, Austria

D. Moss  
Institute for Synchrotron Radiation,  
Forschungszentrum Karlsruhe,  
Postfach 3640, 76021 Karlsruhe, Germany

M. J. Vellekoop  
Institute of Industrial Electronics and Material Science,  
Vienna University of Technology,  
Gusshausstrasse 27–19, 1040 Vienna, Austria

mid-IR detection is already confined to small path-lengths in normal-sized systems due to strong solvent absorption. This especially applies for water, as for measurements in the information-rich fingerprint region the optical path must be kept in the region of  $10\ \mu\text{m}$ . Even shorter paths ( $<8\ \mu\text{m}$ ) are required if the amide I band from proteins is to be measured too [8, 9], because this band heavily overlaps with the bending vibration of the water molecule ( $1640\ \text{cm}^{-1}$ ). An alternative solution would be the use of heavy water, where the solvent absorption bands are shifted away from the amide I band, towards lower frequencies [10]. However, even in this case optical paths must still be kept within the low- $\mu\text{m}$  region.

Therefore, a reduction in the detection volume for on-chip mid-IR detection can only be realized by reducing the beam diameter. The use of an economical beam-condensator already allows a parallel beam taken from an FTIR spectrometer to be focused to a spot diameter of about  $1\ \text{mm}$ , resulting in a probed volume of  $\sim 8\ \text{nl}$  when considering an optical path of  $10\ \mu\text{m}$ . Such a detection volume is rather big for chip-based analysis systems, but appropriate for the time-resolved analysis of a chemical reaction in solution using a microchip device operated in the stopped-flow mode [4, 5]. Such a detection volume has also proven to be adequate for successful on-line FTIR detection in capillary zone electrophoresis [11] and micellar electrokinetic chromatography [12]. For these applications, a dedicated IR transparent chip for detection has been connected to conventional capillaries (i.d.  $75\ \mu\text{m}$ ). However on-chip injection and detection using a chip for infrared detection has not yet been demonstrated. If the beam-condensator is replaced by an IR microscope attached to an FTIR spectrometer, the spot size may be reduced to  $\sim 100\ \mu\text{m}$  without facing degradation in the signal-to-noise ratio due to reduced optical throughput. In this case, again assuming an optical path of  $10\ \mu\text{m}$ , the probed volume can be reduced to  $80\ \text{pl}$ . Such a configuration can already be used to probe different positions on a chip device [6]. This opens up the possibility of studying chemical reactions in solution with better time resolution than stopped flow technique, using continuous flow experiments instead. In such experiments the time resolution is defined by the distance between the mixing point and the sample spot, as well as by the flow rate applied. A further reduction in spot size can be achieved (while still maintaining a high signal-to-noise ratio) if the light source of the FTIR spectrometer (globalar) is replaced by a synchrotron radiation source [13, 14]. Although the number of photons emitted per second in the mid-IR spectral region by the globalar is comparable to the number emitted by the synchrotron source, the synchrotron has a distinct advantage over the globalar in that it naturally produces a highly collimated beam of small diameter. Therefore, the brilliance of a synchrotron source, in terms of photons emitted per second and per solid angle, is significantly higher than that of a globalar – although the throughput advantage of the synchrotron source over a globalar obviously only applies if measurements are to be performed on a small spot size [14]. Using an FTIR microscope and synchrotron radiation, high quality measure-

ments at spot sizes close to the diffraction limit of a given wavelength are possible. For mid-IR detection in a  $10\ \mu\text{m}$ -thick micro-channel with a spot size of  $10\ \mu\text{m}$ , we can achieve a probed volume of only  $0.8\ \text{pl}$ . The realization of this very small volume for mid-IR detection is highly-applicable to chip-based separation and detection systems, as well as to time-resolved experiments with high time resolution and low sample consumption.

It was the aim of this study to produce microchips containing small channels and test them at the new IR beam-line of the synchrotron radiation source ANKA in Karlsruhe (Forschungszentrum Karlsruhe, Germany). For this purpose, two different chip designs, one designed for time-resolved FTIR spectroscopy and the other for on-chip capillary electrophoresis, have been produced. In this paper, the first experimental results obtained from them are reported.

## Experimental

### Microchip fabrication and packaging

Two different microchip geometries have been produced on 4 inch-wide  $\times$  1 mm-thick  $\text{CaF}_2$  wafers. Because standard materials for microchip fabrication, such as silicon, glass or polymer materials, are not transparent in the mid-IR spectral region,  $\text{CaF}_2$  must be used instead. Due to its insolubility in water,  $\text{CaF}_2$  is an appropriate material for producing IR chips [4, 5, 11, 12].

By applying SU-8 technology, structures have been realized on the wafers, and the wafers have been bonded. The geometries of the structures produced are shown in Fig. 1. Design A was intended for time-resolved FTIR spectroscopy in the continuous flow mode, and design B was made for on-chip electrophoresis. For the latter application it was considered important to produce channels made out of one type of material. Therefore, prior to producing the SU-8 structures on the  $\text{CaF}_2$  wafers, they were coated with a  $0.5\ \mu\text{m}$  thick SU-8 layer, and exposed to oxygen plasma for two minutes to make them hydrophilic so that another layer of SU-8 could be deposited (Fig. 2a). Due to the thin nature of the SU-8 layer, the throughput for mid-IR measurements was not impaired despite the fact that the SU-8 characteristic bands were clearly visible in the recorded single beam spectra.

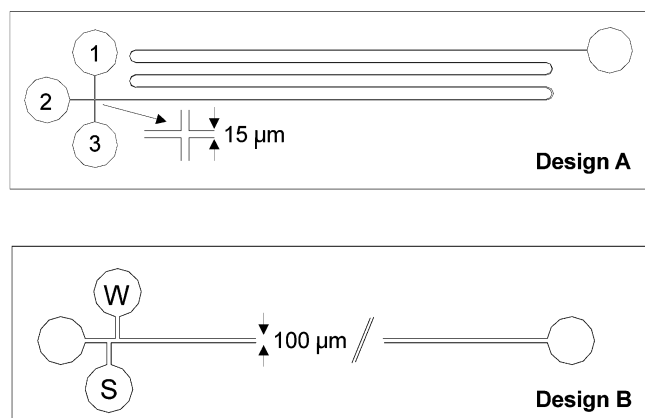
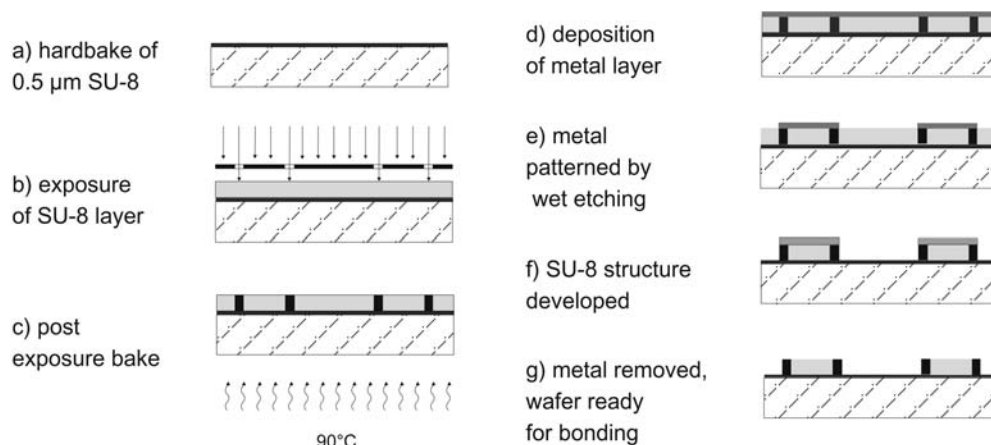


**Fig. 1** Schematic drawing of the structures made on  $\text{CaF}_2$  wafers. Design A was made for time-resolved FTIR spectroscopy of chemical reactions in solution. The reagents are introduced at the inlets 1, 2 and 3. Design B was made for electrophoretic separations with on-chip IR detection. The device is loaded by introducing the sample via hydrodynamic pumping from port S to waste (W)



**Fig. 2** Schematic of the production of micro-devices on CaF<sub>2</sub> wafers using SU-8 structuring technology. For details see text



The flow channel was formed by two lines of epoxy-based photoresist SU-8 (Microchem Corp. Newton, MA), each of them 60 μm wide. The distance between two lines, and therefore the width of the channel formed, was 15 and 100 μm for designs A and B respectively. The height of the SU-8 lines were about 10 μm, equivalent to the desired optical path. One of the CaF<sub>2</sub> wafers already carrying the 0.5 μm thick SU-8 layer was spin-coated with SU-8 and softbaked (90 °C, 30 min). After UV-exposure for 30 s using a SUSS MJB3 mask aligner (Suss Microtech, Munich, Germany) and an appropriate photomask, the resist was post-exposure-baked at 90 °C for 10 min (see Fig. 2b and c). A metal layer (1 μm Ag) was deposited by evaporation on this wafer (Fig. 2d). This layer was patterned by wet etching (Fig. 2e). The areas where unexposed SU-8 was necessary for bonding were surrounded by narrow lines of exposed (hard) SU-8 and covered by metal. After development of the SU-8 with propylene glycol monomethyl ether acetate (PGMEA), the metal layer was removed (Fig. 2f and g). The unexposed and therefore not crosslinked areas of SU-8 were dissolved during the development process. The reason for covering some areas with the metal is to prevent them from getting exposed and to keep them soft, and also to make sure that they are not removed during the development process. The two wafers, with one carrying the structure, were aligned in an EVG AL6 mask aligner (EV group, Schärding, Austria) and the wafer stack was inserted into an EVG 501 wafer bonder (EV group). Bonding was accomplished by applying a contact force of 1000 N while the temperature was increased up to 180 °C with a ramp of 3 °C/min, and left for 1 h. Finally the temperature was decreased to room temperature with a ramp of 2 °C/min and the contact force was removed. This procedure is necessary to induce a complete crosslinking of SU-8 and to develop full mechanical strength and chemical resistance. The soft parts of SU-8 were used to fill small gaps caused by non-uniform layer thickness, meaning that less contact force is necessary when the gaps are filled and so the structures are not deformed and their correct height and shape is maintained during the bonding process. The resulting microchips were placed in dedicated supports made out of PMMA, to facilitate the supply of the chips with reagents and the electrodes as required for the experiments. The connections to the support were all standard flow injection threaded fittings for simple liquid handling. The openings of the chips were sealed to the support with commercially-available O-rings (Zorzi, Vienna, Austria) to ensure tightness. This arrangement made it possible to exchange the microchips easily. The supports carrying the microchips were screwed onto a metal plate that fitted the xy-stage of the IR-microscope attached to the synchrotron source.

#### FT-IR spectrometer and synchrotron source

The IR light used in this study was generated by a synchrotron light source (ANKA, Karlsruhe, Germany), a particle accelerator providing a high-brilliance beam of photons covering a broad spectral

range. The synchrotron radiation is emitted when electrons moving at relativistic speed interact with a magnetic field due to quantum mechanical effects. The radiation covers a spectral range from the hard X-ray to the terahertz range. The infrared beamline is set up where one of the magnets interacts with the electrons and the IR light is guided through a diamond window and a dedicated system of filters and mirrors to the IR spectrometer. A conventional Bruker 66v FT-IR spectrometer (Bruker Optik, Germany) was used throughout all of the experiments. The IR beam was coupled to an IR microscope (Bruker IRscope II) using two parabolic mirrors. The scanner of the spectrometer was operated at a HeNe laser modulation frequency of 100 kHz. Fifty spectra were coadded for each spectrum, with a spectral resolution of 8 cm<sup>-1</sup>.

Reference spectra of myoglobin were recorded using a diamond ATR (attenuated total reflection) unit from SensIR (Danbury, CT) attached to a Bruker IR-cube spectrometer.

#### IR-chip manifolds

To supply the IR chip for the time-resolved experiments (Fig. 1, design A) with reagent, a precise low flow pump (Novodirect, Kehl, Germany) equipped with three 0.5 ml syringes was used. The capillary electrophoresis system was built in-house, and consisted of a high-voltage power supply (Spellman, New York, USA) and two platinum electrodes inserted into standard FIA fittings. The electrodes were attached to the chip by screwing the corresponding fittings into the support such that the electrodes touched the running buffer.

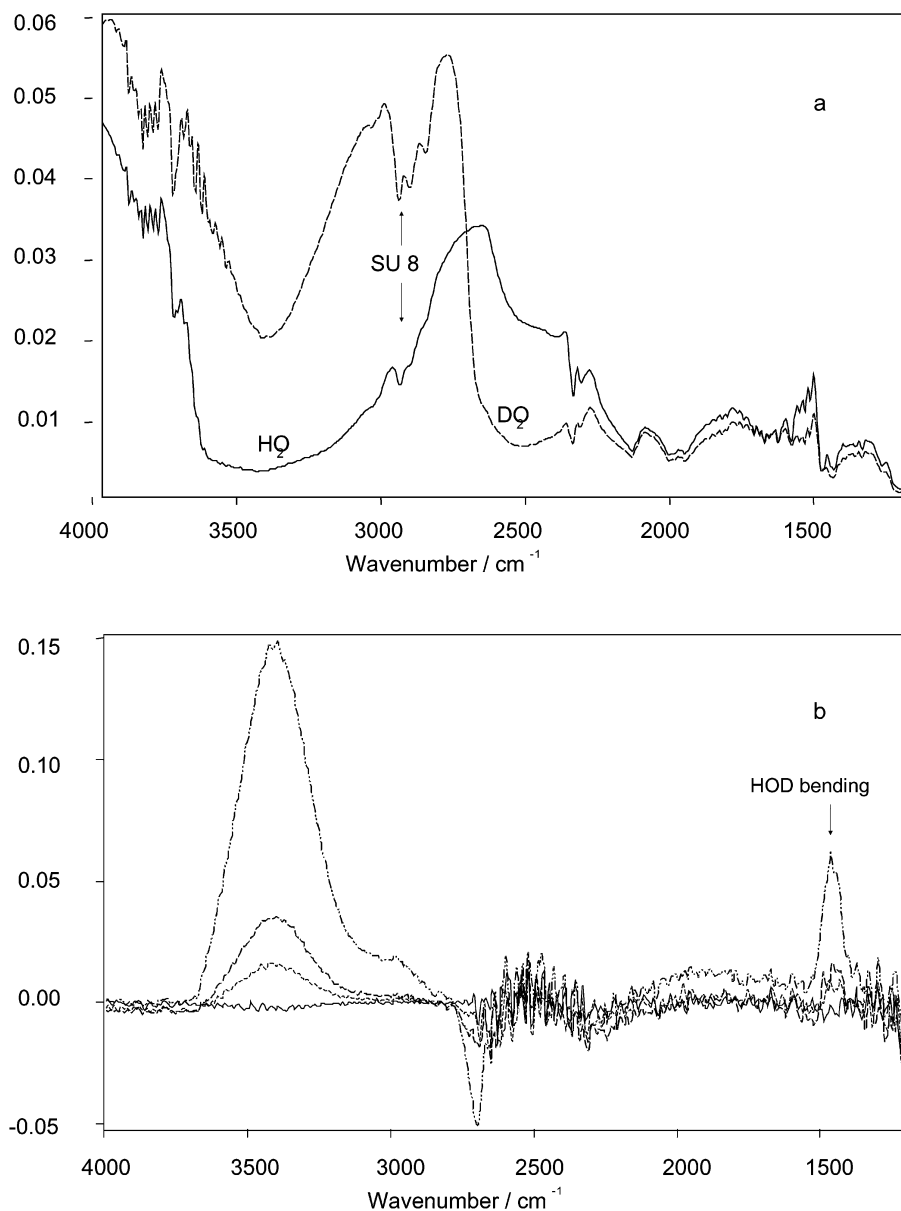
#### Chemicals

HPLC-grade water, heavy water, myoglobin, and borax, all of analytical grade (Fluka, Buchs, Switzerland) were used as received. A 20 mM borax buffer in D<sub>2</sub>O (pD=9.2), and a 2 g/L myoglobin standard in this buffer were prepared. Prior to experiments, the solutions were filtered through a 0.2 μm filter to prevent clogging of the microchip channels.

## Results and discussion

At the start of the measurement campaign at ANKA, the microchip designed for time-resolved FTIR spectroscopic investigation was used. The dimensions of the experimental set-up permitted the use of the 15× objective at the IR-microscope. With this arrangement, a focus spot of 20 μm can be achieved. Spectra of normal and heavy water with clearly-distinct positions of the corresponding absorption

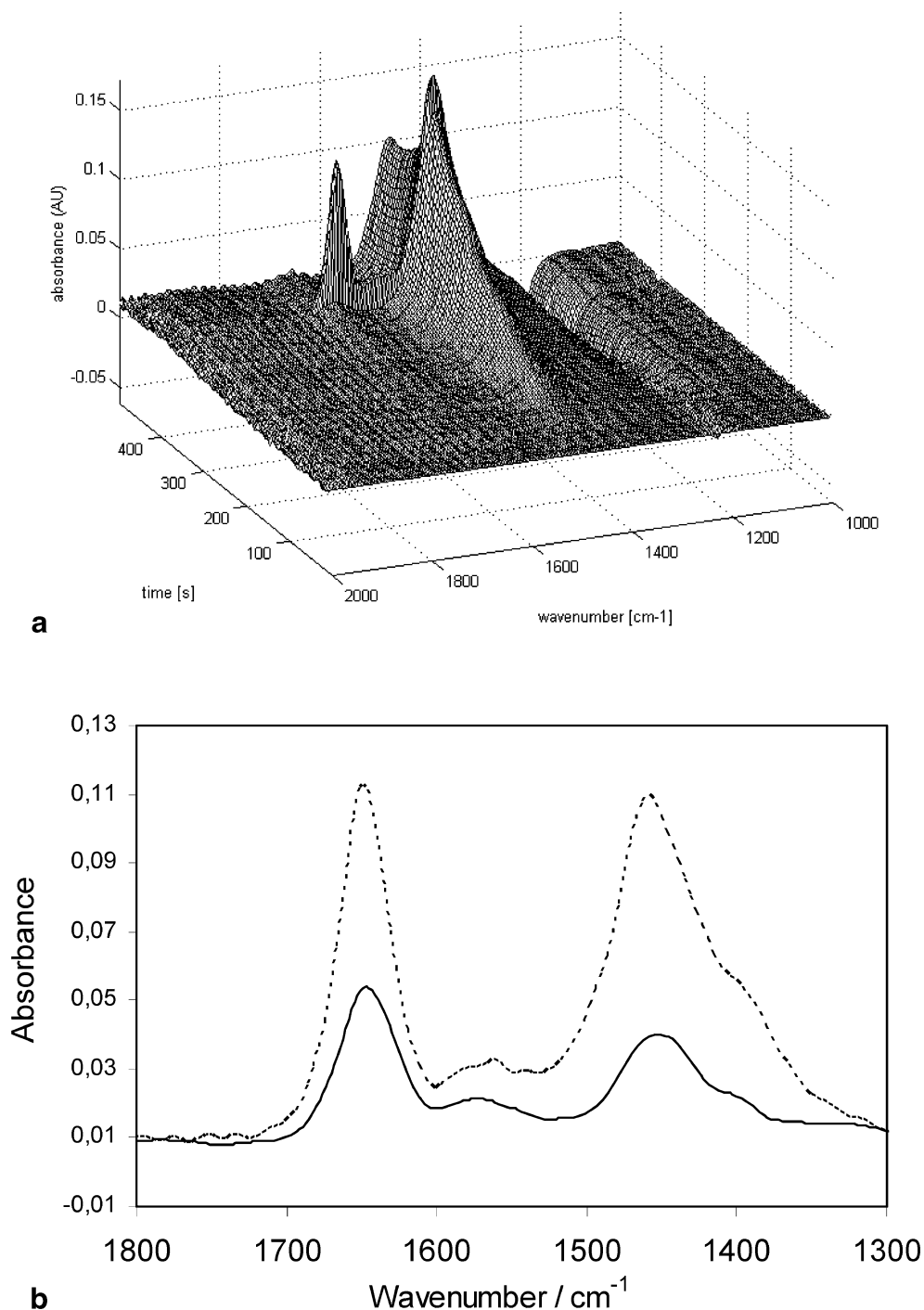
**Fig. 3** **a** Single beam spectra of normal and heavy water as measured in a 15  $\mu\text{m}$ -broad and 10  $\mu\text{m}$ -high channel (sample volume 3 pl). **b** Spectra recorded in the stopped flow mode when feeding the microchip with normal and heavy water. The background was taken at 72 ms reaction time. The spectra display the spectral changes recorded over an 8 min reaction time. The band at 1450  $\text{cm}^{-1}$  indicates the formation of the HOD molecule



bands could be obtained from a volume of 3 pl, as defined by the 15  $\mu\text{m}$ -wide and 10  $\mu\text{m}$ -high fluid channel (Fig. 3a). In an attempt to follow a chemical reaction in these dimensions, heavy water was fed into the microchip via inlets 1 and 3 (see Fig. 1), whereas normal water was introduced via the central channel (inlet 2). The flow rate for each streamline was set to 10  $\mu\text{L}/\text{h}$ . FTIR measurements probing a total volume of approximately 3 pl at a distance of 4 mm after the mixing point were carried out. Taking into account the cross-section of the channel and the flow rates applied, the measured volume corresponded to a reaction time of 0.072 s. Therefore, due to the short diffusion distance between the laminated streamlines (5  $\mu\text{m}$ ) inside the 15  $\mu\text{m}$ -broad channel, and the diffusion coefficients of normal and heavy water ( $\text{H}_2\text{O}$ :  $2.3 \times 10^5 \text{ cm}^2 \text{ s}^{-1}$ ,  $\text{D}_2\text{O}$ :  $1.9 \times 10^5 \text{ cm}^2 \text{ s}^{-1}$  measured at 25  $^\circ\text{C}$  [15]), it may be concluded that complete mixing of the three solutions had

occurred prior reaching the place of measurement. The flow was stopped and subsequent spectra were recorded over the next 8 min and ratioed against the first one. These spectra are given in Fig. 3 and show the formation of HOD molecules (characteristic bending formation at 1450  $\text{cm}^{-1}$ ) from heavy and normal water. In addition to this characteristic spectral feature, an increase in the O–H stretch region (3450  $\text{cm}^{-1}$ ) was recorded too. A full interpretation of the recorded spectral changes must be considered premature at this point, because the spectra of water, despite being a simple molecule, is very complex [16]. This experiment, however, clearly proves the ability of the microchip to follow chemical reactions in aqueous solution within picoliter volumes by FTIR spectroscopy. During measurement, the position of the actual focus spot produced by the optical set-up shifted slightly due to instabilities in the synchrotron source. As a consequence, the full capabilities of

**Fig. 4** **a** 3-D plot of the recording obtained upon loading the CE-IR-chip (design B) with 2g/l myoglobin followed by electrophoretic movement of the analyte through the detection window (~450 s). **b** Comparison of FTIR spectra of the analyte (dashed line), as recorded during the experiment shown in Fig. 4a, with reference spectra (solid line)



the microchip intended for the investigation of chemical reactions could not be fully explored.

In the second study, the microchip designed for electrophoresis and on-chip IR detection was investigated. So far, the use of channels made of SU-8 for electrophoretic separations has not been reported. Before use, the whole chip was flushed with the running buffer. This was accomplished by introducing buffer at the inlets of the separation channel and the sample port by means of a three-channel syringe pump. For sample (myoglobin) loading, the two

exits of the separation channel were blocked and the sample was introduced using the syringe pump. In this way, the sample double tee (Fig. 1) was filled. After loading of the sample, a potential of 3 kV was applied, corresponding to a potential gradient of 680 V/cm. Figure 4a shows a characteristic electropherogram obtained with the passage of the sample through the detection window of the chip. The FTIR spectra corresponding to the peak maximum was extracted from the dataset and is compared with the reference spectra taken of the analyte using an ATR unit. A

characteristic peak at  $1648\text{ cm}^{-1}$ , the C=O stretch vibration of the protein, can be clearly seen in both spectra. In protein analysis this peak is usually called the amide I band, and is the most important peak as it contains direct information about the secondary structure of the protein [8, 17]. Band positions around  $1650\text{ cm}^{-1}$  indicate helical structure, while band positions around  $1630\text{ cm}^{-1}$  are indicative of beta-sheet structure. Band positions in-between show a partial random coil character of the protein. The so-called amide II (out-of-phase N-H bend combined with C-N stretching) can normally be found at  $1550\text{ cm}^{-1}$ , but as  $\text{D}_2\text{O}$  was used in this study a proton exchange can be observed and the amide II' is shifted downwards to  $1450\text{ cm}^{-1}$ . This peak is less important in protein analysis, as it is not influenced directly by the secondary structure. It is mainly used to calculate proton exchange ratios in order to determine the accessibility of the protons to  $\text{D}_2\text{O}$ . The band position of the amide I as recorded on-chip confirms the predominantly helical structure of myoglobin, which is also consistent with X-ray crystallography data. In the spectrum obtained from the electrophoretic run, the amide II band has HDO heavily superimposed on it, which is due to traces of  $\text{H}_2\text{O}$  that have entered the system at the electrolyte reservoir and probably also during sample injection. Even after the analyte has passed the area, the HDO band is still apparent due to the continued presence of this impurity.

## Conclusions

The study detailed in this paper describes, (to the authors' knowledge) the first successful use of micro-chips for reaction and separation monitoring using an IR synchrotron light source. The developed technology for IR-chip fabrication based on the combination of  $\text{CaF}_2$  and SU-8 structuring technology has proven to be a versatile and effective means to produce devices for use with an IR synchrotron radiation source. The results obtained show that a chemical reaction (HD exchange in water) can be monitored in a volume of only 3 pl. Furthermore, using the chip designed for capillary electrophoresis, a protein was successfully injected and recorded as it passed the detector window. From the FTIR spectra recorded, the identity of the analyte could be confirmed by comparison with reference spectra. In addition, the exact position of the amide I band, as recorded on-chip, could be used to determine the secondary structure of the protein.

It is expected that the chip designs developed for separation and reaction monitoring using IR synchrotron detection will be useful for a great many applications, once the stability of the IR focus spot produced by the synchrotron source is improved. In the field of chemical reaction monitoring in particular, including protein folding and bio-ligand interaction studies, the low sample amount required for prolonged experiments is seen as a significant advantage over conventional larger systems. In the case of on-chip electrophoresis, the attractiveness of mid-IR detection is seen in its molecular specific information content and especially in its capability to discern the folding state, as well as the secondary structures of proteins in solution.

**Acknowledgements** Acknowledgement is given to the Austrian Science Fund for support within the project FWF 15531. Furthermore, financial support from the ANKA for carrying out the measurements in Karlsruhe is gratefully acknowledged. J.R.B. also acknowledges support from the Spanish Ministry of Culture, Sport and Science.

## References

1. Limbach P, Meng Z (2002) *Analyst* 127:693–700
2. Jayawickrama DA, Sweedler JV (2003) *J Chromatogr A* 1000(1–2):819–40
3. He L, Natan MJ, Keating CD (2000) *Anal Chem* 72(21):5348–55
4. Hinsmann P, Haberkorn M, Frank J, Svasek P, Harasek M, Lendl B (2001) *Appl Spectrosc* 55:241–251
5. Hinsmann P, Frank J, Svasek P, Harasek M, Lendl B (2001) *Lab Chip* 1:16–21
6. Kauffmann E, Darnton N, Austin R, Batt C, Gerwert K (2001) *P Natl Acad Sci USA* 98:6646–6649
7. Mitchell MC, Spikmans V, Manz A, de Mello AJ (2001) *J Chem Soc Perk T* 1:514–518
8. Fabian H, Mäntele W (2002) In: Chalmers JM, Griffiths P (eds) *Handbook of vibrational spectroscopy*. Wiley, Chichester, UK
9. Koenig JK, Tabb DL (1980) In: Durig JR (ed) *Analytical applications of FT-IR to molecular and biological systems*. D. Reidel, Boston, MA, pp 241–255
10. Arrondo JL, Goni FM (1999) *Prog Biophys Mol Bio* 72(4):367–405
11. Kölhed M, Hinsmann P, Svasek P, Frank J, Karlberg B, Lendl B (2002) *Anal Chem* 74:3843–3848
12. Kölhed M, Hinsmann P, Karlberg B, Lendl B (2003) *Electrophoresis* 24:687–692
13. Mathis YL, Gasharova B, Moss D (2003) *J Biol Phys* 29:313–318
14. Carr GL (1999) *Vib Spectrosc* 19(1):53–60
15. Mills R (1973) *J Phys Chem* 77:685–688
16. Brubach J-B, Mermet A, Filabozzi A, Gerschel A, Lairez D, Krafft MP, Roy P (2001) *J Phys Chem B* 105:430–435
17. Barth A, Zscherp C (2002) *Q Rev Biophys* 35:369–430

### **III**

Kulka, S.; Quintas, G.; Lendl, B.

*"Automated sample preparation and analysis using a sequential-injection (SI)-capillary electrophoresis (CE) interface"*

submitted publication

## **Automated sample preparation and analysis using a sequential-injection (SI)-capillary electrophoresis (CE) interface**

Stephan Kulka, Guillermo Quintás, Bernhard Lendl\*

Institute for Chemical Technologies and Analytics, Vienna University of Technology,  
Getreidemarkt 9-164, A-1060 Vienna, Austria

### *Abstract*

A fully automated sequential-injection (SI)-capillary electrophoresis (CE) system was developed using commercially available components as syringe pump, selection and injection valves and a high voltage power supply. The interface connecting the SI with the CE unit consisted of two T-pieces where the capillary was inserted in one and a Pt electrode in the other T-piece (grounded). By pressurizing the whole system using a syringe pump hydrodynamic injection was feasible. For characterisation the system was applied to a mixture of adenosine and adenosine monophosphate in different concentrations. The calibration curve obtained gave a detection limit down to  $0.5 \mu\text{g g}^{-1}$  (correlation coefficient of 0.997). The reproducibility of the injection was also assessed resulting in a RSD value (5 injections) of 5.4%. The total time of analysis, from injection, conditioning and separation to cleaning the capillary again was 15 minutes. As another application, employing the full power of the automated SIA-CE system myoglobin was mixed directly using the flow system with different concentrations of sodium dodecyl sulfate (SDS), a known denaturing agent. The different conformations obtained in this way were analysed with the CE system and a distinct shift in migration time and decreasing of the native peak of myoglobin could be observed. The protein

samples prepared were also analysed with off-line infrared spectroscopy (IR) confirming these results.

*Keywords:* CE, SIA, Myoglobin, Adenosine monophosphate, Adenosine.

\* e-mail: [blendl@mail.zserv.tuwien.ac.at](mailto:blendl@mail.zserv.tuwien.ac.at) Tel/Fax.: + 43 1 5880115140 / +43 1 5880115199

## 1. Introduction

The last steps of the analytical process generally involve sample pretreatment (can be left out in certain situations), a reaction and/or a separation followed by detection. In most analytical systems, however these steps are not integrated, but carried out subsequently, leading to higher time consumption, higher error probability and also making more manual intervention necessary. Part of these difficulties can be circumvented using a flow injection analysis system (FIA), developed by Ruzicka and Hansen <sup>1</sup> where the analytes and reagents are injected into a constant carrier flow, mixed there reproducibly and finally sent towards the detector using the same carrier flow. In this way the experimental setup needs to be set up only in the beginning and the reaction as well as the detection can be carried out in an automated way. A series of works <sup>2 3 4</sup> show that sample pretreatment steps, like dialysis, solid-phase or liquid-liquid extraction or filtering can be incorporated without difficulty in such a flow system.

However, separations, with resolution power characteristic for HPLC and CE, cannot be achieved when employing these flow systems. In such situations interfaces connect the automated flow system to a separation system where the analytes are separated and detected. In doing so efficient sample pretreatment can be accomplished in the flow system whereas separation and detection is carried out in the connected separation system.

In the last years capillary electrophoresis (CE), a separation technique based on the electrophoretic mobility of the analytes, mainly used in the area of bioanalytical and pharmaceutical chemistry, emerged and is growing steadily



in its applications.<sup>5-9</sup> Already some time ago, the first on-line interfaces between a flow system and a CE system have been demonstrated.

The first interface was developed by Kuban and Karlberg and they applied it to a wide variety of applications like the determination of metallo-cyanides by FI-liquid membrane-CE<sup>10</sup>, use of gas diffusion in measuring volatile species in soft drinks, vinegar and wine<sup>11</sup>, detection of small anions<sup>12</sup>, hydrodynamic sample injection and on-line monitoring for kraft pulping liquors<sup>13</sup>. The other interface developed by Fang et al.<sup>14</sup>, a horizontal splitting device was applied to chiral separations<sup>15</sup>, sample preconcentration using an on-line sorption column<sup>16</sup>, monitoring drug dissociation<sup>17</sup> and analysis of pseudoephedrine<sup>18</sup>.

In both approaches flow injection (FI) was used for sample delivery and replenishing of the background electrolyte (BGE). The sample introduction had to be performed by electrokinetic (EK) injection as hydrodynamic (HD) injection proved to be difficult due to the constant flow generated by continuously working peristaltic pumps. However, EK injection has long been known for sample discrimination<sup>19</sup>, as ions with higher mobility tend to get injected in a higher amount as ions with lower mobility.

This inherent problem of FI leads to the idea to employ sequential injection analysis (SIA) as in this technique a syringe pump is used to generate the flow. This syringe pump that moves both upwards and downwards is able to produce short pressure pulses the flow system and thus HD injection in addition to EK injection is made possible. Fang et al. demonstrated the possibility to interface SI with a specially designed CE chip using laser-induced fluorescence (LIF) to detect amino acids<sup>20</sup>. The first interface to

combine SI and conventional CE was developed by Ruzicka et al. using a  $\mu$ SI system (the so-called Lab-on-a-valve, LOV) <sup>21</sup>. SIA systems perform similar like FIA systems; the main difference lies in the flow generation, as a syringe pump and a selection valve is used. Due to this different setup SIA is more robust and more flexible if the flow injection parameters (flow rate and injection volume) need to be changed due to full computer control of these variables. When interfacing to CE the lower amount of reagents used ( $\mu$ L range as compared to the mL range of FIA), matches the narrow-bore capillaries in CE much better. The feasibility of this concept was shown using the system of small anions also used by Karlberg and Kuban <sup>12</sup> and the results obtained showed the excellent reproducibility of the injection system (about 3 % RSD, n=5). In another application the advantages of a combined flow injection CE system were fully employed as proteins were automatically labeled with a fluorescence marker, separated and subsequently detected.

In this work a fully automated SIA-CE interface with commercially available pumps and valves is presented. The whole analytical process was automated, ranging from the first conditioning of the capillary to the cleaning of the capillary after a separation run. In this way the advantages of SIA, automated and reproducible liquid handling were joined with the advantages of CE, simple and powerful separation without the hassle of work-intensive sample preparation or manual capillary conditioning or cleaning.

The performance of the SIA-CE-UV system is tested for its application in both quantitative and qualitative analysis, evaluating the analytical features of the injection of a mixture of adenosine monophosphate and adenosine and the

effect of increasing concentrations of SDS on a myoglobin solution as described in previous works<sup>22</sup>, respectively.

## **2. Experimental**

### *System components*

The SIA manifold shown in Figure 1 used a Cavro XP 3000 (Cavro Scientific Instruments, Sunnyvale, California) pump equipped with a 100  $\mu$ l syringe, a Valco (Valco Instruments Co. Inc, Houston, Texas) 6 port injection valve and a 8 port selection valve. All the PTFE tubing employed in the manifold were 0.25 mm inner diameter. The manifold was controlled using an in-house written MS Visual Basic 6.0 (Microsoft) based software program (Sagittarius, Version 3.0.25) working under Windows NT operating system. Sagittarius offers the full flexibility of a programmable interface (the server), which coordinates the clients which directly control the devices used. As a client-server architecture is used, as many clients (which equals devices) can be attached to the server as needed and the programming effort for a new experimental setup is very low. As another feature control over a network is possible enabling an even higher degree of automatization.

The capillary electrophoresis system consisted of two electrodes, a fused silica capillary, a UV cell holding the capillary and a high voltage (HV) power supply. The uncoated capillary with an ID of 50  $\mu$ m and an OD of 350  $\mu$ m (Polymicro Technologies LLC, Phoenix, USA) had an effective length of 38 cm and a total length of 50 cm. The electrodes were made out of platinum wire (Pt, 0.5 mm OD, ÖGUSSA), one electrode covered by a Teflon tubing (ID 0.5 mm, OD 1.588 mm) and inserted into a T-piece of the interface. The HV

system was the Spellman CZE 1000R (Spellman New York, USA), capable of delivering up to 30 kV and 300  $\mu$ A. The detection was carried out with an Ultimate UV-Vis detector (Dionex, Sunnyvale, CA, USA) equipped with fiber-optic probes connected to a capillary holder. The absorbance values at two wavelengths (200 and 254 nm) were recorded enabling a better control of artefacts, for further data treatment only one wavelength was chosen. The same computer as to control the whole manifold was used for data collection simplifying the setup.

Infrared spectra were recorded on a 3 bounce diamond attenuated total reflection (ATR) unit attached to a Bruker (Ettlingen, Germany) Matrix-F FTIR spectrometer.

### *Chemicals*

Myoglobin (Mb) from horse heart, sodium dodecylsulfate (SDS), sodium hydroxide, hydrochloric acid and water (HPLC grade) were purchased from Fluka (Buchs, Switzerland) and used as received. Adenosine monophosphate, adenosine and sodium tetraborate (borax) were purchased from Sigma-Aldrich and used as received.

A stock solution of 1 M sodium hydroxide was made by dissolving solid sodium hydroxide and a final concentration of 0.1 M was used. The 0.1 M solution of hydrochloric acid was prepared by diluting concentrated HCl with the appropriate amount of distilled water.

The background electrolyte (BGE) was in both cases borax with a concentration of 20 mM (pH of 9.2). Different concentrations of adenosine monophosphate (AMP) and adenosine were prepared in distilled water, ranging from 0 to 500  $\mu$ g/ml.

The stock solution of 40 mM SDS was prepared by dissolving the correct amount in water. The concentration of myoglobin was 2 g l<sup>-1</sup>, dissolved in water with some careful shaking. All solutions were filtered using filters with a pore size of 0.2 µm. All solutions, except myoglobin were degassed after the filtration in an ultrasonic bath. Using the SIA manifold depicted in Figure 1, different concentrations of SDS between 0.2 and 7.0 mM were prepared immediately prior to the injection in CE, keeping a constant concentration of Mb of 1.7 g l<sup>-1</sup>.

### **3. Results and Discussion**

#### **3.1 SIA-CE Interface**

The interface between the SIA system and the capillary was made using two T-pieces connected through a short tubing where one position was taken by the capillary, one by the electrode (grounded), one inlet and one outlet. The basic principle of injection into the capillary is described below. First the sample was flushed through the interface with the injection valve open to ensure that the sample was close to the capillary inlet, then the injection valve was closed, the syringe could pressurize the system and sample was injected into the capillary. In the next step the interface was rinsed with the background electrolyte (BGE), then the voltage was applied and the separation started while BGE was replenished at a low flow rate using the same pump. The whole injection process was performed in 2 minutes and the separation time was variable (depending on the analytes used). The advantage of the injection in this way lies not only in the hydrodynamic injection as compared to the electrokinetic injection, but also in the complete

automated way of the injection keeping the injection volume constant at 40 nL.

Conditioning or cleaning was performed in the same way as sample injection, the initial conditioning of a new capillary was carried out first with sodium hydroxide (2 min), then water (2 min) and finally BGE (4 min) to ensure complete activation of the capillary surface. The refreshing of the capillary each day in the morning was shorter, 1 min for NaOH, 1 min for water and 2 min for the buffer. The cleaning procedure was the same as the refreshing, either NaOH in the case of adenosine and adenosine monophosphate or HCl in the case of the protein. The flow rate used for flushing the capillary was 5  $\mu\text{L min}^{-1}$  and therefore the volume for the initial conditioning was 40  $\mu\text{L}$  and for the other cleaning processes it was 20  $\mu\text{L}$ .

This procedure simplified the conditioning and the inter-run cleaning of the capillary substantially when compared to manual operation. The complete automation of the injection process and the separation process ensures not only reproducible injections but also retention times easily comparable to each other. As another benefit of the automation the whole sample preparation like the reaction between the sample and the analyte is carried out without any further intervention and the whole analytical process from sample preparation to detection is completely under automated control.

## **3.2 Results and discussion**

### **3.2.1 Quantitative analysis**

In the first step the performance of the interface was evaluated by preparing different mixtures of AMP and adenosine off-line and using the SIA system

only for the injection. As can be seen in Fig. 2 the separation of these two compounds posed no difficulties. The injection volumes were varied to find the optimum amount of sample injected. As a compromise between the error of injection and overloading the capillary a volume of 40 nL (equals to about 4 % of the capillary volume) was chosen (see fig 2). This volume was used throughout the rest of the experiments. Besides the optimization of the injection volume no further optimising was carried out, as this was not the main task of the study.

The mixture of adenosine monophosphate and adenosine was injected in different concentrations and a calibration curve (cf. Table 1) was obtained. It can be clearly seen that in the range of interest the slope of the calibration curve was linear and indicated a reproducible performance of the injection. The same applied also to the retention times, which were reproducible as well after correcting them using the mobility of the electro-osmotic flow (not shown).

As these results suggested that the interface performed in a reproducible way as indicated by the RSD value of 5.4% ( $n = 3$ ), both for the injection as well as for the capillary electrophoresis separation the system was applied to the analysis of the SDS-related denaturation of myoglobin.

### 3.2.2 Qualitative analysis

As in this case the SIA system was also used to perform the sample preparation, an external mixing chamber was integrated into the manifold to ensure complete mixing of the analyte and the reagent. Furthermore, the mixing and the injection process were decoupled which gave better

reproducibility and stability in injection and separation as compared to the case without the external mixing chamber. As another benefit of the external mixing chamber shaking of the mixture could be performed. In this work the concentration of myoglobin was kept constant at 2 g/L to ensure complete comparison with the work of Stutz et al.<sup>22</sup> and also to have the possibility to analyse the same samples with infrared spectroscopy.

Figure 4 shows the influence of increasing concentrations of SDS on myoglobin, where it can be clearly seen that there is a splitting in the peaks and that the retention times of the second peak increase with higher concentration of SDS. In Figure 5 the relation between the peak area of the native form of myoglobin compared to the SDS-induced conformations is plotted where it can be seen that the amount of the non-native states increases with higher SDS concentration.

These results are in accordance with the results from Stutz et al.<sup>22</sup> which show that the interface presented works reproducibly and that the results obtained can be compared to results gained from commercial equipment.

#### *Further results*

As the secondary structure of proteins can be studied using infrared spectroscopy (IR) when regarding the position of the C=O vibration (the so-called amide I band)<sup>23;24</sup> IR spectroscopy was employed to analyse the same samples as in the CE. The position of the amide I band shifted slightly with increasing concentration of SDS (see fig. 6). This finding supports the results from the CE as the increasing migration time indicates denaturation of the protein, which is reflected in the peak shift to lower wavenumbers in the IR.



## *Conclusion*

In this work a successful SIA-CE interface using commercially available pumps and valves is presented. The advantages of SIA were employed and the automated injection into the capillary gave very reproducible results giving a RSD of 5.4% (n = 5, injection volume 40 nL) using adenosine as internal standard (see table 1) showing the feasibility of such an interface using off the shelf components and self-written software.

Compared to commercially available CE instruments the presented system can perform many sample preparation tasks ranging from solid phase extraction over mixing several components to heating and shaking solutions in an external mixing chamber. The interface presented gives rise to many possibility in sample preparation, preconcentration and reactions immediately prior the actual separation. This interface and its possibilities are in the trend to further integrate and simplify chemical analysis. Another option using such a fully automated flow system would be to take advantage of the highly reproducible dispersion profile produced by the SIA system. In the myoglobin-SDS system under study in this paper “electronic dilution” of SDS might be an appropriate technique to give insight into concentration and time-dependent processes.

## *Acknowledgements*

S.K and B.L are grateful for financial support received within the project 15531 of the Austrian Science Fund. G.Q. is grateful for post-doctoral grants

from the Ministerio de Educación y Ciencia, Secretaría de Estado de Universidades e Investigación (Spain) (EX2004-1245).

#### Reference List

1. Ruzicka, J.; Hansen, E. H. *Flow Injection Analysis*, 2nd ed.; New York, 1988.
2. Fang, Z.-L. *Flow Injection: Separation and Preconcentration*, 1st ed.; Weinheim, 1993.
3. M. Miró and W. Frenzel , *Trends in Analytical Chemistry* 2004, **23**, 624-36.
4. J. Wang and E. H. Hansen , *Trends in Analytical Chemistry* 2005, **24**, 1-8.
5. Haleem J. Isaaq , *Electrophoresis* 2000, **21**, 1921-39.
6. Hu Shen and Dovichi Norman J. *Analytical Chemistry* 2002, **74**, 2833-50.
7. Sentenellas Sonia, Puignou Luis and Gordon Manuel J. *Journal of Separation Science* 2002, **25**, 975-87.
8. P. R. Powell and A. G. Ewing , *Analytical and Bioanalytical Chemistry* 2005, **382**, 581-91.
9. D. C. Simpson and R. D. Smith , *Electrophoresis* 2005, **26**, 1291-305.
10. P. Kuban, W. Buchberger and P. R. Haddad , *Journal of Chromatography A* 1997, **770**, 329-36.
11. P. Kuban and B. Karlberg , *Talanta* 1998, **45**, 477-84.
12. P. Kuban and B. Karlberg , *Analytical Chemistry* 1998, **70**, 360-65.
13. Petr Kuban and Bo Karlberg , *Analytica Chimica Acta* 2000, **404**, 19-28.
14. Z. L. Fang, Z. S. Liu and Q. Shen , *Analytica Chimica Acta* 1997, **346**, 135-43.
15. Z. S. Liu and Z. L. Fang , *Analytica Chimica Acta* 1997, **353**, 199-205.
16. H.-W. Chen and Z.-L. Fang , *Analytica Chimica Acta* 1997, **355**, 135-43.
17. H.-W. Chen and Z.-L. Fang , *Analytica Chimica Acta* 1998, **376**, 209-20.
18. H. W. Chen and Z. L. Fang , *Analytica Chimica Acta* 1999, **394**, 13-22.

19. J. W. Jorgenson and K. D. Lukacs , *Analytical Chemistry* 1981, **53**, 1298-302.
20. Q. Fang, F. R. Wang, S. L. Wang, S. S. Liu, S. K. Xu and Z. L. Fang , *Analytica Chimica Acta* 1999, **390**, 27-37.
21. C.-H. Wu, L. Scampavia and J. Ruzicka , *The Analyst* 2002, **127**, 898-905.
22. H. Stutz, M. Wallner, H. Malissa, Jr., G. Bordin and A. R. Rodriguez , *Electrophoresis* 2005, **26**, 1089-105.
23. A. Barth and C. Zscherp , *Quarterly Reviews of Biophysics* 2002, **35**, 369-430.
24. Fabian Heinz; Mäntele Werner *Handbook of Vibrational Spectroscopy*, Chalmers J.M.; Griffiths P., Eds.; John Wiley & Sons Ltd.: 2002.

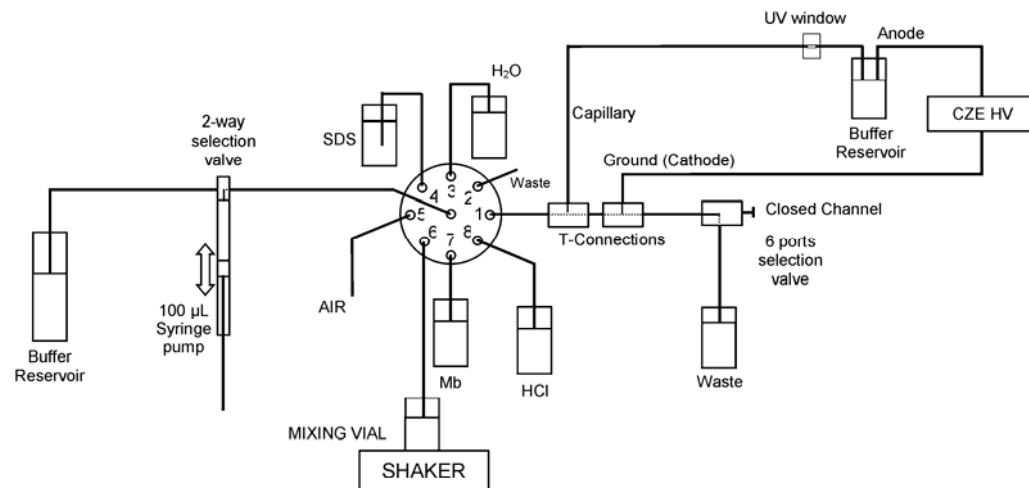


Figure 1. Schematic view of the SIA-CE manifold detailed description of the valve positions: 1, Capillary; 2, Waste; 3, H<sub>2</sub>O; 4 SDS (Mb analysis) or AMP/A standard solutions (AMP analysis); 5, Air; 6, Mixing vial; 7, Mb (Mb analysis) or samples (AMP analysis); 8, HCl (Mb analysis) or NaOH (AMP analysis).

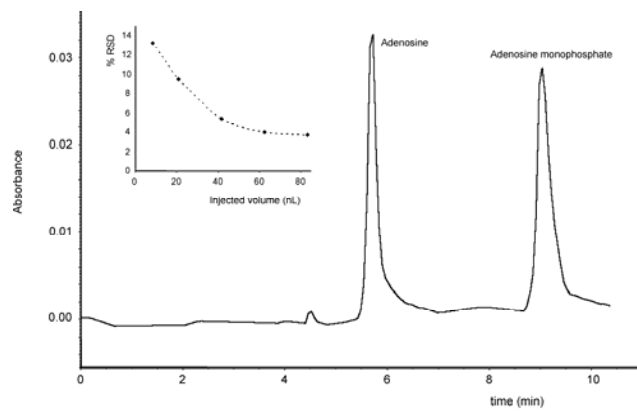


Figure 2. Electropherogram of a solution containing adenosine and AMP in water using the injection conditions indicated in the text. Inset: effect of the injection volume on the RSD of the adenosine peak (ret time 5.7 min).

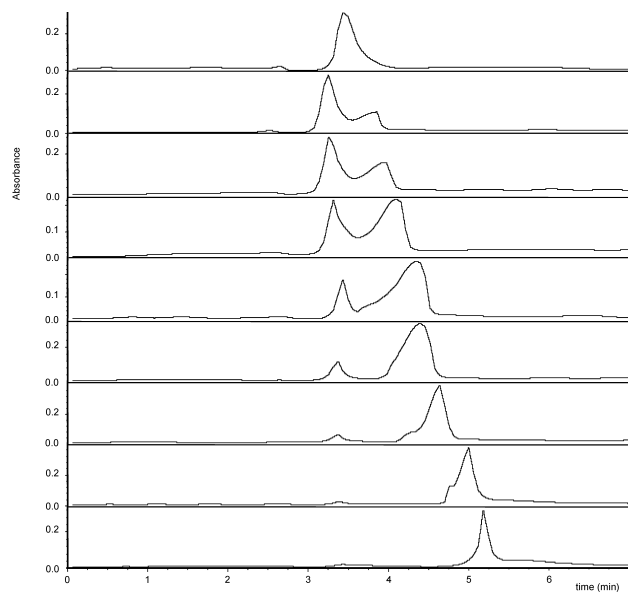


Figure 3. CE-electropherograms of Mb (1.7 gl<sup>-1</sup>) at different SDS concentrations. From top to bottom SDS concentration: 0.0, 0.2, 0.4, 0.6, 0.8, 1.0, 1.3, 2.5 and 5.6 mM.

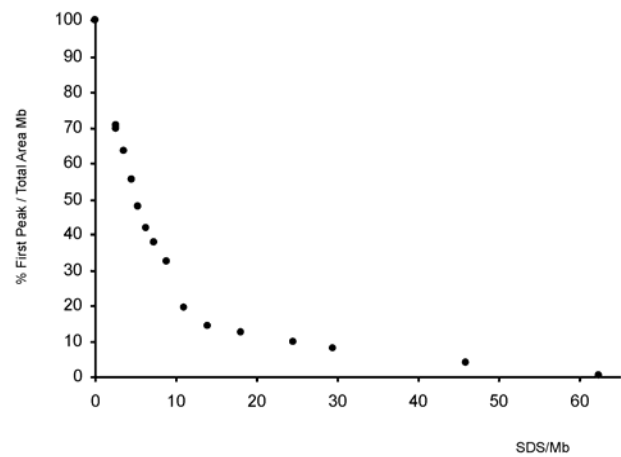


Figure 4. Effect of increasing SDS / Mb ratios (molar ratios) on the first peak area compared to the total peak area of myoglobin.

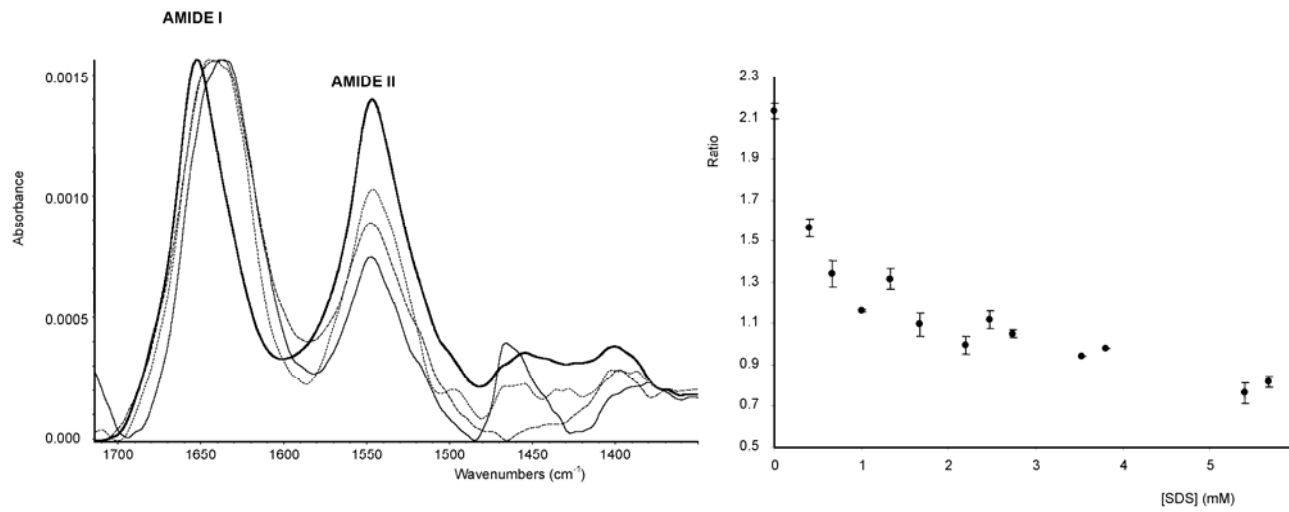


Figure 5. Measurement conditions for A): Concentration of myoglobin 2 g/L, pH 7, concentrations of SDS ranging from 0-5.67 mM, resolution used 4 cm<sup>-1</sup>, background was water  
 Figure B) shows the Peak height ratio between 1652 and 1630 cm<sup>-1</sup>, indicating a shift away from the alpha-helical structure of myoglobin with higher SDS concentrations.



Table 1

	Calibration line <sup>a</sup>	R <sup>2</sup>	LOD <sup>b</sup>	LOQ <sup>c</sup>
<b>External calibration</b>	$A = (-1 \pm 9) 10^{-5} + (2.68 \pm 0.04) 10^{-5} C_{AMP} \text{ (ppm)}$	0.997	6	22
<b>Internal standard calibration<sup>d</sup></b>	$R = (0.000 \pm 0.006) + (1.040 \pm 0.007) C_{AMP/A} \text{ (ppm)}$	0.9995	0.5	1.7

<sup>a</sup>, Adenosine monophosphate (AMP) regression lines using peak area measurements and 5 standards in the range 0 – 500 ppm; <sup>b</sup>, Limit of detection in  $\mu\text{g g}^{-1}$ , obtained from the standard deviation of 6 measurements of a standard solution ( $50 \mu\text{g g}^{-1}$ ), established for a probability level of 99.6 % ( $k=3$ ); <sup>c</sup>, Limit of quantification calculated for a probability level of  $k=10$ ; <sup>d</sup>, Regression line calculated using an Adenosine (A) solution ( $220 \mu\text{g g}^{-1}$ ) as internal standard.  $R = \text{Area AMP} / \text{Area A}$ .

## IV

Kulka, S.; Lendl, B.

*“Vibrational spectroscopic detection in capillary electrophoresis  
(CE)”*

in *“Analysis and detection by capillary electrophoresis”*, eds. Marina, M.L;  
Rios, A.; Valcarcel, M., Elsevier: Amsterdam, 2005

Stephan Kulka, Bernhard Lendl\*  
Institute of chemical Technologies and Analytics  
TU Vienna  
Getreidemarkt 9, 1060 Vienna  
Austria  
E-Mail: blendl@mail.zserv.tuwien.ac.at

## **1 Vibrational spectroscopic detection in capillary electrophoresis (CE)**

### ***Analytical information in vibrational spectroscopy***

Vibrational spectroscopy embraces infrared (IR) and Raman spectroscopy. Both techniques provide direct molecular specific information by measuring vibrational and rotational transitions in molecules. For measurement in condensed phase such as required for detection in capillary electrophoresis only vibrational transitions are observed. According to Hooke's law the frequencies of the observed fundamental vibrations depend on the strength and the masses of the atoms involved and are characteristic for a given functional group or structural subunit. As a consequence it is possible to determine the presence of these in the molecule under investigation if bands are observed at the corresponding wavenumbers (wavelengths) in the recorded spectra. Due to the sensitivity of the vibrational transitions that involve large part of the molecule on its structure (finger print) IR and Raman spectroscopy are powerful techniques to distinguish between structurally similar molecules and isomers. When considering the whole vibrational spectrum it is therefore possible to confirm the identity of a given molecule in case appropriate reference spectra are available against which a visual or computer aided comparison can be made. Reference spectra recorded under comparable conditions are important because the exact position and intensities of the bands in IR and Raman spectra are different for neat (powders, liquids) or dissolved analyte spectra. Furthermore, they will depend on the solvent and pH value because different hydrogen bonding as well as dissociation may occur which strongly alter the appearance of the obtained spectra. The sensitivity of vibrational spectra on inter- and intra-molecular interactions can, however, also advantageously be used for the determination of secondary structures of proteins as well as for differentiation of diastereomers. In addition to the qualitative information on the separated compounds IR and Raman spectroscopy also allows to obtain quantitative information in the concentration of the measured analytes.

## **1.1 Infrared spectroscopy (IR)**

Whereas both, infrared and Raman spectroscopy, provide information on the vibrational transitions in molecules their physical fundamentals are different. To give rise to bands in the infrared spectra it is required that the dipole moment of the part of the molecule involved in the vibration changes during vibration. In principal infrared spectroscopy can be divided in three different ranges, near infrared (NIR, 10000-4000  $\text{cm}^{-1}$ ), mid infrared (MIR, 4000-400  $\text{cm}^{-1}$ ) and far infrared (FIR, 400-100  $\text{cm}^{-1}$ ). In NIR overtones and combination of vibrations can be found. Molar absorptivities in the NIR are much smaller than in the MIR spectral region where the fundamental vibrations are observed. Furthermore, the structural information gained from NIR are less detailed than in MIR. Therefore NIR, while it is advantageously being used in modern process analytical chemistry, has found no applications as a detection technique in capillary electrophoresis so far. FIR spectra give information about long-range intermolecular interactions. This part of IR spectrometry is currently experiencing an important development with new powerful light sources and detectors being introduced [1];[2];[3]. However, no application of FIR in capillary electrophoresis has been reported yet. Mid-infrared spectroscopy in capillary electrophoresis is an absorption technique and uses thermal, broad band light sources with an interferometer to record the transmitted light. For quantitative analysis Beer's law can be used. The hyphenation of MIR spectroscopy to capillary electrophoresis is difficult due to the low amount of sample available for measurement in capillary electrophoresis. Therefore high quality Fourier transform spectrometer are required to achieve a successful hyphenation. However, miniature, powerful and room temperature operated quantum cascade lasers may soon come up as an alternative for sensitive functional group specific detection in capillary electrophoresis.

### **1.1.1 On-line mid-infrared spectroscopic detection in capillary electrophoresis**

The advantage of on-line detection lies mainly in the real-time acquisition of data allowing to record the whole electrophoretic peak over time. However, to achieve on-line MIR detection important experimental difficulties had to be overcome. Fused silica capillaries are not transparent in the MIR spectral region and therefore transmission measurements through the

capillaries, as done in the UV – visible spectral region, are not possible in the MIR. In addition the buffers employed in capillary electrophoresis also show strong absorptions in the MIR spectral region. In case of aqueous solutions the optical path must be in the low micrometer region (typically between 8-25  $\mu\text{m}$ ) to allow measurements in the information rich fingerprint region. However, also in case of such short optical path lengths part of the spectral region will be blocked in regions of strong solvent absorption. To record the spectra of the eluting analytes the spectrum of the buffer must be subtracted from the spectra recorded during the separation. This can efficiently be achieved by taking the spectrum of the buffer as the background spectrum. As measurements are done on-line there are, in contrast to off-line detection, no limitations concerning the employed buffer system. However, as spectra are recorded in solution spectral reference libraries, which usually contain spectra of neat analytes can not be used.

Köhlhed et al.[4] showed first that the use of a micromachined IR-transparent flow cell (CE cell) made out of calcium fluoride (Fig.1) and inserted between two pieces of standard fused silica capillaries makes on-line MIR detection in capillary zone electrophoresis possible. This CE cell is placed in a holder and standard capillaries are attached on both sides and sealed off with o-rings (Fig.2).

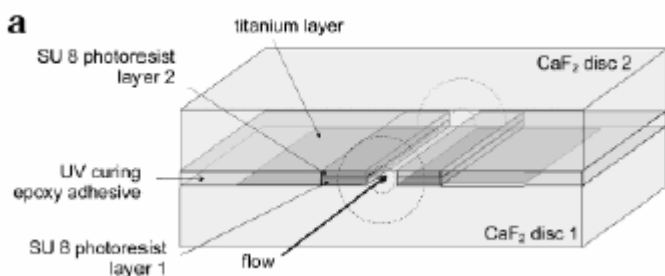


**Figure 1**

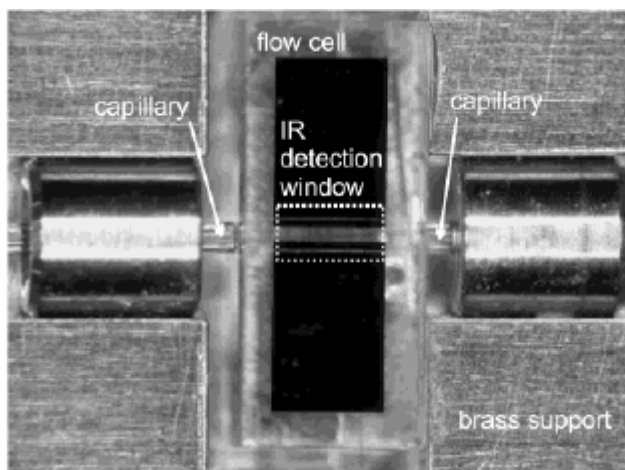


**Figure 2**

It was shown that this cell did not influence the separations as checked with a standard UV detector. In this study adenosine, guanosine and adenosine-5'-monophosphate (AMP) were separated and analyzed (Fig. 2). A linear calibration was made ranging from 0.8 mM to 8 mM for adenosine and AMP and for guanosine from 0.64 mM to 3.2 mM leading to correlation coefficients higher than 0.99.

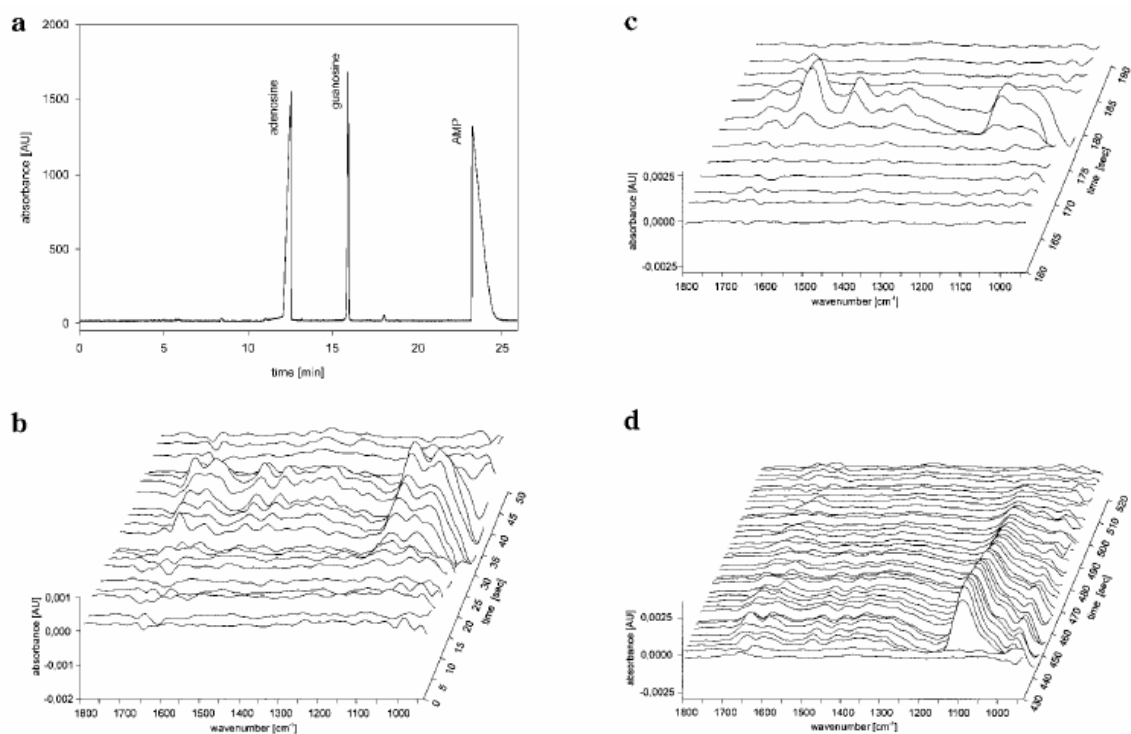


**Figure 3**

The same technology was applied to a micellar electrokinetic chromatography (MEKC)[5] separation where neutral analytes can be separated as well. In this work paracetamol, caffeine,

p-nitrobenzyl alcohol, m- and p-nitrophenol were studied. It was shown that also in case of a background electrolyte containing 40 mM of SDS in addition to the borax buffer FTIR detection still achieved useful results. Also in this application MIR spectra for substance identification could be recorded. Linear calibration for all analytes have been shown covering the low mM concentration range (from 1.08 mM to 1.44 mM). Thus, on-line FTIR detection for different modes of capillary electrophoresis might be of great interest for applications where not only the quantification but also the identification plays a role.

Hinsmann et al.[6] applied the already discussed technology with the CE cell to non-aqueous capillary electrophoresis expanding the application range of CE to charged hydrophobic compounds. It was applied to study the separation and direct identification of (R,S)-3,5-dinitrobenzoyl leucine (DNB-Leu) enantiomers using O-(tert-butyl carbamoyl) quinine (tBuCQN) as a chiral selector. The background electrolyte was a mixture of ethanol and methanol containing some modifiers and the chiral selector. It could be shown that the formed diastereomers could be directly distinguished by FTIR spectroscopy (Fig. 4). In this paper, however, no quantitative results were reported.

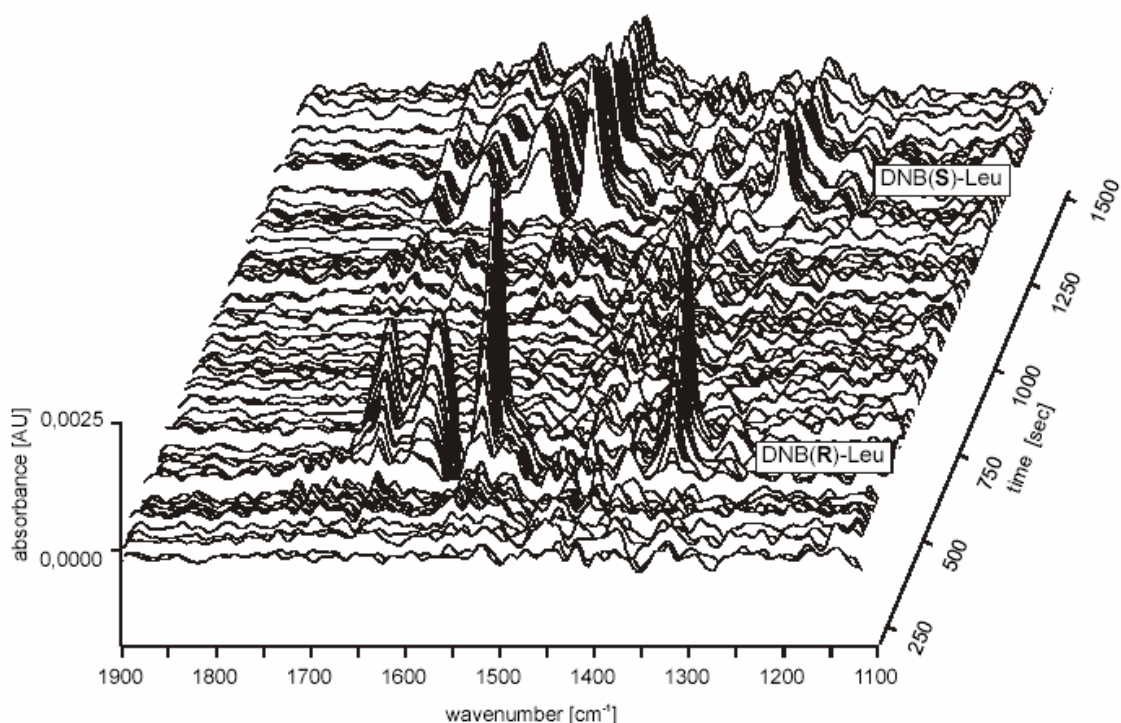


**Figure 4**

Recently also research efforts have been directed to develop mid-IR detection for chip based separation systems. For this purpose IR compatible chip materials such as CaF<sub>2</sub> need to be

used. Because of the reduced overall dimensions in chip based separations microscopic detection is mandatory. High quality IR spectra close to the diffraction limit (sample spot 10-20  $\mu\text{m}$  in diameter) can be obtained using a synchrotron radiation source coupled to a FTIR microscope. Kulka et al.[7] carried out the first IR detection in CE-IR chips using synchrotron powered IR microscopy as a detection system. These experiments already showed that the secondary structure of proteins can be determined on-chip.

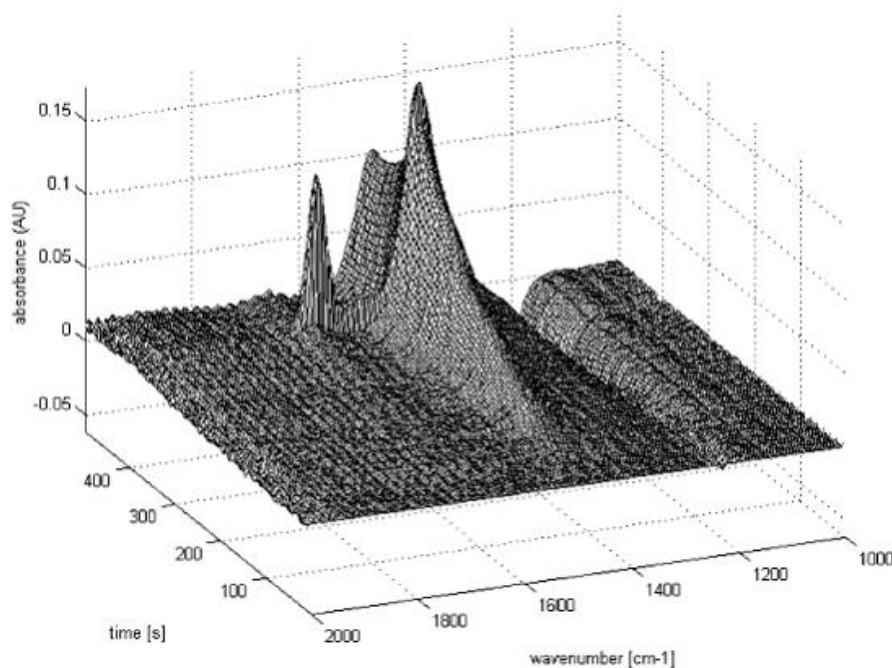


**Figure 5**

In a different work using a conventional thermal light source and etched channels on a  $\text{CaF}_2$  chip Pan et al.[8] showed that spectra from the produced channels could be recorded with a conventional IR microscope.

Another approach was taken by Patterson et al.[9] as they used attenuated total reflectance (ATR) infrared microspectroscopy as a detection technique for CE. The tip of the capillary was placed about 1  $\mu\text{m}$  above the Ge ATR crystal where the spectra were taken. A plastic reservoir around the ATR prevented evaporation of the sample and allowed for the grounding of the Pt wire (fig. 6).



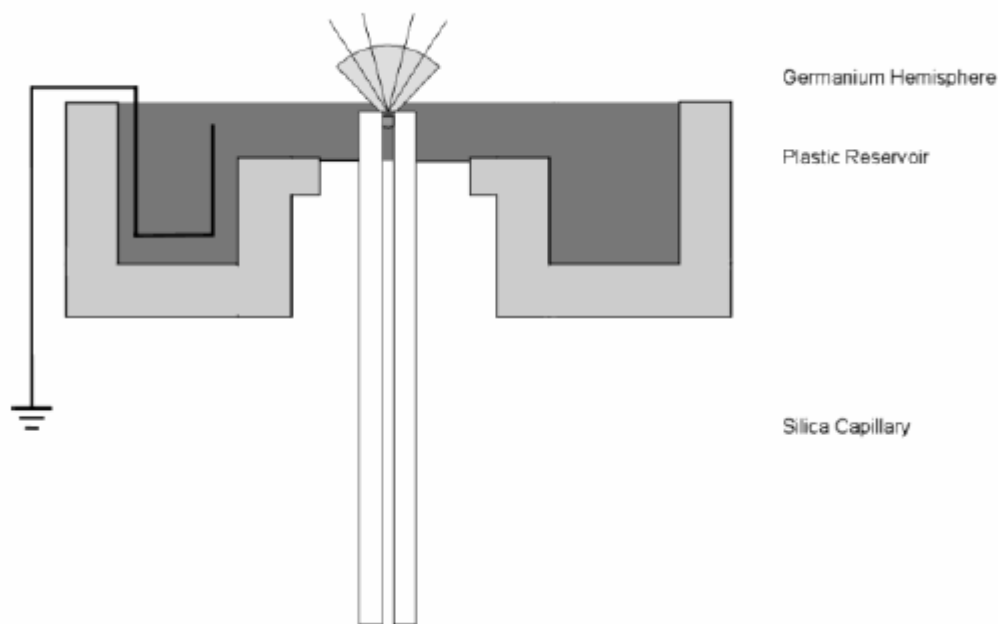


**Figure 6**

The analytes studied were citrate and nitrate, as well succinylcholine chloride and sodium salicylate using acetone as a neutral marker. It could be shown that these analytes could be separated using capillaries of different diameters and concentrations to study the effect of dead volume and sample concentration on the ATR detection. As the time to collect a spectrum was quite low the signal-to-noise ratio would be improved as pointed out in the outlook when using another equipment. However, the spectra obtained were equivalent to the ones taken in a conventional ATR measurement. The advantage of this setup is the simplicity of the design and the minimal broadening of the eluted analytes. The limit of detection achieved in an injection of 820 pL of succinyl chloride was 1.3 mM.

### **1.1.2 FTIR spectroscopic detection in capillary electrophoresis after solvent elimination**

Solvent elimination techniques aim to deposit the separated analytes on a target surface and to measure them after the solvent has been evaporated. In doing so spectral contributions from the solute molecules shall be eliminated. As the analytes are measured in dry state available spectral libraries can, in principle, be applied to these spectra. Furthermore, as spectrum acquisition is decoupled from the time scale of separation signal averaging over a prolonged

period of time can be carried out at a given analyte deposit if required. Todebush et al.[10] introduced this approach using a nebulizer interface, made out of stainless steel. The elute from the capillary was deposited onto a calcium fluoride or zinc selenide window which was moved to prevent mixing of the deposited analytes (fig. 7).

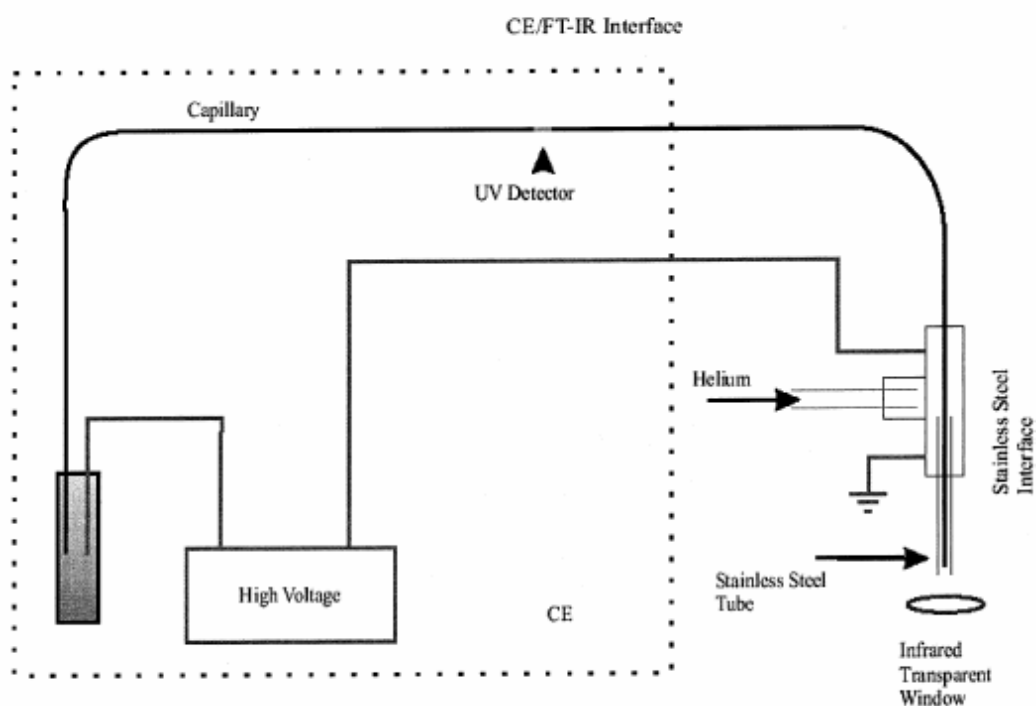


**Figure 7**

A typical deposit was round in shape and had a diameter between 200 and 400  $\mu\text{m}$ . The spots were dried and analyzed offline with an FTIR microscope (fig. 8).

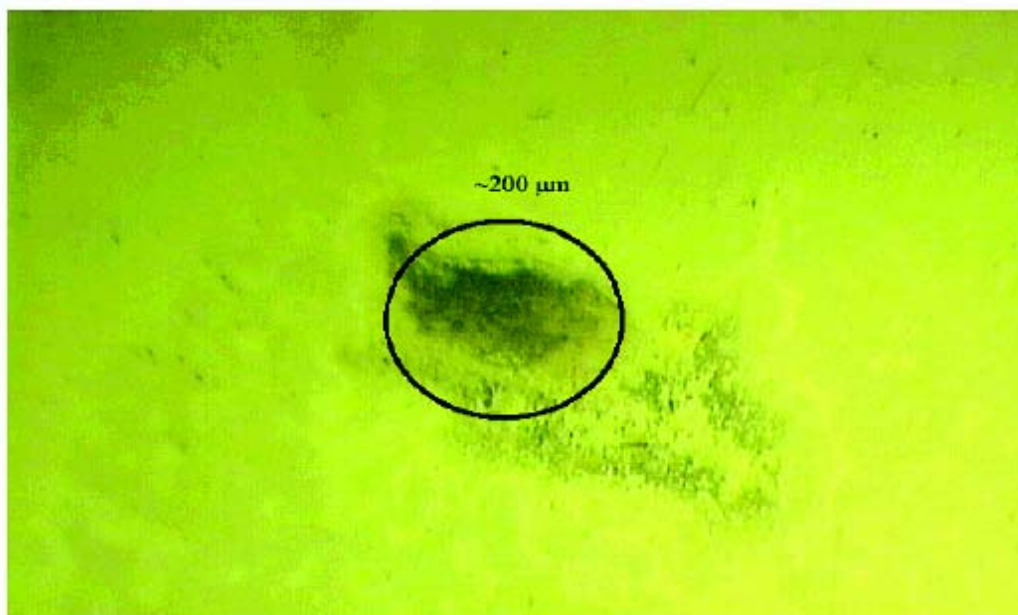


**Figure 8**

In this work the analytes studied were p-aminobenzoic acid, acetylsalicylic acid, sodium benzoate, N-acetyl-D-glucosamine (GlcNAc), nicotinamide, caffeine and salicylic acid in concentrations varying from  $5.0 \times 10^{-2}$  to  $1 \times 10^{-3}$  M. A separation was run with caffeine, salicylic acid, p-aminobenzoic acid and sodium benzoate, while the other analytes were used to study the performance of the hyphenated system compared to conventional IR microscopy measurements of manually deposited analytes. These results showed that the spectra obtained were not influenced by the presence of the background electrolyte used during the separation if it was volatile enough to be removed through the nebulizer interface.

As the deposits with the metal nebulizer exhibited a significant amount of splatter patterns and interference patterns Jarman et al.[11] introduced a glass nebulizer interface to overcome these problems. It could be shown that the new design of the nebulizer with an appropriate orifice allowed the uniform deposition of the analyte. The analytes used to test the stability and separation ability of the interface were caffeine, salicylic acid and GlcNAc with final concentrations of  $5.0 \times 10^{-3}$  M.

In contrast to on-line MIR detection no quantitative results have been reported for off-line MIR detection so far.

## **1.2 Raman spectroscopy**

For a vibration to be active in Raman spectroscopy the polarizability of the bonds involved must change during vibration. In contrast to MIR spectrometry a monochromatic light source situated in the UV-NIR spectral region is employed and the inelastically scattered light is detected. The energies of the vibrational transitions are then calculated as the difference between the laser frequency and the frequency of the detected light. The absolute wavelength of the detected light is shifted toward the excitation wavelength and is in general found in the Vis-NIR spectral regions. Raman spectroscopy has experienced a dramatic development in recent years. FT-Raman instruments are used when excitation in the NIR spectral region (mostly 1064 nm) is undertaken whereas dispersive instruments are in use when UV and Vis laser are used to induce Raman scattering[12];[13]. The main problem of Raman spectroscopy remains the low probability of the Raman scattering process ( $10^{-10}$  when compared to Rayleigh scattering) and therefore the inherently low concentration sensitivity. Raman spectroscopy, when combined with a confocal microscopy, however, can reach surprising sensitivities as seen e.g. in single cell imaging[14];[15]. To increase concentration sensitivities two different approaches can be used. One is the surface-enhanced Raman scattering (SERS) where small deposits of noble metals, mostly Ag are used as substrates for the analytes, the other is Resonance Raman scattering (RRS) which makes use of the possibility to enhance the signal of analytes absorbing in the wavelength of the exciting light. These effects can generate different enhancements of the signal ranging from  $10^2$  to  $10^6$ , depending on the experimental circumstances. An important advantage of Raman compared to FTIR spectroscopy (MIR) for detection in capillary electrophoresis results from the shorter wavelengths that need to be measured as in these spectral regions the fused silica capillaries are transparent. Therefore on- capillary measurements are possible in contrast to MIR detection. A further advantage of Raman compared to MIR detection is the fact that water shows only weak Raman scattering whereas it is a strong IR absorber. Therefore it is understandable that so far more work has been done on coupling of Raman and CE.

### **1.2.1 Raman scattering in capillary electrophoresis**

The first work coupling CE and Raman detection was reported by Chen and Morris[16] where optical fibers were used to collect Raman scattered light direct from a capillary. The capillaries were aligned and focused onto the entrance slit of spectrometer fitted with a PMT. The analytes used were methyl orange and methyl red at  $1.10^{-4}$  M which were detected on

base of the intense Raman band at  $1410\text{ cm}^{-1}$  using an excitation wavelength of  $442\text{ nm}$ . As a high spectral resolution was not necessary in this application it was set to  $30\text{ cm}^{-1}$  to increase the signal-to-noise ratio.

In a slightly modified system a charge-coupled device (CCD) and lenses were employed and therefore the collection efficiency was enhanced. The spectral resolution could be set to  $12\text{ cm}^{-1}$  again using methyl orange and methyl red as test analytes[17]. In this work pre-resonance Raman spectra were taken with an integration time of  $5\text{ s}$  to achieve detection limits as low as  $6 \cdot 10^{-7}\text{ M}$ . Further increase of integration time lowered the detection limit but was incompatible with the fast separation process, therefore the voltage was reduced when the sample zone arrived at the detector window to allow integration times until  $40\text{ s}$  and a limit of detection of  $1 \cdot 10^{-7}\text{ M}$ .

The intensity of the Raman signal can be increased if the concentration of the sample zone in the capillary directly is increased. One possibility to achieve this goal is sample stacking, using the conductivity differences between the dilute sample zone and the higher concentrated background electrolyte. Therefore the electric field is higher in the dilute sample zone than in the background electrolyte. Consequently, the sample ions move faster to the boundary with the background electrolyte where they slow down and stack up. This preconcentration method was used by Kowalchuk et al.[18] in their work where a  $1 \cdot 10^{-5}\text{ M}$  mixture of nitrate and perchlorate was separated and detected. They used nitrate and perchlorate as model analytes at an excitation wavelength of  $532\text{ nm}$ .

As the analyte concentrations in the steady state in isotachopheresis (ITP) can be between  $0.01\text{ M}$  and  $0.03\text{ M}$  when using electrolytes with a concentration of  $0.1\text{ M}$ , it is the preferred separation and preconcentration method for Raman detection.[19]

Analytes in a matrix containing a high concentration of background electrolyte cannot be preconcentrated via sample stacking methods. ITP requires leading electrolyte (LE) of higher mobility and a trailing electrolyte (TE) of lower mobility than any of the ions of interest. This technique is also called “moving boundary” techniques as all zones move at the same velocity. This velocity occurs since the electric field is self-adjusting to maintain the constant velocity as velocity equals mobility. Walker et al.[20] employed ITP with Raman microscopic detection for the first time separating adenosine 5'-triphosphate, adenosine 5'-diphosphate and adenosine 5'-monophosphate in phosphate buffer. The exciting laser was a Nd-YAG laser at  $532\text{ nm}$  (fig. 9). Limits of detection in the range of  $5 \cdot 10^{-6}\text{ M}$  were achieved for the studied analytes.

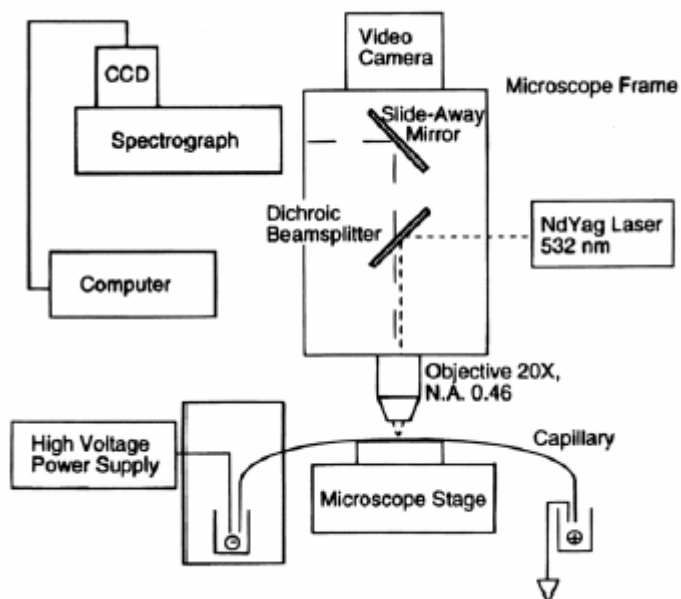


**Figure 9**

As Raman spectroscopy deals with absolute wavelengths in the UV-Vis-NIR spectral region where high performance optics are available fiber-optic probes have also been used for detection in capillary electrophoresis[21]. In this work Walker et al. again separated adenosine 5'-triphosphate, cytidine 5'-monophosphate, guanosine 5'-monophosphate and uridine 5'-monophosphate. The fiber-optic head is much smaller than a microscope giving the possibility to couple it inside the safety housing of the CE system. Due to coupling and insertion losses the signal intensity of the fiber-probe was only about 28% of the signal gained with the conventional Raman microscope. However, spectra of the ribonucleotides with an initial concentration of  $2 \cdot 10^{-5}$  M could be obtained with a similar quality as in the previous work[20], only the absolute signals were lower (fig. 10).

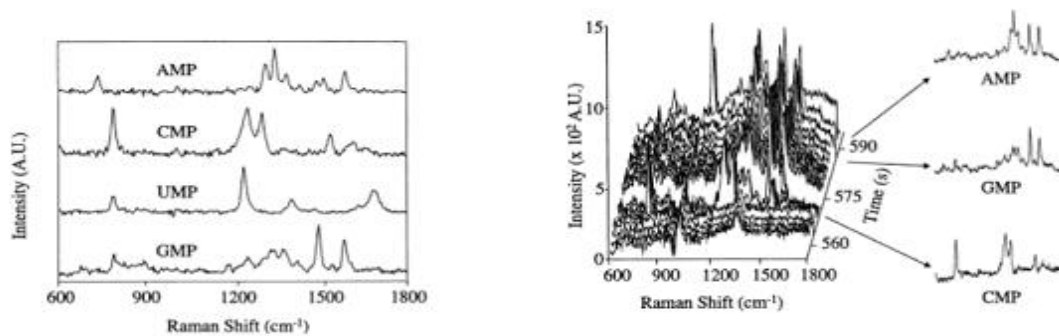


**Figure 10**

Walker et al.[22] furthermore employed statistical methods to the results of a isotachophoretic separation of paraquat and diquat detected by a Raman microscope, again using 532 nm as excitation wavelength. The detection limit could be lowered substantially when using decorrelation against the leading electrolyte Raman spectrum with a t-test ( $t = 5$ , significant difference with 99% confidence level) and factor analysis to extract spectra of analytes during the electrophoresis run. As the factor analysis is a form of signal averaging, good spectra could be achieved considering the low starting concentration of about  $10^{-7}$  M. Paraquat could be detected at initial concentrations of 180 ppb visually and 90 ppb using statistical methods (fig 11).

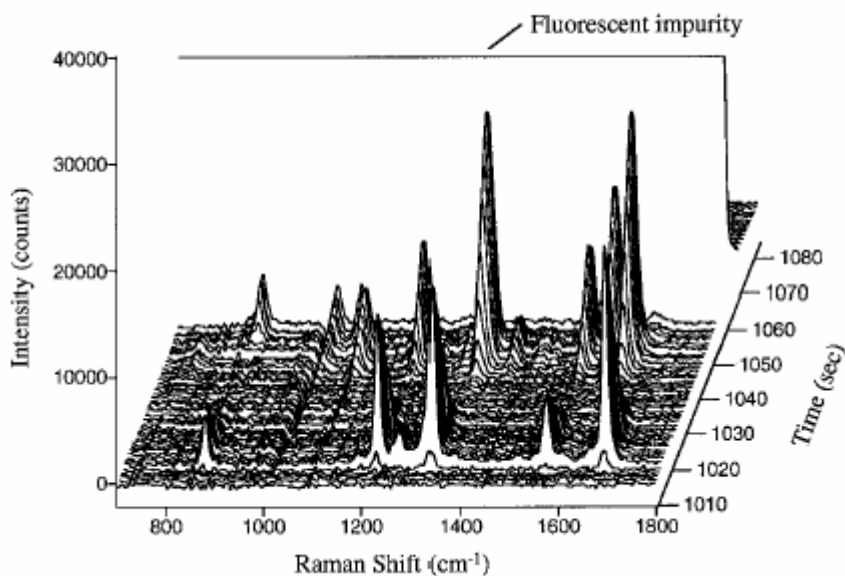


**Figure 11**

Raman microscopes can be employed for probing small volumes down to a few femtoliters so that the microchip is directly coupled to the Raman microprobe. In the field of electrophoresis the miniaturization is advantageous as the speed of the separation increases and the heat dissipation due to a high surface to volume ratio is very efficient, particularly useful for ITP as high-concentrated buffers are used. Walker et al.[23] using the same analytes as in the previous work[22] carried out the separation in a serpentine designed chip with a total length of 21 cm. The interface between the Raman microscope and the microchip was straightforward as the microchip was directly attached to the microscope stage using clips making this interface even simpler than for discrete capillaries (fig. 12).



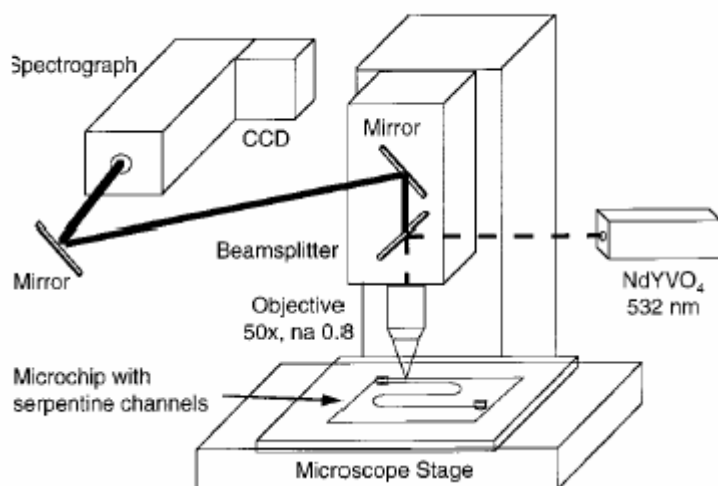


**Figure 12**

The detected concentrations of paraquat and diquat in this work were  $2.3 \cdot 10^{-7}$  M with no statistical treatment employed in this case.

### **1.2.2 Surface-enhanced Raman scattering in capillary electrophoresis**

As already mentioned in the introduction SERS is an important method to increase the signal intensities obtained in Raman spectroscopy. Therefore methods to use this enhancing factor also in the coupling of capillary electrophoresis and Raman spectroscopy were developed. Most of them are off-line methods as the eluents are deposited onto different SERS substrates and are detected subsequently.

However, one on-line method where silver colloids were added to the background electrolyte was developed[24] which is also the first work which employed SERS as a detection method for capillary electrophoresis. The analytes used were riboflavin and the very SERS-active Rhodamine 6G; the detection limits were  $1 \cdot 10^{-6}$  M for riboflavin and  $10^{-9}$  M for Rhodamine (S/N = 10) (fig 13) using a microprobe spectrometer operated in a confocal mode with an excitation wavelength of 515 or 488 nm. The silver colloidal solutions was prepared as described by Lee and Meisel[25], it could be shown that the silver colloid had only little influence on the separation performance when compared to a capillary electrophoresis with laser-induced fluorescence detection (CE-LIF). Different concentrations of silver colloid in the background electrolyte were checked for their influence of the S/N of the SERS spectra, however the particle size of the colloids was not optimized. The only obvious disadvantages

of this work lies in the necessity of cleaning the capillary after each run as the spectra degraded due to decreased resolution and increased background fluorescence due to an assumed gradual buildup of silver particles on the walls of the capillary.

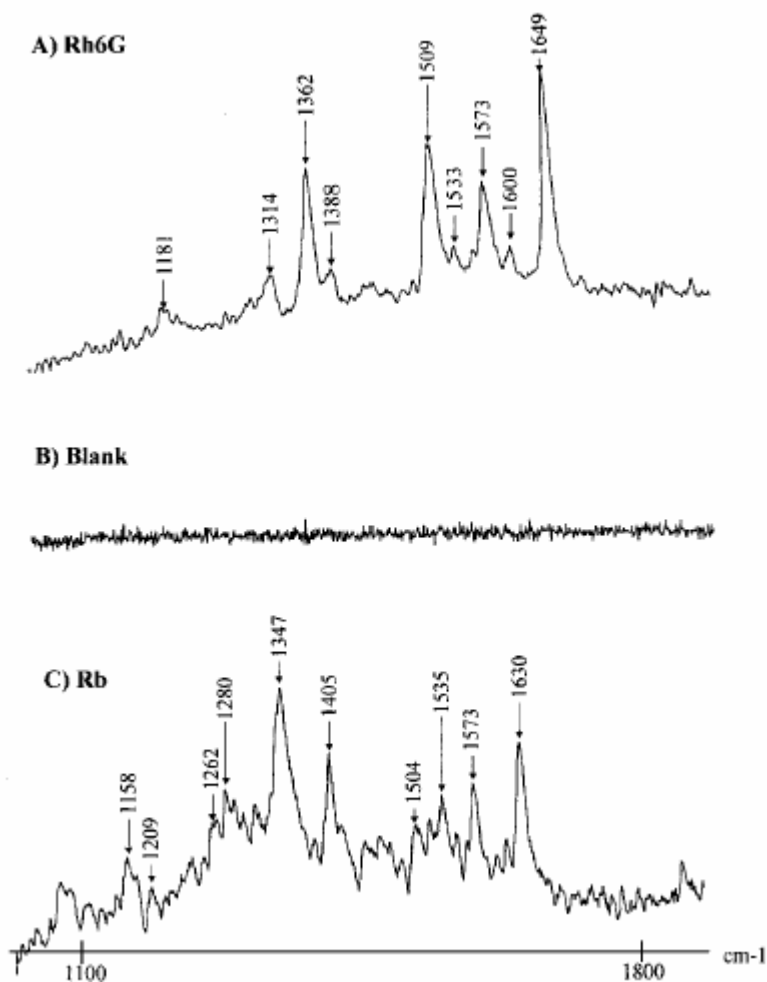
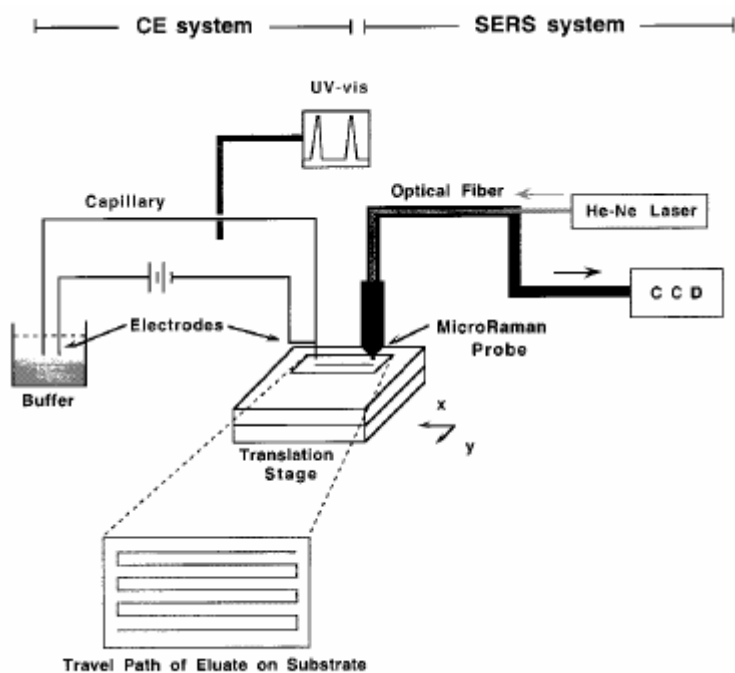


Figure 13

He et al.[26] were the first to couple CE and Raman spectroscopy off-line. The interface used consisted out of the CE system, a computer-controlled translation stage and a fiber-optic Raman microprobe using a He-Ne laser (632.8 nm) as excitation source (fig 14).



**Figure 14**

For confirmation of the separation achieved by the CE-SERS system standard on-line UV detection was used. The retention times obtained corresponded well. The authors evaluated four different substrates for deposition of the eluate, namely Au-LI Ag, Ag colloid, sputtered Ag and Au-LI Ag-Ag film substrates with Au-LI Ag-Ag showing the strongest enhancements. The Au-LI substrate were prepared using a collidial Au solution ( $\sim 17$  nM) and reimmersing the colloidal Au into a mixture of equal volumes of LI silver initiator and enhancer solutions (Nanoprobes, Inc.). The sputtered substrates were prepared using a Ar plasma sputterer, while the Ag colloid was prepared by reduction with EDTA (fig. 15).

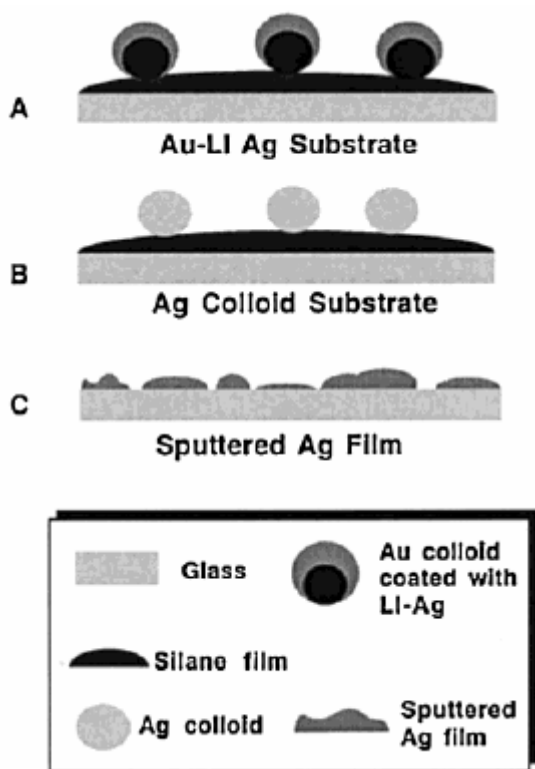


**Figure 15**

The analytes used were trans-1,2-bis(4-pyridyl)ethylene and N,N-dimethyl-4-nitrosoaniline. The CE-SERS system was also applied to the amino acids tyrosine and tryptophan and also to the environmental pollutants chlorophenol and dichlorophenol. As this work was mainly intended as a feasibility study, no quantification was done in this work.

DeVault and Sepaniak[27] explored another approach for deposition as they used electrofilament deposition onto a moving SERS substrate using an argon-ion laser (514 nm) as excitation source.. The on-column separation was checked by LIF. The analytes used were benzyloxyresufin, riboflavin and resorufin (all  $10^{-5}$  M), all compounds of biological significance. In this work the preparation of the SERS substrates was carefully evaluated and optimized as were the separation conditions (fig. 16).

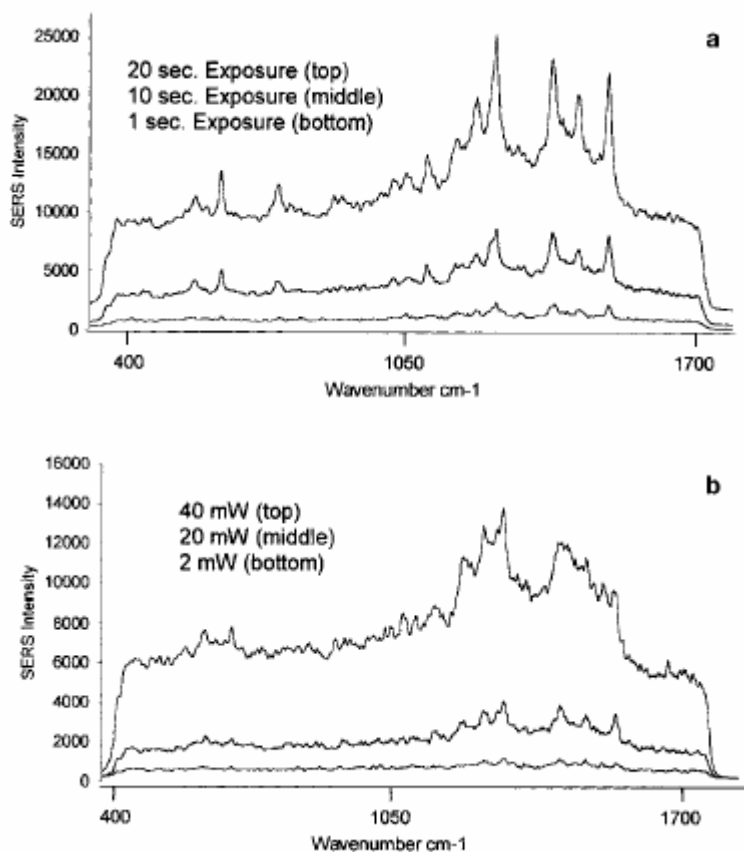


**Figure 16**

The possibility to optimize the separation and the detection step in an off-line experiment separately is one of the main advantages of such an approach. Besides the use of a self-assembled monolayer (SAM) formed out of dodecanethiol to enhance the SERS signal by selective absorption was studied for resorufin. Using a SAM the sample deposited was better spatially focused and the detection limit could therefore be lowered by a factor of 10, resulting in a limit of detection of  $10^{-6}$  M (fig. 17).

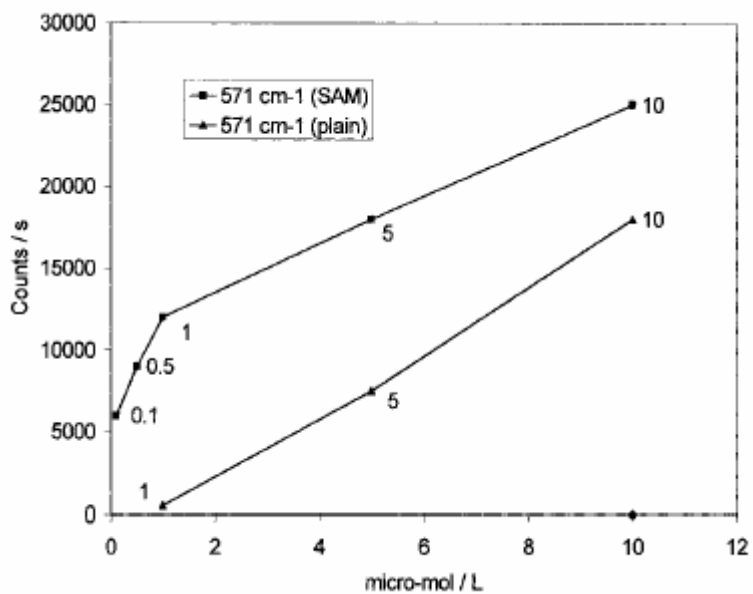


Figure 17

In the approach of Seifar et al.[28] thin layer chromatography (TLC) plates were used as substrates followed by application of the silver sol after the deposition (fig. 18).

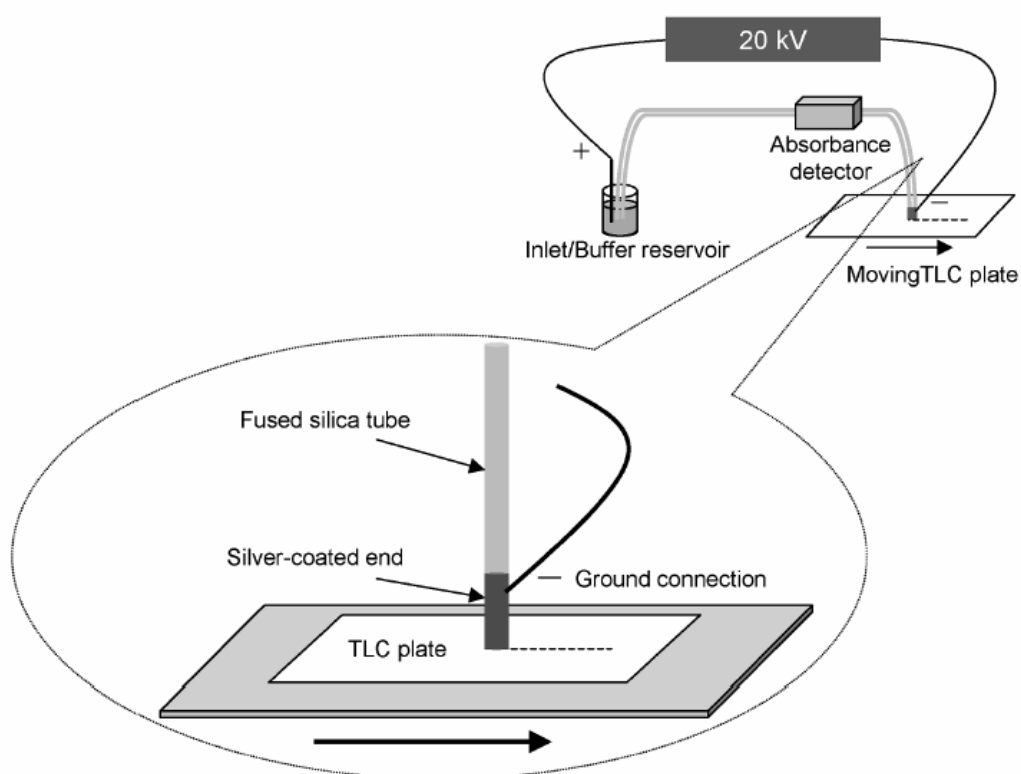
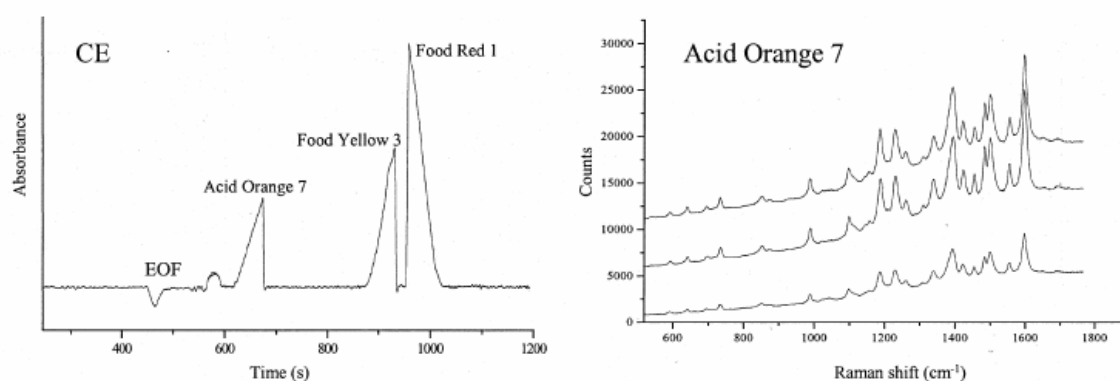


Figure 18

The analytes used in this experiment were three different dyes, Acid Orange 7, Food Yellow 3 and Food Red 1. The excitation wavelength was 514.5 nm, an argon-ion laser. The eluate of the CE run was immediately absorbed on moving TLC plates so that no dispersion of the spot was observed. The detectable amount deposited on the TLC plate was 2-3 pmol (about 1 ng) (fig. 19).



**Figure 19**

The possibility to use resonance Raman spectroscopy (RRS) to enhance the signal was first employed by Chen and Morris[17] using a laser line of 532 nm. In a more recent work by Dijkstra et al.[29] the possibilities of CE-UV-RRS were explored. The employment of excitation light in the UV range makes the application of the RRS more widely usable as more compounds show absorption in the UV rather than in the visible region. In this work two excitation wavelengths (244 and 257 nm) were used that were generated by a frequency-doubled argon ion laser. The analytes studied were aromatic sulfonic acids, nucleotides and substituted pyrenes (fig. 20, right upper 257 nm, lower 244 nm)

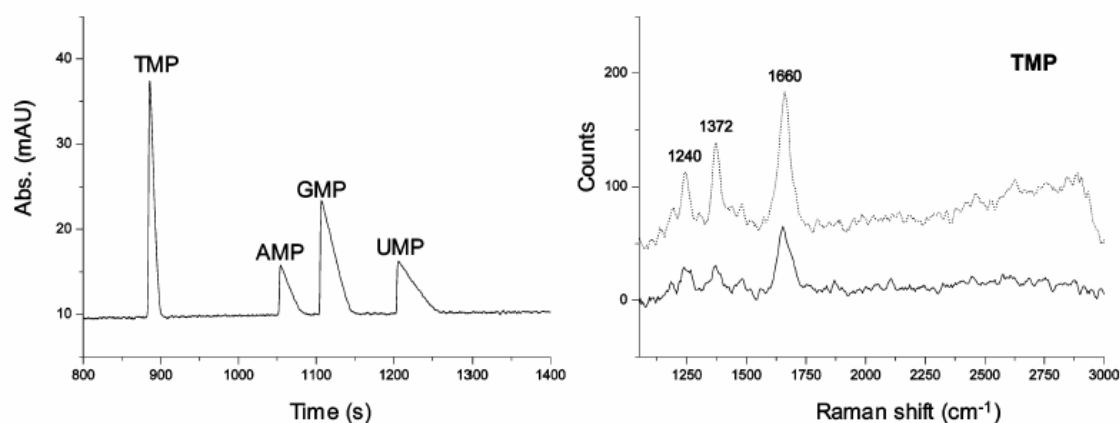


**Figure 10**

The detection was carried out on-line and therefore experiments were carried out to improve the detectability of the analyte by increasing the volume of the injection and sample stacking. It could be shown that the overall sensitivity was increased while only some peak-broadening could be observed. The limit of detections for the nucleotides were calculated and reached from 25  $\mu\text{M}$  for Thymidine-5-monophosphate disodium salt (TMP) to 190  $\mu\text{M}$  for uridine-5'-monophosphate disodium salt (UMP).

As can be clearly seen from the advantages stemming from SERS and RRS the idea to combine both methods to SERRS (surface-enhanced resonance Raman spectroscopy) lies close. The mechanism of SERRS is somewhat different from SERS, as SERRS is less sensitive to changes in molecular orientation on the substrate. Dijkstra et al.[30] studied different substrates in off-line SER(R)S experiments. Again, the procedure was similar as before[28], the eluate was deposited onto the substrates, dried and detected and the excitation wavelength was 514.5 nm- The substrates studied were an etched silver foil, a vapour-deposited silver film, a silver-oxalate-precoated silica TLC plate and silica TLC plate to which colloid and poly(L-lysine) were added after deposition. As in this work the effect of SERS and SERRS was studied using trans-1,2-bis(4-pyridyl)ethylene (BPE) as a model compound for SERS and crystal violet (CV) for SERRS, respectively. The limits of detection was 50  $\mu\text{M}$  for BPE and 0.5  $\mu\text{M}$  for CV, respectively (fig 21).

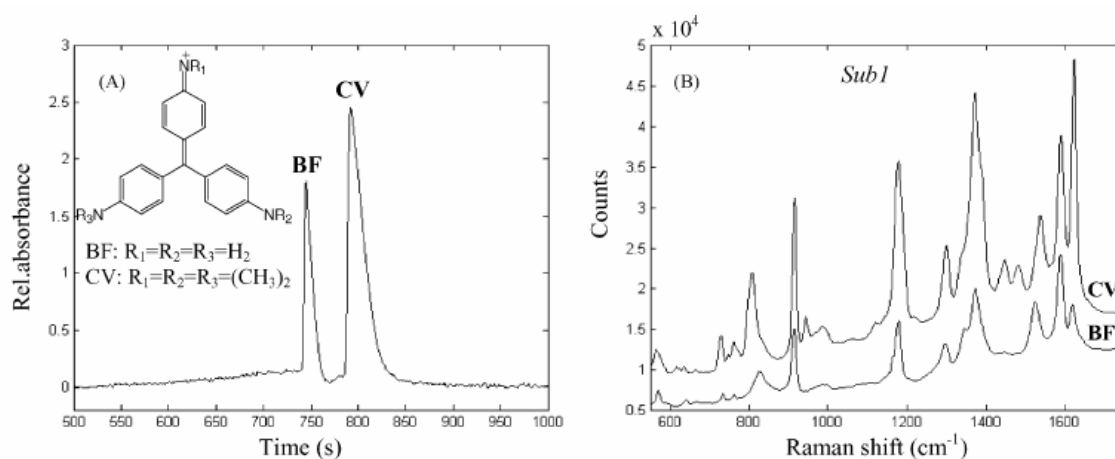


**Figure 21**

Except the silver-oxalate coated TLC plate all substrates used showed good results, while in the case of the TLC plate the background signals increased with time, obviously a drying process attributable to amorphous carbon.



## Reference List

- 1 Abo-Bakr, M.; Feikes, K.; Holldack, K.; Kuske, P.; Peatman, W. B.; Schade, U.; Wustefeld, G.; Hübers, H.-W. *Physical Review Letters* **2003**, *90*, 094801-1-094801/4.
- 2 Taday, P. F.; Bradley, I. V.; Arnone, D. D.; Pepper, M. *Journal of Pharmaceutical Science* **2002**, *92*, 831-38.
- 3 Miller, L. M.; Smith, G. D.; Carr, G. L. *Journal of Biological Physics* **2003**, *29*, 219-30.
- 4 Kölhed, M.; Hinsmann, P.; Svasek, P.; rank, J.; arlberg, B.; endl, B. *Analytical Chemistry* **2002**, *74*, 3843-48.
- 5 Kölhed, M.; Hinsmann, P.; Lendl, B.; Karlberg, B. *Electrophoresis* **2003**, *24*, 687-92.
- 6 Hinsmann, P.; Arce, L.; Svasek, P.; Lämmerhofer, M.; Lendl, B. *Applied Spectroscopy* **2004**, *58*, 662-66.
- 7 Kulka, S.; Kaun, N.; Baena Rodriguez, J.; Frank, J.; Svasek, P.; Moss, D.; Vellekop, M. J.; Lendl, B. *Journal of Analytical and Bioanalytical Chemistry* **2004**, *378*, 1735-40.
- 8 Pan, T.; Kelly, R. T.; Asplund, M. C.; Woolley, A. T. *Journal of Chromatography A* **2004**, *1027*, 231-35.
- 9 Patterson, B. M.; Danielson, N. D.; Sommer, A. J. *Analytical Chemistry* **2004**, *76*, 3826-32.
- 10 Todebush, R. A.; He, L.-T.; de Haseth, J. A. *Analytical Chemistry* **2003**, *75*, 1393-99.
- 11 Jarman, J. L.; Todebush, R. A.; de Haseth, J. A. *Journal of Chromatography A* **2002**, *976*, 19-26.
- 12 Chalmers, J. M.; Griffiths, P. R. *Handbook of Vibrational Spectroscopy*, Wiley: Chicester, 2002.
- 13 Lyon, L. A.; Keating, C. D.; Fox, A. P.; Baker, B. E.; He, L.; Nicewarner, S. R.; Mulvaney, S. P.; Natan, M. J. *Analytical Chemistry* **1998**, *70*, 341R-61R.
- 14 Rösch, P.; Schmitt, M.; Kiefer, W.; Popp, J. *Journal of Molecular Structure* **2003**, *661-662*, 363-69.
- 15 Schuster, K. C.; Reese, I.; Urlaub, E.; Gapes, J. R.; Lendl, B. *Analytical Chemistry* **2000**, *72*, 5529-34.
- 16 Chen, C.-Y.; Morris, M. D. *Applied Spectroscopy* **1988**, *42*, 515-18.
- 17 Chen, C.-Y.; Morris, M. D. *Journal of Chromatography* **1991**, *540*, 355-63.

- 18 Kowalchyk, W. K.; Walker III, P. A.; Morris, M. D. *Applied Spectroscopy* **1995**, *49*, 1183-88.
- 19 Morris, M. D. *Handbook of Vibrational Spectroscopy*, Chalmers John M., Ed.; Wiley: Chicester, 2002.
- 20 Walker III, P. A.; Kowalchyk, W. K.; Morris, M. D. *Analytical Chemistry* **1995**, *67*, 4255-60.
- 21 Walker III, P. A.; Morris, M. D. *Journal of Chromatography A* **1998**, *805*, 269-75.
- 22 Walker III, P. A.; Shaver, J. M.; Morris, M. D. *Applied Spectroscopy* **1997**, *51*, 1394-99.
- 23 Walker III, P. A.; Morris, M. D.; Burns, M. A.; Johnson, B. N. *Analytical Chemistry* **1998**, *70*, 3766-69.
- 24 Nirode, W. F.; DeVault, G. L.; Sepaniak, M. J.; Cole, R. O. *Analytical Chemistry* **2000**, *72*, 1866-71.
- 25 Lee P.C.; Meisel D.J. *Journal of Physical Chemistry* **1982**, *86*, 3391-95.
- 26 He, L.; Natan, M. J.; Keating, C. D. *Analytical Chemistry* **2000**, *72*, 5348-55.
- 27 DeVault, G. L.; Sepaniak, M. J. *Electrophoresis* **2001**, *22*, 2303-11.
- 28 Seifar, R. M.; Dijkstra, R. J.; Gerssen, A.; Ariese, F.; Brinkman, U. A. Th.; Gooijer, C. *Journal of Separation Science* **2002**, *25*, 814-18.
- 29 Dijkstra, R. J.; Efremov, E. V.; Ariese, F.; Brinkman, U. A. Th.; Gooijer, C. *Analytical Chemistry* **2003**, 5697-702.
- 30 Dijkstra, R. J.; Gerssen, A.; Efremov, E. V.; Ariese, F.; Brinkman, U. A. Th.; Gooijer, C. *Analytica Chimica Acta* **2004**, *508*, 127-34.

# Curriculum vitae

# DI Stephan Kulka

---

## Persönliche Informationen

- Familienstand: ledig
  - Nationalität: österreichisch
  - Alter: 28
  - Geburtsort: Wien
  - Eltern: Dr. iur. Friedrich Kulka und Dr. iur. Gabriele Kulka
- 

## Ausbildung

2002-2005 Technische Universität Wien  
Doktoratsstudium Technische Chemie

1998-2002 Technische Universität Wien  
Diplomstudium Technische Chemie

- Spezialisierung auf analytische und physikalische Chemie
- Diplomarbeitsthema: *Determination of Aluminium in Seawater using Flow Injection with Micelle-Enhanced Lumogallion Fluorescence Detection* (durchgeführt an der Universität Plymouth am Institute for Environmental Science bei Professor Worsfold; verbunden mit einem neunmonatigem Aufenthalt in Plymouth)

1996-1998 Eidgenössische Technische Hochschule Zürich  
Diplomstudium Interdisziplinäre Naturwissenschaften

ab 1998 Wirtschaftsuniversität Wien  
Diplomstudium Betriebswirtschaftslehre

- Spezialisierung auf „Investmentbanking und Katallaktik“ und „Wirtschaftsinformatik“
- Studium mehrmals durch Auslandsaufenthalt und Abfassung der Dissertation unterbrochen

1986-1995 Piaristengymnasium Wien  
Humanistischer Zweig

- Matura mit Auszeichnung
- Chefredakteur und Gründer der Schülerzeitung; mehrmals stellvertretender Schulsprecher

## Tätigkeiten neben dem Studium

- 1996-1997 Finanzreferent des Vereins Chemischer Studierender
- 1997-1998 Finanzreferent des Verbands der Studierenden an der ETH

- 1998-2000 Mitglied des Umweltreferates der Wirtschaftsuniversität Wien (Mitorganisator der jährlich stattfindenden Ökowoche)
  - 1999-2001 Studienberater der Österreichischen Hochschülerschaft
- 

## Sprachkenntnisse

- Deutsch: Muttersprache
  - Englisch: ausgezeichnet in Wort und Schrift
  - Italienisch: hohes Niveau in Wort und Schrift
  - Französisch: mittleres Niveau in Wort und Schrift
  - Polnisch: Grundkenntnisse
- 

## Berufserfahrung

2002-2005                      Technische Universität                      Wien  
Angestellter (Dissertant)

- Forschungsarbeit, administrative Tätigkeiten, Projektarbeit und Verfassen von wissenschaftlichen Publikationen und Berichten
- 

## Publikationen

- Kulka, S.; Kaun, N.; Baena J.R.; Frank, J.; Svasek, P.; Moss, D.; Vellekoop M.J.; Lendl, B. "Mid-IR synchrotron radiation for molecular specific detection in micro-chip based analysis systems" Analytical and Bioanalytical Chemistry 378 (2004) 1735-1740
  - Kulka, S.; Lendl, B. Buchkapitel in „Detection Systems For Capillary Electrophoresis“, eds. Marina, M.L; Rios, A.; Valcarcel, M., Elsevier: Amsterdam, 2005
  - Kulka, S.; Lendl, B. "On-line capillary electrophoresis FT-IR detection for the separation and characterization of proteins", eingereichte Publikation
  - Kulka, S.; Quintas, G.; Lendl, B. "Automated sample preparation and analysis using a sequential-injection (SI)-capillary electrophoresis (CE) interface", eingereichte Publikation
  - Kaun, N.; Kulka, S. ; Frank, J.; Schade,U.; Vellekoop, M.J.; Harasek, M. and Lendl, B. "Towards Biochemical reaction monitoring using FT-IR Synchrotron radiation" eingereichte Publikation
- 

## Ferialpraktikum

1993                                      U-Bahn Arge                                      Wien  
Ferialpraktikant

- Bürotätigkeiten, Verfassen von Plänen und Baustellenbegehungen
- 

## Wehrdienst

- 1995-1996 abgeleistet in Graz und Neulengbach
-